PHILOSOPHICAL TRANSACTIONS OF THE ROYAL SOCIETY A MATHEMATICAL, PHYSICAL & ENGINEERING SCIENCES

The Magnetic Properties of Igneous Rocks from the Ocean Floor

N. D. Watkins and T. P. Paster

Phil. Trans. R. Soc. Lond. A 1971 **268**, 507-550
doi: 10.1098/rsta.1971.0011

Phil. Trans. Roy. Soc. Lond. A. **268**, 507–550 (1971) [507]
Printed in Great Britain

The magnetic properties of igneous rocks from the ocean floor

By N. D. Watkins
Graduate School of Oceanography, Narragansett Marine Laboratory, University of Rhode Island, Kingston, Rhode Island 02881, *U.S.A.*

and T. P. Paster*
Department of Chemistry, University of Wisconsin, Madison, Wisconsin, 53706, *U.S.A.*

[Plates 7 to 9]

The measured magnetic properties of submarine igneous rocks, comprising data from approximately 300 specimens, are summarized. Basaltic rocks dominate the collection numerically, and are distinguished by their high Q (ratio of remanent to induced magnetic intensities). Limited numbers of altered samples indicate that spilitization, chloritization, and serpentinization can drastically reduce the intensity of magnetization. The available thermomagnetic data suggest that low Curie points may be typical of quenched basalts.

The limited range of submarine igneous rock types examined, and the strong bias towards quenched samples necessitates a supplement to this summary in the form of a discussion of studies of magnetic properties from selected igneous rocks outcropping above sea level. In these studies, serpentinization of ultrabasic rocks has been observed in one case to increase the intensity of magnetization; chloritization and spilitization are confirmed as being magnetically destructive; maghaemitization may have destructive effects; titanomagnetite oxidation variation dominates in magnetic change of basaltic lavas (and some corresponding chemical changes are likely to occur); basaltic intrusives have a much more limited titanomagnetic oxidation range than is generally observed in lavas; and spontaneous demagnetization with time probably exists, at least in basalts.

New data are presented. These include the magnetic properties of harzburgites dredged from the Macquarie Ridge, and eight pillow basalts from the South Pacific and Scotia Sea. The former suggest that harzburgite is capable of creating strong magnetic anomalies. Samples for the latter study were sufficiently large for study of the variation of magnetic and petrological properties with depth beneath the cooling surface. Systematic texturual changes from glassy exterior, through a variolitic zone to aphanitic interior characterize the silicates in most samples. Chloritization is present in some aphanitic parts. Serpentinization is present in some aphanitic zones and also next to joints. The opaque minerals were studied in detail in one pillow. The titanomagnetites are all fine and of low oxidation state. Very fine sulphides are common. The intensity of magnetization and susceptibility variation are closely related to the changes in titanomagnetite grain size. Although optically undetectable in the titanomagnetites, a zone of slightly higher oxidation is inferred to exist towards the centre of the pillow by the presence of higher Curie points and magnetic stability, and lower sulphide content.

New data are also presented from traverses of Icelandic lavas and dykes, and from spilites of St Thomas, Virgin Islands.

It is concluded that the submarine basalt magnetic properties which have so far been determined are largely a function of quenching, in contrast with the data from lavas outcropping above sea level which have generally experienced longer cooling periods, and which therefore include a greater range of titanomagnetite grain size and oxidation states. The quenching process can apparently proceed faster than the oxidizing process in basalts. Magnetic properties of the surface of submarine basalts are therefore largely a function of cooling history, rather than any upper mantle phenomenon. The new data confirm that deuteric or post-cooling alteration of basalts and ultrabasic rocks can be magnetically destructive: chloritization is always associated with a decreasing intensity of magnetization and Q ratio. Spilitization is similarly destructive. The magnetic effect of serpentinization, however, is not uniquely predictable. The magnetic data for submarine ultrabasic rocks show much variation, but are too limited for further generalization.

* Present address: Molybdenum Corporation of America, Louviers, Colorado 80131, U.S.A.

Introduction

Study of the magnetic properties of igneous rocks from the ocean floor has increased greatly since 1966. This is to a large extent in response to successful application of the Vine–Matthews (1963) hypothesis to examination of linear magnetic anomalies in all oceans of the world, in terms of the crustal spreading model (for a summary of such applications see Bullard 1968, 1969). It is somewhat paradoxical that these globally significant analyses of data associated with most of the Earth's surface are at present matched by study of the magnetic properties of only 300 or so specimens of the rocks actually involved (at least in part) in creating the anomalies: this represents the order of one specimen per million square kilometres.

As Watkins & Haggerty (1967) have observed, the magnetic properties of rocks have tended to become considered as 'geophysical' parameters, remote from the interest of petrologists and geochemists. This historical accident is unfortunate since titanomagnetites in basalt, for example, are much more sensitive than the silicates to variation in the initial cooling oxygen fugacity, and are therefore quite clearly useful petrological indices. The post-cooling or lower temperature changes can also be expressed in magnetic property variation (Watkins & Haggerty 1965, 1967; Wilson & Watkins 1968). It would seem reasonable, therefore, to suggest that finer petrological definitions could utilize magnetic properties, but this has not occurred to date.

The purpose of this paper is to summarize the results of the studies so far made of the magnetic properties of submarine igneous rocks. These include some descriptions of the apparent effect on the magnetic properties of alterations which have been detected by examination of the silicates in thin section. Only one detailed opaque mineralogical description of submarine rocks has been presented (Carmichael 1970) at the time of writing. Because of the great lack of data from non-basaltic rocks, some results from studies of rocks which outcrop above sea level are included. We shall present and discuss limited new results involving submarine rocks taken from the Macquarie Ridge, and spilites from the Virgin Islands. The effect of variations in cooling rate on silicate and titanomagnetite petrology (and the corresponding magnetic property differences) will then be examined by presentation of new data. These are from traverses between the glassy margins and crystalline interiors of several submarine pillow basalts collected from the South Pacific and Scotia Sea. Because of the very limited size of the pillows involved (and, therefore, the limited durations of cooling), we supplement the results with previously unpublished traverses between the cooling faces of some Icelandic lavas and dykes.

Magnetic properties

(*a*) *Fundamentals*

Study of the magnetic properties of igneous rocks can be a very broad discipline. Nagata (1961) has summarized in detail the results of the great range of studies of the many parameters in natural and synthetic specimens, which are contributing to an understanding of rock magnetism.

In this presentation we shall restrict our discussion to the magnetic properties which are most readily associated with geological and geophysical studies of igneous rocks. These are discussed below.

The *intensity of magnetization* of material can be discussed at four ascending levels: the magnetic moment of electron spins in an atom; the magnetism of domains (discrete collections of alined

spins); the magnetism of grains, crystals, or phenocrysts (which are generally collections of domains) of the magnetic material; and the magnetism of the whole rock, which is a collection of grains, crystals, or phenocrysts. The process of magnetization is generally one of domain rotation or effective rotation by displacement of domain walls or boundaries. Two different types of intensity of magnetization are distinguished: the permanent or *remanent magnetization* (J), and the *induced magnetization*. J in an igneous rock is dependent on the phase, size and volume of the ferromagnetic constituent and the ambient geomagnetic field intensity during cooling. *Thermal remanent magnetism* (t.r.m.) therefore dominates in most igneous rocks, but post-emplacement or lower temperature phenomena can contribute to net J values in the form of *chemical remanent magnetism* (c.r.m.) which can, however, form at higher temperatures. The direction of J is generally that of the ambient geomagnetic field during cooling. This property is the foundation of the field of palaeomagnetism. The intensity of induced magnetization is dependent on the phase and size of the ferromagnetic constituents, but is a function of the ambient magnetic field during the measurement only: the induced intensity of magnetization is therefore zero in zero field. The direction of the induced intensity of magnetization is that of the ambient geomagnetic field during measurement of the induced intensity. The ratio of induced intensity of magnetization to ambient geomagnetic field intensity is the *susceptibility* (χ) of the material. The ratio of the remanent to the induced intensity of magnetization is called the Q *value*, so that $Q = J/\chi H$.

The parameter Q is very important in an understanding of the cause of anomalies in magnetic surveys over rocks of any type: if $Q \ll 1$, the induced component dominates and the direction of the intensity of magnetization is readily available, being that of the geomagnetic field during the measurement. This therefore can only be normal in its polarity. If $Q \gg 1$, the remanent component is dominant however, so that the direction of the intensity of magnetization reflects most commonly the direction of the geomagnetic field during the initial cooling. This can be reversed or normal, since the geomagnetic field has reversed many times in the past. Without a high Q, past reversals of the geomagnetic field would not be detectable as reversed magnetic anomalies over igneous bodies. If $Q \approx 1$, then the remanent and induced magnetism have about the same intensity. This can reinforce the observed anomaly intensity, if the direction of the remanent component is normal, but can oppose it (perhaps creating no observable anomaly) if the direction is reversed.

The intensity of magnetization is zero in rocks containing only diamagnetic minerals, such as quartz and feldspar: no net alinement of electron orbits exists. Paramagnetic minerals such as olivine, pyroxene and biotite are only slightly magnetic: the individual atoms are uncoupled, each behaving independently of each other. When the crystal structure allows, however, overlapping of electron orbits occurs and coupling exists: *ferromagnetism* features parallel coupling, which results in maximum alinement of electron spins and strong intensity of magnetization. Other coupling configurations are used to finely distinguish additional magnetic states. The intensity of magnetization resulting from such coupling is destroyed at the *Curie temperature* (T_C), when the coupling energy becomes less than the thermal energy. It follows that this is also the temperature at which a rock or mineral begins to aquire magnetism on cooling from high temperatures.

A single ferromagnetic domain (or aggregate of atoms with parallel coupled electron spins) is of the order of 1 μm in size, but can be larger. A single crystal can be made of many such domains, of differing sizes. The degree of alinement of the adjacent domains determines the

PHILOSOPHICAL TRANSACTIONS OF THE ROYAL SOCIETY A MATHEMATICAL, PHYSICAL & ENGINEERING SCIENCES

net J of the crystal. Similarly, the net J of a rock depends on the overall alinement of the domains. The alinement can be increased by the application of a strong constant ambient field, up to the saturation intensity of magnetization (J_{sat}), when alinement is total.

The stability of a rock is a term used to express the degree to which the original direction and intensity of magnetization is retained. Forces tending to change these original parameters can be later ambient thermal or magnetic activity, and a spontaneous self-demagnetization. The stability is dependent on the length of domain wall per unit volume, as well as other factors. Therefore the smaller the constituent domains, the higher the magnetic stability. The *coercivity* is an expression of stability: alternating magnetic fields can be applied to rotate or migrate the domain walls away from their original configuration. The size of this 'demagnetizing field' is a measure of the coercivity of the domain. A spectrum of domain sizes invariably exists in a rock, and so a *coercivity spectrum* results from the application of progressively higher demagnetizing fields: this is in practice accomplished by mechanically tumbling the rock sample around several axes simultaneously during the application of an alternating magnetic field which sweeps up to a peak value and down again. This is sometimes called 'magnetic washing' because randomizing the lower coercivity domains results in the cancellation of unstable components (acquired after the initial cooling), to more closely arrive at, in the case of igneous rocks, the direction of the original t.r.m. An *isothermal remanent magnetism* (i.r.m.) is generally a magnetization acquired spontaneously in the Earth's magnetic field following emplacement of the rock: this would be to some extent a function of the age of the rock and is usually contained in one of the lower coercivity components which are readily randomized by 'magnetic washing'.

(*b*) *Mineralogy*

By far the most dominant magnetic minerals in igneous rocks are the titanomagnetites. Their relationships and some of their properties are summarized in figure 1 (*a* and *b*). It should be noted that figures 1*a* and 1*b* result from study of synthetic rocks. Addition of foreign ions such as Al or Mn, can drastically affect magnetic properties.

The major factor contributing to change in magnetic properties is oxidation (Meitzner 1963), although quenching or any factor inhibiting crystal growth is also critical.

Watkins & Haggerty (1967) and Wilson & Watkins (1967) have described the development of an oxidation index system, whereby the relative oxidation state of the titanomagnetites in a basalt is determined optically. The oxidation index system employs the following six categories, for use with Reichert Zetopan-pol reflexion microscope, using oil immersion with up to 1200 times magnification:

Index I. Homogeneous titanomagnetite.

Index II. Titanomagnetite containing a single or a small number of 'exsolved' ilmenite lamellae.

Index III. Titanomagnetite with abundant oxidation-'exsolution' lamellae of ilmenite.

Index IV. The sharp, well-defined ilmenite lamellae of III become mottled and distinctly lighter in colour. The submicroscopic and heterogeneous nature of the inversion products at this oxidation stage does not permit identification of individual mineral phases, and is best termed 'meta-ilmenite' (Buddington & Lindsley 1964, p. 326). The titanomagnetite shows signs of incipent alteration to titanohaematite.

Index V. With increasing oxidation the products become more coarsely crystalline. The characteristic mineral phase at this stage is rutile. Both ilmenite and the titanomagnetite are oxidized to

oriented intergrowths of rutile in a host of titanohaematite. Relic areas of titanomagnetite may still persist and in these cases contain exsolution rods of alumino-spinels.

Index VI. This represents the maximum degree of oxidation and is characterized by the high temperature (> 585 °C) index mineral pseudobrookite. The original titanomagnetite–ilmenite intergrowth is completely changed to pseudobrookite in a host of titanohaematite, in which accessory rutile may or may not be present.

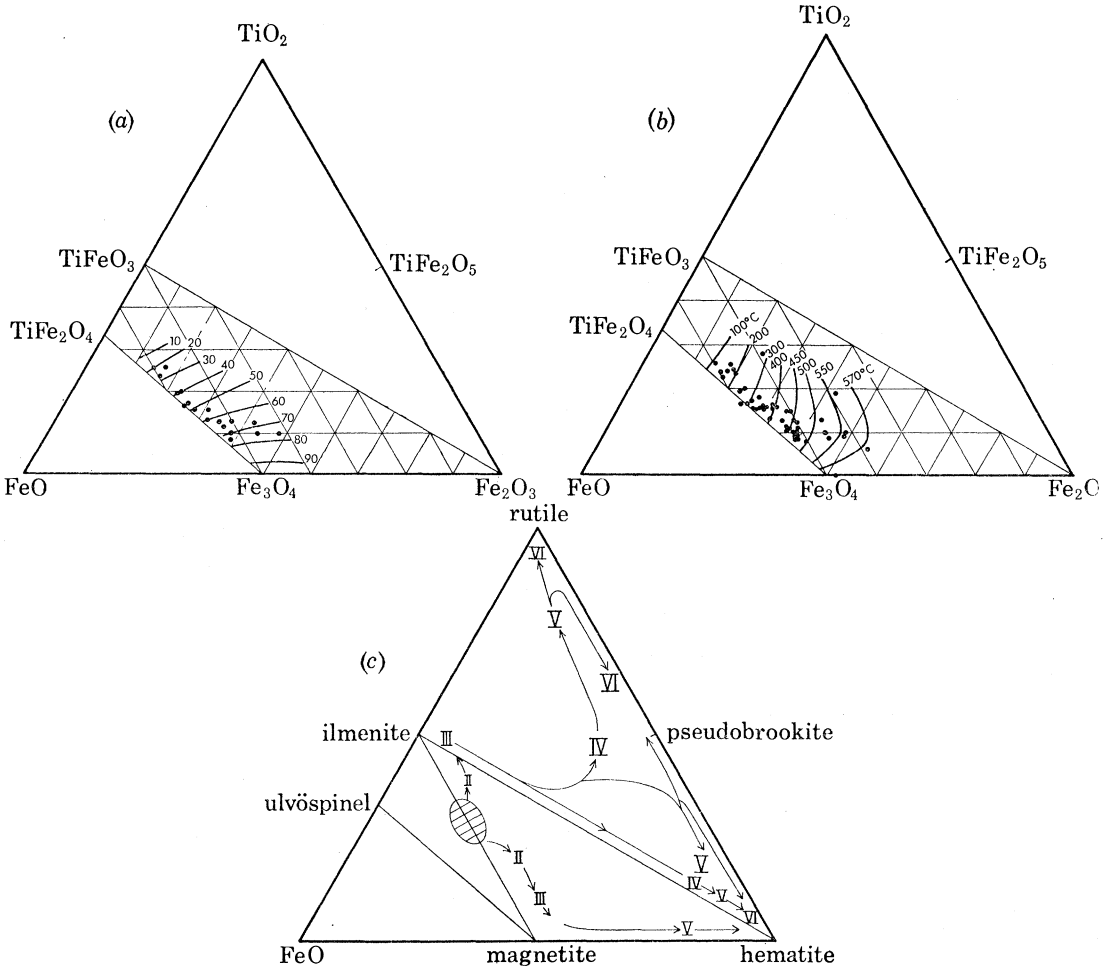

FIGURE 1. Relations between the iron–titanium oxides, some magnetic properties, and optically defined mineralogical trends in basalts: (*a*) variation of the saturation intensity of magnetization in e.m.u. g^{-1} and titanomagnetite composition; (*b*) variation of the Curie point and titanomagnetite composition; (*c*) generalized trends of oxidation of high temperature titanomagnetite in basalts from oxidation index I to oxidation index VI, as employed in the optically defined system of Wilson & Watkins (1967); Watkins & Haggerty (1967), and others. See text for discussion: note that the bifurcation of trends may indicate either separate phases evolving as textures within the original titanomagnetite, or its complete replacement; it is emphasized that these trends are based purely on the optically-defined system and do not involve at this stage any significant number of essential chemical analyses. The upper two figures are after Akimoto (1957).

The progressive oxidation of coarse discrete grains of ilmenite, which coexist with titanomagnetite, is exactly the same as that described for the 'exsolved' ilmenite, starting at class IV with the development of meta-ilmenite through rutile-titanohaematite at V and pseudobrookite as the major phase in class VI.

The oxidation product titanomaghaemite may be superimposed on the high temperature

oxidation sequence, but is not found in oxidation states higher than homogeneous titanomagnetite containing 'exsolution' lamellae of ilmenite (Oxidation Index III). Maghaemite inverts to haematite between 590 and 650 °C (Gheith 1952). The oxidation of magnetite to maghaemite has been reported to take place as low as 200 °C (Lepp 1957), and may also form as a lower temperature weathering product (Akimoto & Katsura 1960). Maghaemite has not been reported in association with titanohaematite, rutile, or pseudobrookite.

Several studies (Watkins & Haggerty 1965, 1967; Wilson *et al.* 1968) have shown systematic relations between the optically-defined oxidation index and other parameters thereby showing the meaningful nature of the above definitions.

Figure 1*c* attempts to show the general directions of changes taking place during the development of these titanomagnetite oxidation indices from an original magnetite-ilmenite solid solution, which appears to be dominant initially in most extrusive basaltic material. In the system of Watkins & Haggerty (1967) about 300 grains in a given polished section are scanned, and an average oxidation index is estimated. This system has been superseded by the more quantitative *magnetite oxidation number* system (Wilson *et al.* 1968; Ade-Hall & Watkins 1970) which involves assigning an oxidation index to 100 grains, and computing the magnetic oxidation number (M) where $M = \sum_{i=1}^{n} \frac{n_i x_i}{n}$ and n is the number of grains in a given oxidation index x. Some of the observed relations between the oxidation state of the titanomagnetites and various magnetic properties will be presented in the following section.

Magnetic minerals other than titanomagnetite are generally rare in basaltic rocks. The sulphides pyrite and pyrrohotite are magnetic, but rarely occur in extrusive igneous rocks since they are particularly susceptible to oxidation, readily converting to iron oxide and a gas phase at high temperatures. When observed, sulphides are usually in intrusive igneous or metamorphic rocks. Low-temperature iron-sulphur oxyhydroxides can be weakly magnetic, but are generally unimportant magnetically in igneous rocks.

Summary of previous studies

(*a*) *Petrology and magnetic properties of submarine rocks*

In order to define the linear magnetic anomalies which are now being recognized over much of the Earth's oceans (Heirtzler *et al.* 1968), magnetic profiles totalling of the order of millions of kilometres in length have been made. As Heirtzler, Le Pichon & Baron (1966) have emphasized: 'While a detailed magnetic survey gives accurate information about the structural trend of a region, it provides much less information about the materials causing the anomalies.' Nevertheless, this important property of magnetism in rocks (that the bulk intensity and direction of magnetization, at least, can be monitored by remote sensing) can provide important limits to the magnetic properties of rocks. For example, Hess (1964, 1966) modified his earlier ideas about the existence of a magnetically dominant oceanic serpentinite layer because of the fact that the measured J values of the Puerto Rico Mohole test core serpentinite (Cox, Doell & Thompson 1964) were too low to account for the observed linear magnetic anomalies over oceanic ridges.

Measurement of the basic magnetic properties of igneous and metamorphic rocks from the ocean floor are restricted to eleven studies. These are summarized in table 1. The total number of specimens is about 300.

PHILOSOPHICAL TRANSACTIONS OF THE ROYAL SOCIETY A MATHEMATICAL, PHYSICAL & ENGINEERING SCIENCES

TABLE 1. SUMMARY OF PREVIOUS MEASUREMENTS OF THE MAGNETIC PROPERTIES OF SUBMARINE ROCKS

Reference	sample locality	rock type	N	$J \times 10^{-4}$ c.g.s.	$\chi \times 10^{-4}$ c.g.s.	Q	remarks
Matthews 1961	North Atlantic	basalt	41	44.0	5.0	20.0	—
Cox & Doell 1962	Northeast Pacific	basalt	23	5.4	3.0	40.0	—
Bullard & Mason 1963	Mendocino-Pacific	basalt	?	177.0	18.0	20.0	includes data from Ade-Hall (1964)
Ade-Hall 1964	Atlantic and Pacific	basalt	97	50.0	5.0	18.0	one third of samples 'decomposed'
Vogt & Ostenso 1966	M.A.R., 44° N	basalt	10	50.0	3.0	48.0	—
Opdyke & Hekinian 1967	M.A.R., 30° N	basalt	24	290.0	9.2	64.0	includes 'altered' samples
Luyendyk & Mason 1967	M.A.R., 22° N	basalt	8	63.0	18.0	12.0	—
Ozima *et al.* 1968	Pacific	basalt	9	35.7	2.7	24.8	—
Dymond *et al.* 1968	Cobb Sea Mount	basalt	1	4.5	0.8	10.4	—
DeBoer *et al.* 1970	Reykjanes Ridge	basalt	38	500.0	5.0	173.0	many samples from a few boulders
Carmichael 1970	M.A.R., 45° N	basalt	17	1680.0	—	110.1	—
Luyendyk & Melson 1967	M.A.R., 22° N	basalt breccia	9	7.4	4.9	3.41	much saponite present
Opdyke & Hekinian 1967	M.A.R., 30° N	spilitized basalt	4	0.04	0.55		—
Luyendyk & Melson 1967	M.A.R., 22° N	greenstone	3	0.06	0.53	0.2160	—
Carmichael 1970	M.A.R., 45° N	metabasalt and diabase	2	1.33	—	13.3	—
Opdyke & Hekinian 1967	M.A.R., 30° N	chloritized basalt	1	0.0016	1.84	0.0017	—
		Anorthosite gabbro	1	3.11	1.46	4.26	—
		olivine gabbro	1	5.40	3.35	3.22	—
		amphibolite	1	0.0032	0.81	0.0078	—
		serpentinite	1	23.2	38.5	1.2	—

N = number of specimens measured. J and χ values are sometimes e.m.u. g^{-1} and mass susceptibility, or e.m.u. cm^{-3} and volume susceptibility, respectively. $Q = J/\chi H$ where H = present ambient geomagnetic field intensity in oesteds. Refer to original reference for details of data averaging, which is sometimes per unit sample (several specimens) or per unit specimen. M.A.R. = Mid-Atlantic Ridge

As far as is possible, the data listed in table 1 have been divided on a silicate petrological basis, following the respective author's description. The basalt category includes some 'altered' materials: for example, Ade-Hall (1964) reports that 35 % of his specimens were 'decomposed'; and Opdyke & Hekinian (1967) include 'altered and decomposed' basalts in their study. It is therefore highly probable that there is some overlap between the basalt and other categories in table 1. 'Chloritized basalt' and 'greenstone' are virtually certain to be synonymous between some authors. It is also not clear if there is any significant petrological difference between 'basalt' and 'basalt breccia'. The very limited study of Dymond, Watkins & Nayudu (1968), was the first reflected light observation of the opaque minerals, describing the phases and textures of the ferromagnetic minerals present. Carmichael (1970) has since presented detailed description of the titanomagnetites in dredged rocks from the mid-Atlantic Ridge at 45° N, but no other similar work has been carried out. In this summary of previous work, discussion of measured magnetic properties is therefore by necessity almost completely restricted to their association with the given silicate petrological type. It is, of course, unlikely that the more common silicate alterations are not accompanied by some form of change in the titanomagnetites, which are, as stated earlier, much more susceptible to oxidation changes (for example) than the silicates.

The data (table 1) fall into three distinct groups: the basalts with $Q > 10$; the basalt breccias, gabbro, and serpentinite with $1 < Q < 5$; and the spilitized and chloritized basalt, greenstone, and amphibolite, with $Q < 1$. Not all data fit this simple scheme: those of Carmichael (1970) present exceptions. There is considerable (but not perfect) parallelism between these divisions and the respective J values. From these limited data, it appears that chloritized basalt, which is generally believed to result from hydrothermal or deuteric alteration of biotites and ferromagnesians, is strongly correlated with J and Q values diminished to less than unity. It is suggested that the latter could be considered for use as a diagnostic property of chloritized basalt.

The number of specimens other than basalts is clearly too limited for further generalizations. Some discussion of three of the studies in table 1 is warranted, however. These are the measurement of the magnetic properties in the only oceanic basalt core so far studied (Cox & Doell 1962); the self-reversal studies of Ozima & Kaneoka (1968) using oceanic basalts; and data from a traverse of the M.A.R. by Carmichael (1970).

The study of Cox & Doell (1962) was made on 23 specimens from the Mohole test core. The result is reproduced in figure 2. A higher coercivity is observed in specimens closer to the surface. The grain size increases from 2–4 μm at the surface, to 9–100 μm deeper in the core. The systematic decrease in Q with depth in the core is attributed to the more rapid cooling towards the surface, resulting in diminished grain size. This can diminish χ (and therefore increase Q) in line with Gottshalk's (1935) observed experimental data, and also increase J and stability since retentivity and coercivity are inversely correlated with grain size. The higher coercivity could also be due in part to a more rapid cooling since cooling produces abundant imperfections in crystal lattices.

Ozima & Ozima (1967) examined the thermomagnetic behaviour of several South Pacific samples, the basic magnetic properties of which were reported elsewhere (Ozima *et al.* 1968). They show (figure 3) that on heating for a limited period the original magnetic component (T_C of 250 °C) is gradually transformed in part to another component (T_C of 300 °C) which is antiparallel to the parent. This results in a diminishing net J value, and finally a t.r.m. which

is reversed in direction relative to the original. This does not mean that the polarity recorded by the basalt is not the ambient polarity during the initial cooling, but it does mean that under very restricted circumstances a reheating to 300 °C could lead to an irreproducible polarity change. The very limited temperature range involved (figure 3) suggests that such self-reversals are unlikely to be relevant to observed magnetic anomaly patterns. Wasilewski (1968) has detected similar self reversals in some Atlantic and Puerto Rico trench oceanic basalts, which

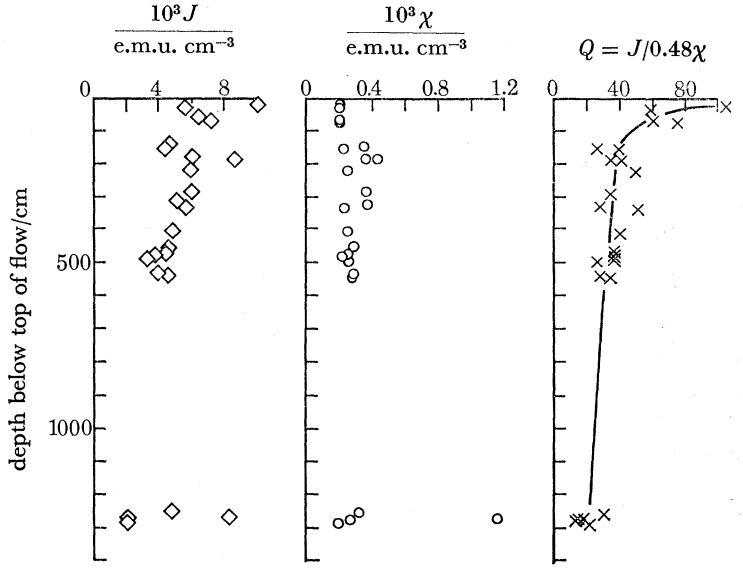

FIGURE 2. Variation of the intensity of magnetization (J); susceptibility (χ); and Q factor with depth in the Mohole test basalt core, taken from west of Baja California in 3568 m of water. After Cox & Doell (1962, figure 4).

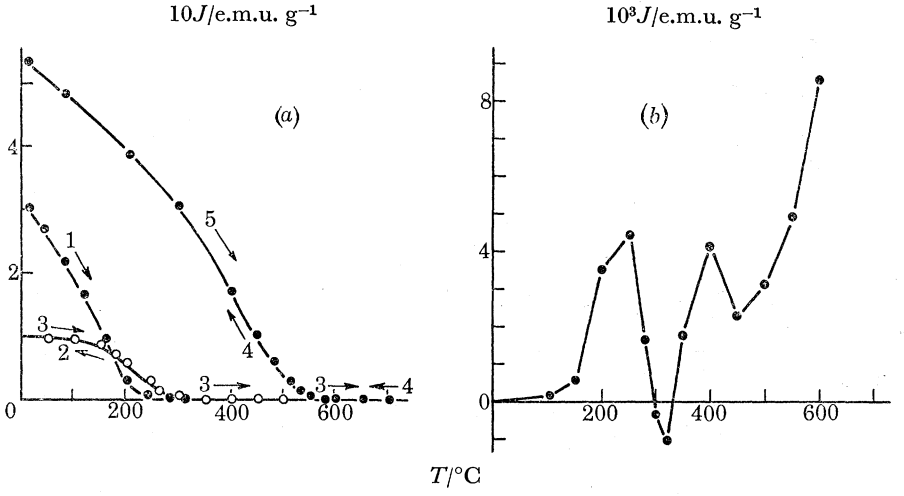

FIGURE 3. Thermomagnetic behaviour of some oceanic basalt from the northwest central Pacific: (*a*) On original heating (1) the Curie point is about 250 °C. After continuing heating to 400 °C, the cooling process (2) results in a *decrease* in the high field intensity of magnetization by a factor of about 3, indicating the development of a new phase with magnetic moment antiparallel to that of the original component. A second heating to above 600 °C (3) yields a Curie point of about 300 °C. Subsequent cooling (4) produces an *increased* high field intensity of magnetization, and a Curie point of about 575° C, which is reproducible on further heating (5). In *b* this behaviour is illustrated for a thermal remanent magnetism acquired by heating in air to various temperatures for ten minutes and cooling: a reversed component is apparent at about 300 to 320 °C. Both figures from Ozima & Ozima (1967).

he believes may be consistent with Verhoogen's (1959) theoretical self reversal mechanism which involves both high temperature of crystallization and rapid cooling. The production of a higher T_C during heating, however, suggests that oxidation is the mechanism occurring.

Carmichael (1970) has made a detailed study of the magnetic properties and opaque mineralogy of submarine igneous rocks from the M.A.R. at 45° N. Figure 4 is taken from his paper. A decrease of J away from the ridge is apparent. Since J_{sat} varies little across the traverse, mineralogical differences cannot account for the high J. To some extent a normal polarity unstable component contributes to the high J. A large range of titanomagnetic oxidation states and grain sizes suggests that some of the specimens examined are not surface (quenched) materials.

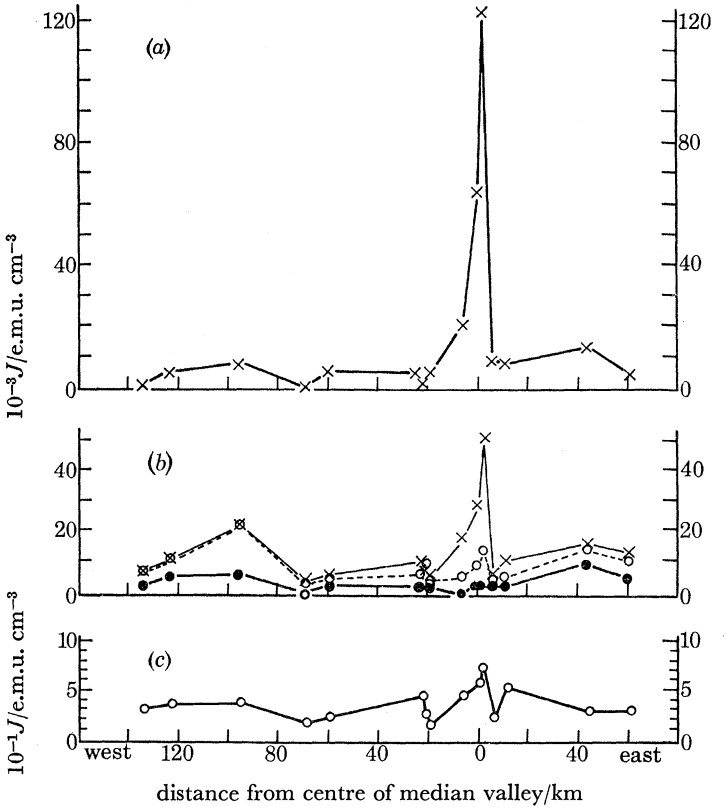

FIGURE 4. Variation of some magnetic properties with distance from the centre of the median valley of the M.A.R at latitude 45° N. From figure 5 of Carmichael (1970). The specimens are fine-grained basalts only. Upper diagram (*a*) shows intensity of magnetization (J) of n.r.m. Middle diagram (*b*) shows the same data normalized to unit palaeointensity (crosses); after demagnetization in $H = 100$ Oe (open circles); and after demagnetization in $H = 200$ Oe. This demonstrates that the high J of diagram (*a*) resides in low coercivity components. Lower diagram (*c*) shows the saturation intensity of magnetization: some slight increase in ferromagnetic content is indicated for the sample with the highest J of n.r.m. (*a*).

By comparing the behaviour of the intensity of the natural remanent magnetism (n.r.m.) on heating to that of a t.r.m. produced artificially in a known field (H) in the same sample over the same temperature range, a measure of the intensity of the geomagnetic field during the initial cooling may result. Such data could conceivably be relevant to oceanic crustal genesis, as well as an understanding of the geomagnetic field behaviour. Ozima *et al.* (1968) have made five measurements of this parameter on oceanic basalt specimens. They show that the geomagnetic field intensity recorded by the samples involved was not appreciably different to the present value. Carmichael (1970) has produced results on his M.A.R. collection showing a

range from 0.3 to 2.0 times the present value. This is similar to results from palaeointensity studies on lava outcropping above sea level (Smith 1967). To some extent, the high J in the younger rocks of Carmichael's traverses is due to a high palaeointensity (figure 4).

Under exceptional circumstances a dredged boulder may possess external features to suggest the top and bottom of the sample. If such samples are from high latitudes (DeBoer, Schilling & Krause 1969) the polarity of the samples is readily determined. It is implied by some authors that such polarity determinations may significantly assist in resolving details of crustal spreading history. Watkins & Richardson (1969) believe, however, that the geological value of such determinations may be very restricted for the reasons discussed below.

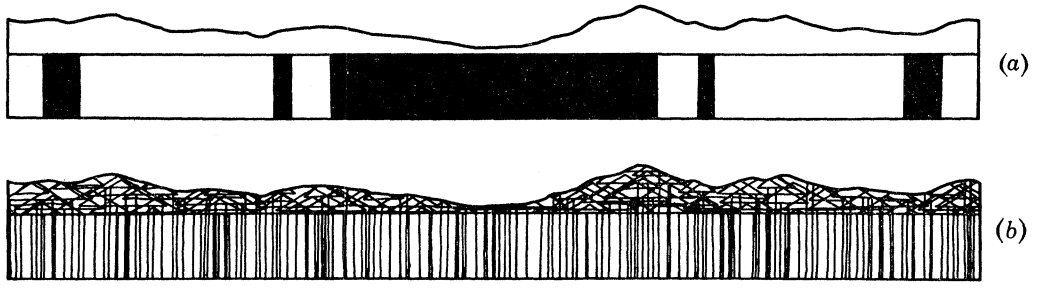

FIGURE 5. West to east bathymetric profile across the M.A.R. at 22.5° N, after van Andel & Bowin (1968), with (*a*) a finite block of normal (black) and reversed (clear) polarity, as used to explain the observed sea-level magnetic profile across the area. The magnetic configuration of this block is most readily explained as the result of repeated dyke injection superimposed on a geomagnetic polarity changes. (*b*) a suggested (Watkins & Richardson 1969) geologically more plausible representation, where the zone between the blocks of (*a*) and the bathymetric profile is filled with material extruded by the dykes forming the blocks of (*a*).

The commonly accepted method of analysis of linear magnetic anomalies is a fitting of the observed anomaly pattern to a finite two-dimensional block. The polarity boundary positions are ideally a linear function of the known geomagnetic polarity history (figure 5*a*). This would appear to be a very reasonable practice in most circumstances. A dyke injection model is envisaged as the actual mechanism, by several authors (figure 5*b*). An intuitive objection to this simple model is the generally ignored magnetic effect of extrusive bodies, which are known to exist. Watkins & Richardson (1969) have investigated the magnetic effect of adding extrusives above a series of dykes which may plausibly constitute the finite horizontal blocks of figure 5*a*. These extrusives would be in the region made available between the blocks and the bathymetric limits (figure 5*b*). Assuming that the dyke and extrusive configuration is as in figure 6*a*, computations (figure 6*b*) show that the effect of adding extrusives is to *sharpen* the linear anomalies (figure 7) for a considerable range of extrusive sizes rather than to smear them as might be expected.

Since such extrusives are certain to overlap with others of opposite polarity (but the essential centre peak of the magnetic anomaly is nevertheless the most probable survivor of such overlapping), it follows that the determination of the polarity of submarine basalt lumps is unlikely to have any meaning in terms of the actual source of the sign of the anomaly (and therefore inferred polarity) at the sea level.

The above conclusion is supported by Cox & Doell's (1962) measurement of the Mohole basalt core, where the palaeomagnetic inclination readily provided a polarity determination. If it is assumed that the host body caused the anomaly then the clearly reversed polarity of the core is incompatible with the observed positive magnetic anomaly at sea level above the test site, the dominant source of which is clearly not the body from which the core was recovered.

Even if no substantial extrusives existed in order to overlap with adjacent opposite polarity anomalies, polarity determinations on dredged or cored rocks will not offer definitive testing of the crustal spreading hypothesis, by comparison with the predicted polarities of Heirtzler *et al.* (1968). This is simply because the predicted polarities are a minimum number: as Vine (1966) pointed out, short duration polarity events even if perfectly recorded in a spreading crust will not be resolved in the sea-level anomaly pattern from which the predictions are made. It would appear that if the predicted polarity were to be found in every appropriate sample, some information on the limits of extrusives could conceivably result; but a conflict with the predicted polarities can have little meaning because of the two available degrees of freedom available in the interpretation.

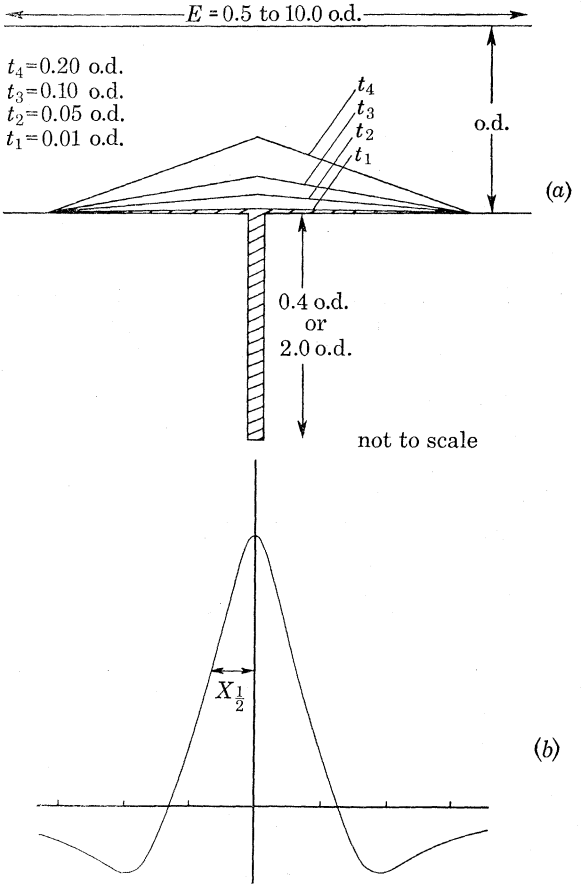

FIGURE 6. (*a*) Idealized model of submarine intrusive–extrusive configuration. Parameters *E*, *t*, and the width and vertical extent of the dyke are generalized being fractions or multiples of the ocean depth (o.d.). (*b*) Diagram illustrating definition of half width of generalized anomaly ($X_{\frac{1}{2}}$) due to any of bodies in (*a*). From Watkins & Richardson (1969).

Because of the above arguments it would therefore seem that polarity determinations on unoriented dredged lumps is of minimum value. In any case, totally reliable polarity determinations are not possible at this stage. Irving (1968) has suggested that since the i.r.m. resulting from the present field will add to normal polarity and subtract from reversed polarity rocks, observation of the n.r.m. during removal of the i.r.m. will essentially reveal the polarity of the host. He specifically proposed that if an anhysteritic remanent magnetism (a.r.m.) is added to the specimen, its removal behaviour will be polarity dependent, although collected samples

which are not definitely *in situ*, having rotated after the initial cooling, will not possess this ideal property. No account was taken of the role of the magnetic mineralogy. Watkins (1967) has shown that a.r.m. is more readily added to low oxidation state and maghaematized titanomagnetites, with the higher oxidation states clearly discriminating against the addition of an a.r.m. It would therefore appear that low oxidation state or maghaemitized titanomagnetites are essential for successful application of Irving's method.

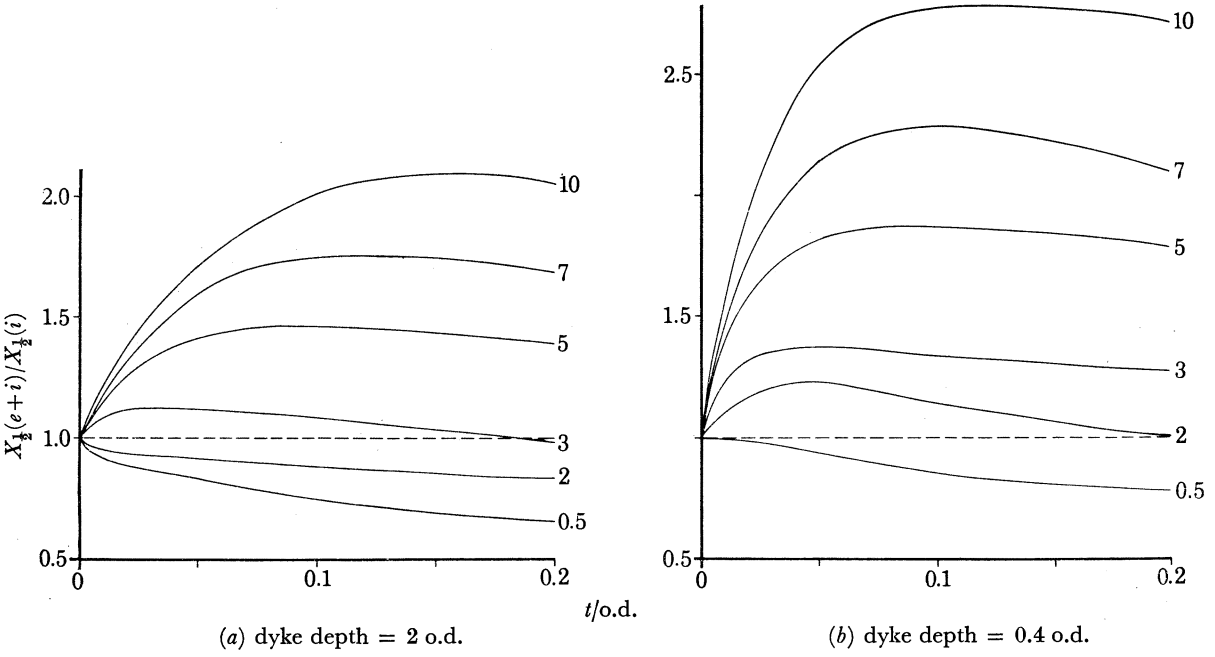

(*a*) dyke depth = 2 o.d. (*b*) dyke depth = 0.4 o.d.

FIGURE 7. Relation between the ratio of $X_{\frac{1}{2}}$ for a dyke alone (i) to $X_{\frac{1}{2}}$ for the dyke with added submarine extrusive (e and i); for various values of E, and t as illustrated in figure 6. The width of the dyke is 0.01 o.d.u. For values of E less than about 2.0 o.d.u. $X_{\frac{1}{2}}$ for the dyke with added idealized extrusive is less than that for the dyke alone.

(*b*) *The petrology and magnetic properties of selected non-submarine rocks*

The number of specimens of submarine rocks (other than basalts) so far studied is obviously too limited for satisfactory generalizations about the magnetic properties of oceanic igneous rocks. This is particularly the case in altered rocks, which may be important as a cause of some oceanic magnetic anomalies. None of the studies so far made, with the exception of the Mohole test basalt core (Cox & Doell 1962) provide any indication of the variation of properties with depth in the crust: inference of magnetic properties for bodies several kilometres thick (as required in crustal spreading analyses of marine magnetic anomalies) by the study of the outer few centimetres of the bodies may not be meaningful, particularly when cooling rate differences with depth are considered. A summary is therefore made of the magnetic properties of some altered igneous rocks, which occur above sea level, but which nevertheless appear relevant to submarine rock properties. We shall not describe the magnetic properties of fresh basalts in general: these are well documented in the literature. Wherever possible we shall include such description as part of the variation of magnetic properties in some of the few single cooling units which have been studied. This will also serve in some cases to demonstrate some relationships between the titanomagnetite oxidation states and magnetic properties.

The processes causing changes in magnetic properties fall naturally into three categories.

These three categories are independent of simple variation in rock type: phonolites are less magnetic than basalts; and acid igneous rocks are of course generally less magnetic than basic rocks. The processes are therefore more significant absolutely in their effect on the more magnetic rocks (the basics and ultrabasics).

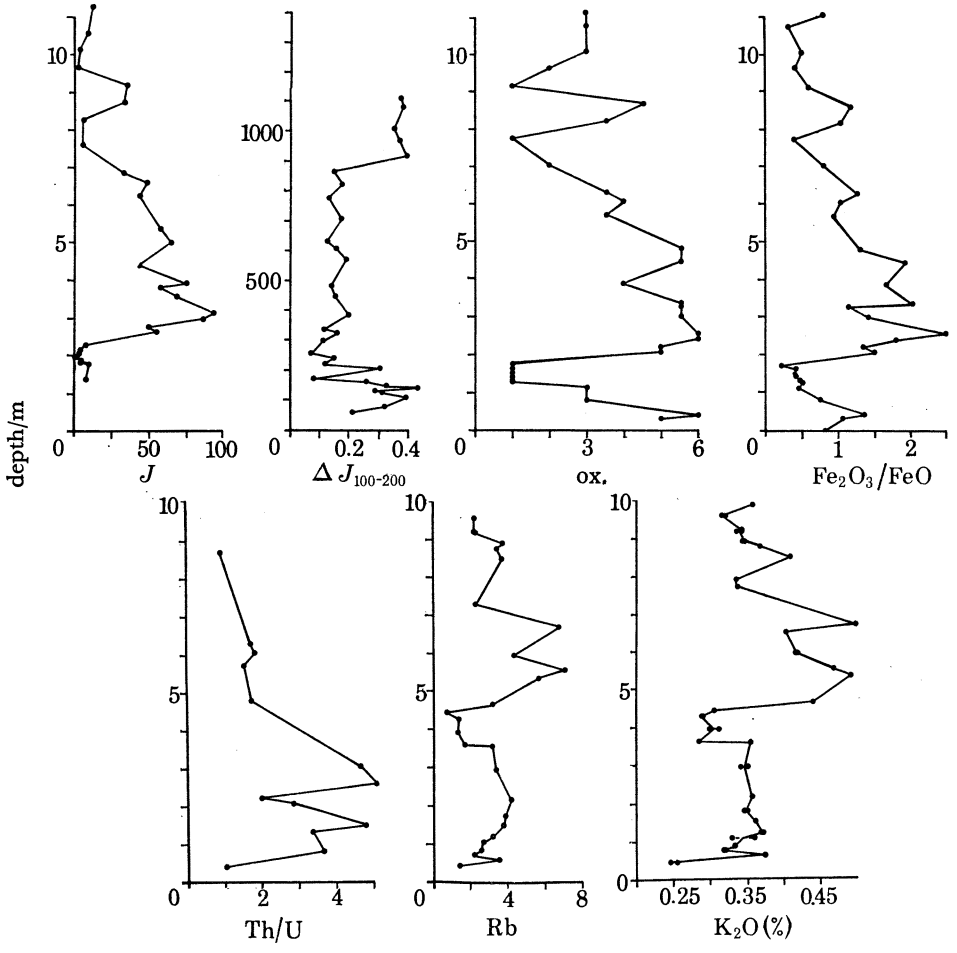

FIGURE 8. Variation of some magnetic, mineralogical, and chemical properties between the upper and lower surfaces of a single 11 m thick Icelandic Lava. J, intensity of magnetization in e.m.u. $g^{-1} \times 10^{-4}$, $\Delta J_{100-200}$ = a measure of the magnetic stability, being the difference between J following demagnetization in alternating magnetic fields of 100 and 200 Oe; ox. = optically defined high temperature titanomagnetite oxidation index (see text for definition); Rb in parts/10^6. For details of all aspects of the data see Watkins & Haggerty (1967) and Watkins *et al.* (1967, 1970*a*).

(i) *Primary cooling processes.* These take place during the initial cooling of the igneous body.

Differentiation has long been recognized as an initial cooling process capable of producing petrological inhomogeneities in single cooling units. The corresponding variation of J and χ in some differentiated dolerite sills in Australia has been described by Jaeger & Joplin (1955), Jaeger & Green (1958), Bull, Irving & Willis (1962) and Kazmi (1961). Rösler (1962) and Clark (1969) have described the magnetic variations in some highly differentiated sills in Thuringia and Oregon, respectively. The former describes an increase in χ by a factor of 30 in the picritic phase of the diabase studied. Beck (1966) has devised a genetic sequence with a J and χ increase resulting from crystal fractionation in some systematically variable diabase sills in Pennsylvania.

Even when megascopic variations are not evident, however, considerable systematic magnetic variations may exist in a single cooling unit. In the case of single lava, the silicate variations accompanying the magnetic change may be only slight or virtually undetectable. The variation of the intensity of magnetization, a function of the coercivity spectra, and the high temperature titanomagnetite oxidation index between the upper and lower surfaces of a single Iceland lava (Watkins & Haggerty 1967) is shown in figure 8. This considerable variation and the interior

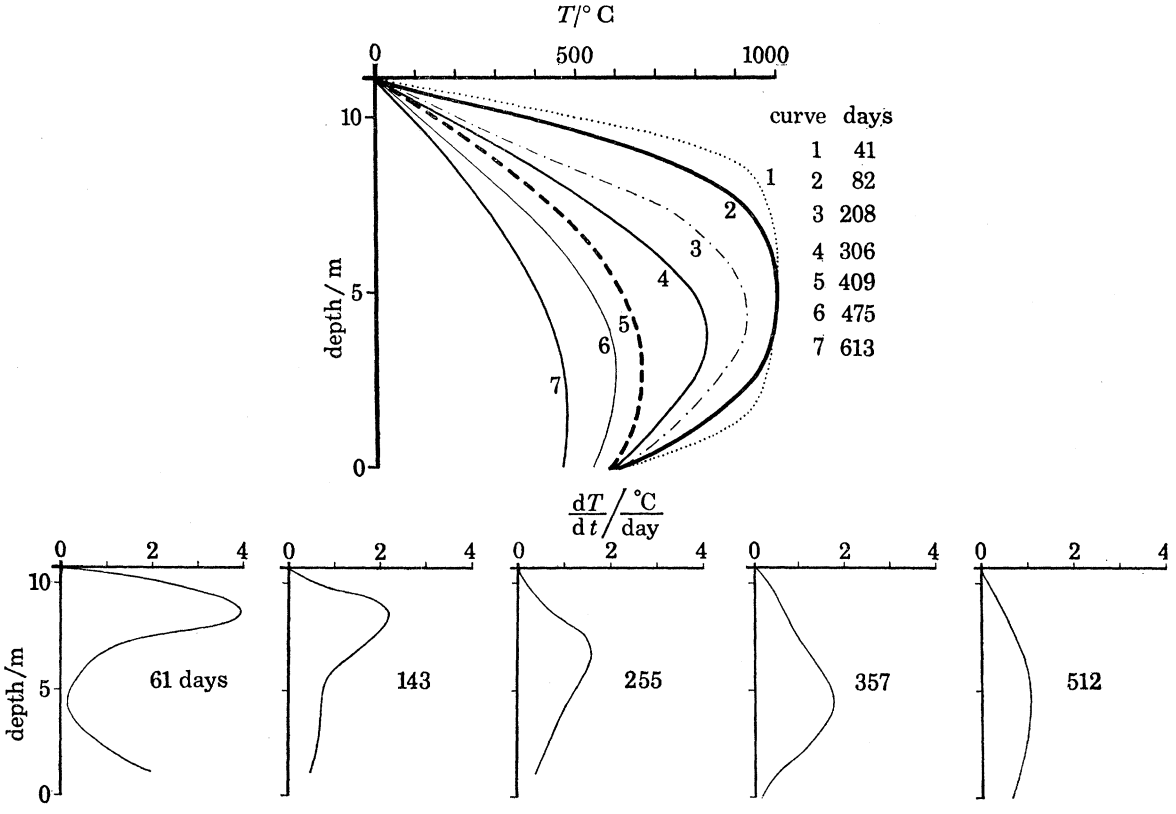

FIGURE 9. Theoretical cooling curves for a single 11 m thick lava (as sampled for the studies summarized in figure 8). Upper curves show the temperature distribution at the given times after the initiation of cooling. Lower series of curves show the variation of the cooling rate in different parts of the lava (°C/day), at the arbitrarily selected times (in days) after the inititation of cooling. Curves calculated using method and constants detailed by Jaeger (1968).

maxima are interpreted to be initial cooling phenomena. In order to emphasize the relation between magnetic and some chemical parameters we include in figure 8 the results of subsequent geochemical analyses from the same body. The Fe_2O_3/FeO results are not surprisingly parallel to the optically defined oxidation index. The Th/U (Watkins, Holmes & Haggerty 1967), which varies by a factor of five, appears to be related to the interior oxidation maxima. The K_2O and Rb variations (Watkins, Gunn & Coy-Yll 1970*a*) are due to other factors. The source of these variations is complex, but the inherent cooling rate variations of different parts of the lava (figure 9) must contribute to the chemical configurations. Such variations exist, of course, in all cooling bodies. Whether or not the actual temperature distribution at a fixed time (figure 9 upper) or the variation of the cooling rate (figure 9 lower) are of equal relevance to the lower temperature products is not known.

By electrochemical means Sato & Wright (1966) have detected a high oxygen fugacity developing during the initial cooling of a modern lava. The high oxidation is accompanied by a marked increase in χ and 'reddening of the olivines'.

Augenheister & Turkowsky (1964) have shown systematic variations and J, Q, and stability (which can be inferred from the scatter of n.r.m. inclination) in a series of cores from 25 separate Vogelsberg basalt lavas. Wilson *et al.* (1968) have recently made another examination of magnetic properties and titanomagnetite grain size and oxidation state across a single lava. In

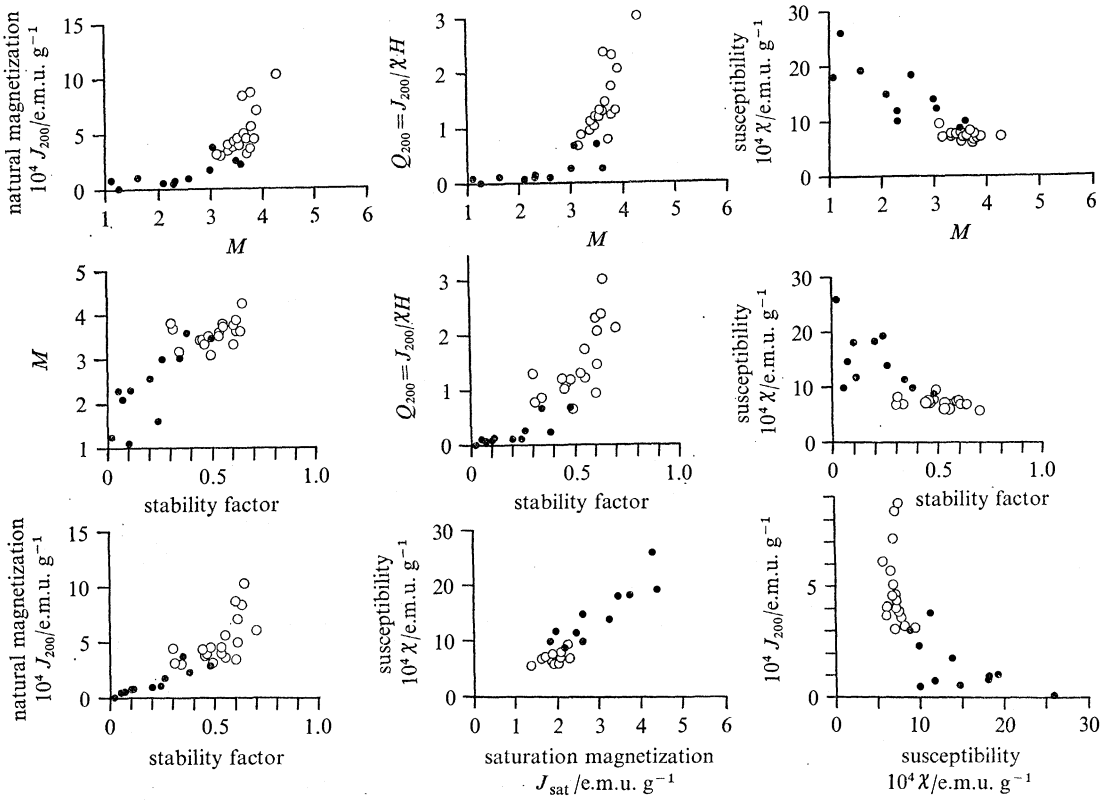

FIGURE 10. Relations between various magnetic parameters which were obtained from a traverse of a single 16 m/thick Icelandic lava (Wilson *et al.* 1968). Left and centre columns show some positive correlations. Right column shows some inverse correlations. ○, Data from the lower one-third of the lava; ●, upper two-thirds of the lava. J_{200}, intensity of magnetization after demagnetization in $H = 200$ Oe; for explanation of M (magnetic oxidation number), J_{sat}, and χ, see text. Stability factor $= R_{200}/R_{200}+r$, where R_{200} is the magnetization remaining after demagnetizing in $H = 200$ Oe; and r is the non-vector sum of the change in magnetization resulting from treatments in $H = 100$ and 200 Oe (if $r \ll R$, as is the case in very stable rocks, then the stability factor approaches unity; whereas if $r > R$, as is the case in very unstable rocks, then the stability factor approaches zero).

this case the lava, of 16.8 m thickness, features both normal and reverse polarity n.r.m., as the result of very variable coercivities superimposed on an original reversed polarity. The relation between the various parameters measured (irrespective of position on the lava) are illustrated in figure 10. Several conclusions emerge:

(1) The stability (expressed as S_{200} in this particular study; see caption of figure 10 for explanation) depends more on oxidation state than on measured grain size. This is probably because increasing oxidation subdivides the grain by creation of lamellae into smaller units, approaching single domain size.

(2) The stability also correlated with J_{200} (which is J after the removal of unstable components by a demagnetizing field of $H = 200$ Oe†) because smaller grains have larger retentivities. The inverse correlation of the stability with χ and J_{sat}, which is dominantly a function of bulk fraction for a given constituent supports the belief that the range in J is a function of effective grain size or oxidation, and not simple bulk content. The oxidation has not produced more magnetic phases, according to the microscopic and T_C analyses.

(3) The range in Q_{200} is due more to a change in J_{200}, than in χ.

(4) The lava examined does not feature any quenched parts, but the variation in titanomagnetite grain size appears to be related to cooling rate (figure 11).

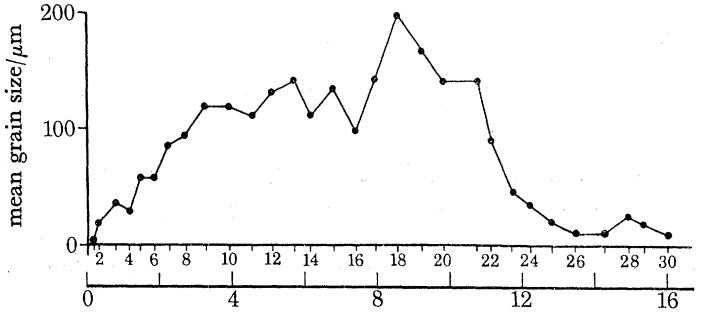

FIGURE 11. Variation of average magnetite grain size (in micrometres) with position between the upper and lower face of a single 16 m thick Icelandic lava. (From Wilson *et al.* 1968).

It is clear that given sufficient time during the initial cooling, considerable magnetic variations can evolve within a single igneous body. It is highly probable that such variations will be found in submarine lavas, if they are large enough to possess equivalent cooling rates.

(ii) *Secondary processes.* These are thought to take place after the initial cooling, but are not always distinguishable from phenomena occurring during the late stages of the initial cooling.

Very low J and Q values have been obtained by Grommé & Gluskoter (1965) from Mesozoic spilites in California. The origin of spilites is both marine and secondary (Amstutz 1968).

Akimoto & Katsura (1960) have shown that low J and low stability in basalts are strongly associated with maghaemitization of the titanomagnetites. Watkins (1967) obtained similar results. Although maghaemitization has been reported to require a temperature as low as 250 °C (Gheith 1952) in the laboratory, it can also result from normal weathering: this is most readily demonstrated by its decrease inward from a weathered surface of some basalts. This may be relevant to Manley's (1956) observation of a very marked decrease of J, χ and Q in the weathered rind of a doleritic boulder, relative to its fresh inner core.

Metamorphism of any type is considered secondary, although normal surface temperatures may in some cases not be approached by the parent material during the initial cooling.

An understanding of the magnetic effect of serpentinization may be very relevant to formulating oceanic genesis models. Mention has already been made of the relevance of the magnetic properties of the Puerto Rico serpentine core (Cox *et al.* 1964) to Hess's (1964, 1966) ideas on oceanic crustal genesis. The observed values of J, χ and Q in this core are plotted as a function of density in figure 12. The density is used because of its relation with degree of serpentinization:

† 1 Oe $\approx$ 79.6 A m^{-1}.

it is well established (see, for example, Barnes, Lamarche & Himmelberg 1967) that serpentinization results in density decrease. The data show an inverse correlation between inferred degree of serpentinization and J, χ and Q. This was confirmed petrographically, by the observation of more magnetite in the less serpentinized rocks. It was this observation which apparently led Hess (1964, 1966) to dismiss serpentinite as a magnetically dominant material in oceanic rocks. Cox *et al.* (1964) also showed an increase in stability with serpentinization. Wagner (1967) made a similar observation: in this case serpentinization and magnetic stability increased with depth in a core. The Puerto Rico serpentinite observations are explained by Cox *et al.* (1964) as follows: the magnetite increases in early stages of serpentinization but is later removed as serpentinization proceeds; so that a peak in the J–density curve at something greater than 2.7 g cm^{-3} should be expected. Hess & Otalora (1964) have commented on this suggestion: they support the concept of a serpentinization: density inverse relation for densities above 2.6 g cm^{-3}, but they point out that serpentinization is complete at $\rho = 2.55$ g cm^{-3}. Any decrease in ρ below this value can only be due to porespace increase and water sorption. With an increase of water, the ferric to ferrous ratio increases, which may in turn change any titanomagnetites present to less magnetic ferric hydrates or limonites.

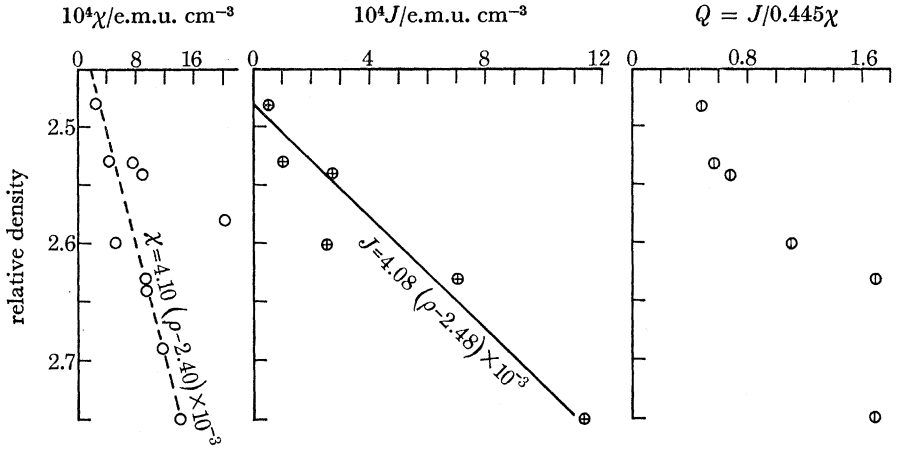

FIGURE 12. Variation of intensity of magnetization (J), susceptibility (χ) and Q factor with relative density in the Mohole serpentinite test core, drilled near Mayaguez, Puerto Rico, in 1962. (From Cox *et al.* 1964.)

This observation of an inverse relation between serpentinization and J is completely at variance with results from the study by Komarov, Moskaleva, Belyayev & Ilyina (1962) of the Kraka Massif, in the Urals. The central and western part of the massif are largely completely unserpentinized ultrabasics (dunites), and are associated with a weak negative aeromagnetic anomaly. The aeromagnetic signature is in fact indistinguishable from those due to adjacent quartz sandstones. In contrast, the margins and east part, composed of serpentine and minor pyroxenite bodies, are associated with strong positive aeromagnetic anomalies. These characteristics are repeated in local late faults and associated serpentinization. Measurement of the magnetic properties of the various petrological types reveal the following facts: the dunite is the most weakly magnetized rock, and J is proportional to the optically defined degree of serpentinization. The table of results is reproduced graphically in figure 13. Komarov *et al.* (1962) believe from these observations that ultrabasics are not significantly magnetic: the magnetization results from metamorphism (serpentinization) which is accompanied by deposition of magnetite.

PHILOSOPHICAL TRANSACTIONS OF THE ROYAL SOCIETY A MATHEMATICAL, PHYSICAL & ENGINEERING SCIENCES

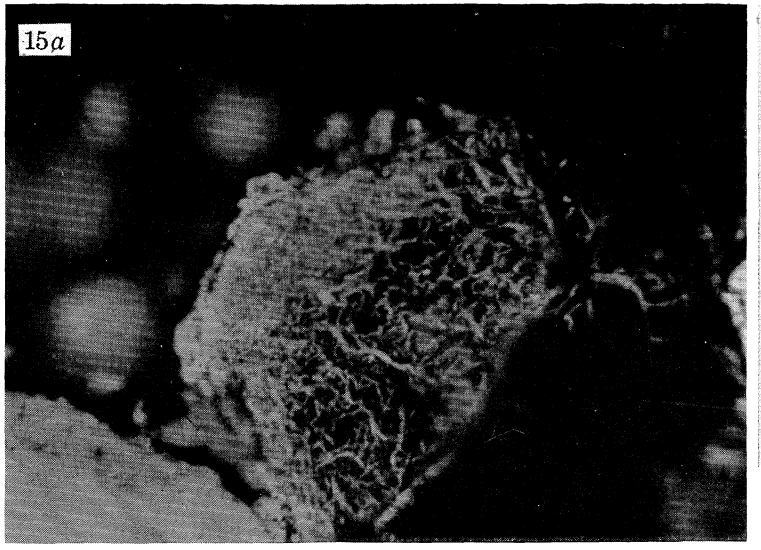

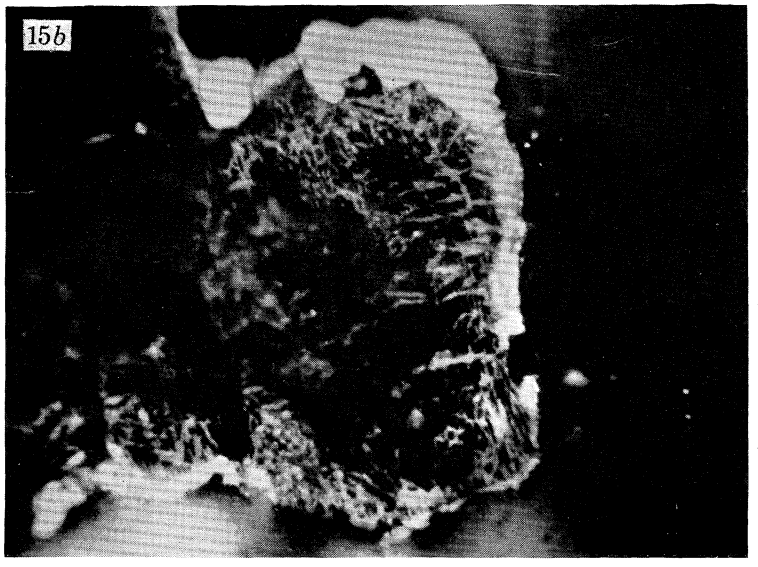

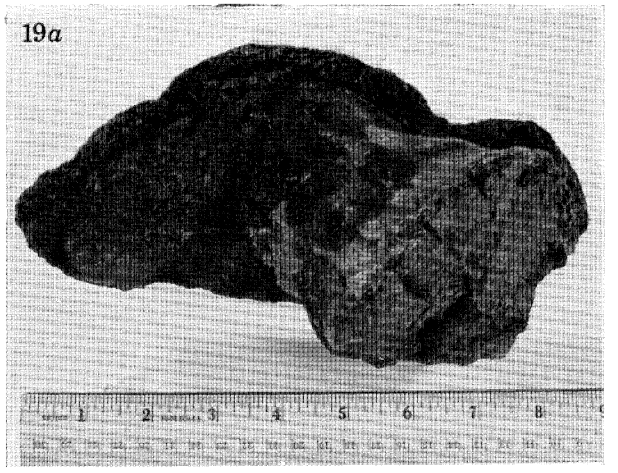

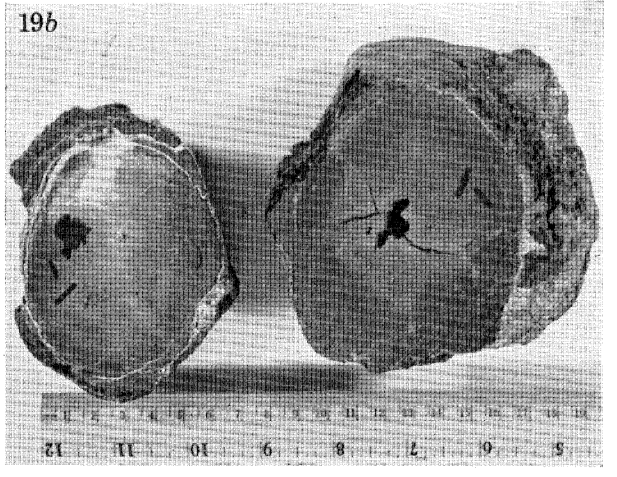

FIGURE 15. Photomicrographs of secondary magnetite and haematite in olivine grains. The magnetite is light grey and has a web-like texture. The haematite increases towards and at the rim of the grains. Conversely, the fraction of magnetite decreases towards the centres of the grains. (From Watkins (1969); field of view 140 μm $\times$ 100 μm.)

FIGURE 19. Photographs of two samples: (*a*) is pahochoe toe E24–15 with a ferromanganese crust from 1.0 to 1.4 cm thick and (*b*) is section through toe E 05–04 showing central cavity and concentric fractures in glass rim, filled with phillipsite.

(*Facing p. 525*)

Watkins & Haggerty (1967) have since shown the marked magnetic effect of oxidation of the olivines in a single lava: figure 14 shows the correlation between J and oxidation index, and J and the fraction of pseudobrookite in the total titanomagnetite fraction. Since pseudobrookite is diagnostic of oxidation index VI the correlation between J and oxidation index

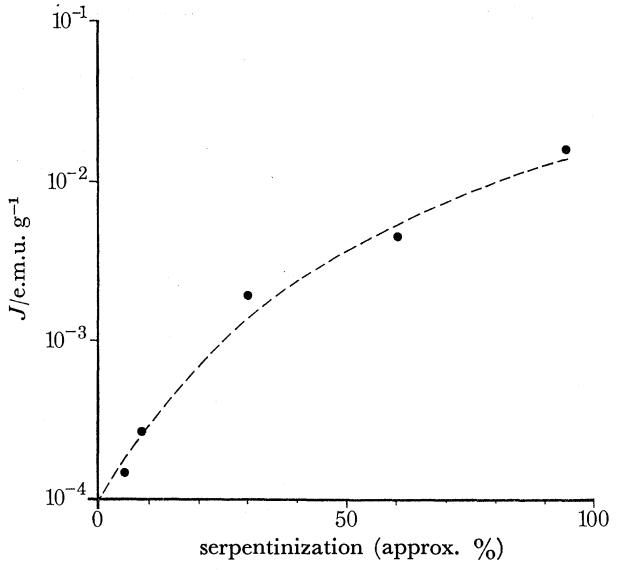

FIGURE 13. Relation between intensity of magnetization (J) and optically defined degree of serpentinization in samples from the Kraka massif (Ural Mountains). (From table 1 of Komarov *et al.* 1962.)

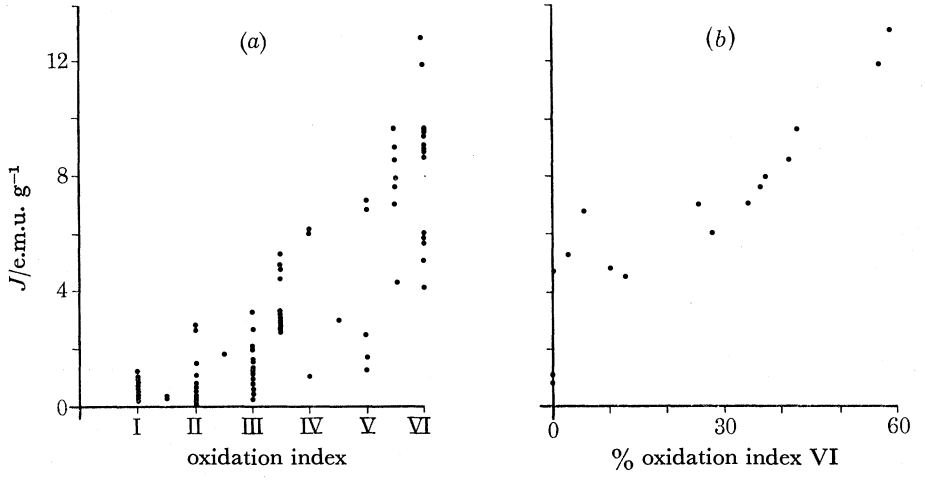

FIGURE 14. Relation between intensity of magnetization (J) and (*a*) optically-defined high temperature titanomagnetic oxidation index for all specimens or (*b*) the percentage of oxidation index VI grains (dominantly pseudobrookite–haematite intergrowths) in the total opaque mineral grains in selected specimens taken from a traverse between the upper and lower surfaces of a single 11 m thick Icelandic lava. (From Watkins & Haggerty 1967.)

(which is unexpected, as oxidation destroys primary magnetite, pseudobrookite being diamagnetic) is explained by production of magnetite in the olivines at high oxidation states. Photomicrographs of such magnetite in olivines are shown in figure 15, plate 7. It would appear that serpentinization can occur during the initial cooling of a simple extrusive basalt. The term 'serpentinization' is clearly in need of finer definition. The use of density and magnetic measurements may assist in this.

Komarov (1962) also believes the following about the magnetic effects of secondary processes, as detailed in a discussion about the suitability of ultrabasics for paleomagnetic study:

(1) Pyroxenites (particularly the monoclinic types) are the most stable ultrabasics, and are therefore most suitable, if study of the original magnetic state is desired.

(2) Ultrabasics containing olivine (and this is the overwhelming majority of ultrabasics) are always serpentinized to some extent.

(3) The magnetic effect of serpentinization must vary depending which is the dominant end member—forsterite or fayalite.

(4) Dunite as a rule does not contain primary magnetite, since olivine (in contrast with pyroxene) is generally non-magnetic. Therefore the J of a dunite, peridotite, or pyroxenite will be proportional to the amount of pyroxene contained, as well as the degree of serpentinization. Unaltered dunites (except for the sideronitic variety) are virtually non-magnetic, whereas peridotite and pyroxenites are strongly magnetic. If hydrothermal metamorphism is superimposed on a primary serpentinized ultrabasic, the magnetite could be removed: a deeply serpentinized body *could* be non-magnetic (in contrast to Komarov's result shown in figure 11).

Some of the details of Komarov's (1962) observations are certainly debatable but they are very consistent with his observed field relationships and aeromagnetic data. The discrepancy between the observations of Cox *et al.* (1964) in figure 12, and those of Komarov *et al.* (1962) in figure 13 could be due to the respective serpentinites coming from totally different density rocks. Might the Kraka massif be high density (early stages of serpentinization)? It appears unlikely, according to the ordinate of figure 13. Perhaps the Kraka massif is a richly fayalitic olivine? Whatever the answer, further work on the magnetic effect of serpentinization is clearly appropriate: the possibility of some significant oceanic anomalies being due to serpentinization cannot be dismissed.

(iii) *Spontaneous processes*. These are magnetic changes which take place simply as a function of time. This is most readily envisaged as domain wall movement under the influence of the Earth's magnetic field, but more significantly, as a result of the internal demagnetizing fields. Konigsberger (1938) compared the n.r.m. and artificially induced t.r.m. in a series of igneous rocks. The results, showing that the J of n.r.m. $<$ J of t.r.m., led Konigsberger to suspect the existence of a spontaneous demagnetization with time. Thellier's (1959) suggestion of a weaker past geomagnetic field intensity causing the observations is not supported by recent palaeointensity data (Smith 1967) which show a varying palaeo-intensity from less than to more than the present value.

Komarov (1962) cites six independent examples to support his belief that Q and age are inversely related, in reply to Mikailova's (1961) refutation of his idea, in which she cites observation of the variation of Q by a factor of 15 in a single body of mixed gabbro and pyroxenite. The result shown in figure 10 supports Mikhailova's argument, it is far from impossible, however, that given normalized petrology, Q and J may be subject to a decay rate (Muratov 1964). Nagata (1961) has speculated on the relaxation time involved: if the decay rate is expressed as $J_t = J_0 e^{-\alpha t}$, where J_0 = the original J value, t = age of the rock, and α = the decay coefficient, Nagata shows that as J/J_0 has been observed to be about 0.6 to 0.7 for t of about 10^5 years, and about 0.1 for 10^8 years, then $\alpha = 10^{-16}$.

Carmichael's (1970) data, shown in figure 4 as a traverse across the M.A.R. are relevant to the spontaneous demagnetization process. A high palaeointensity may explain in part the peak of J at the ridge axis, where the youngest materials are found. The crustal spreading model

requirements and the radiometric and fission-track data which Carmichael quotes show that older rocks flank the central rift. The lower J (figure 4) is equivalent to a demagnetization by $H = 100$ Oe for rocks of a few hundred thousand years age, according to Carmichael. The change in J is greater than Nagata suggests in his analysis. Perhaps weathering of the Mid-Atlantic rocks has contributed to the steep change of J with age over the ridge.

In this sort of study, the problem arises as to which part of a given sample is used for such a comparison? If an 'average value' for a submarine sample is suggested, how many specimens must come from the sample?

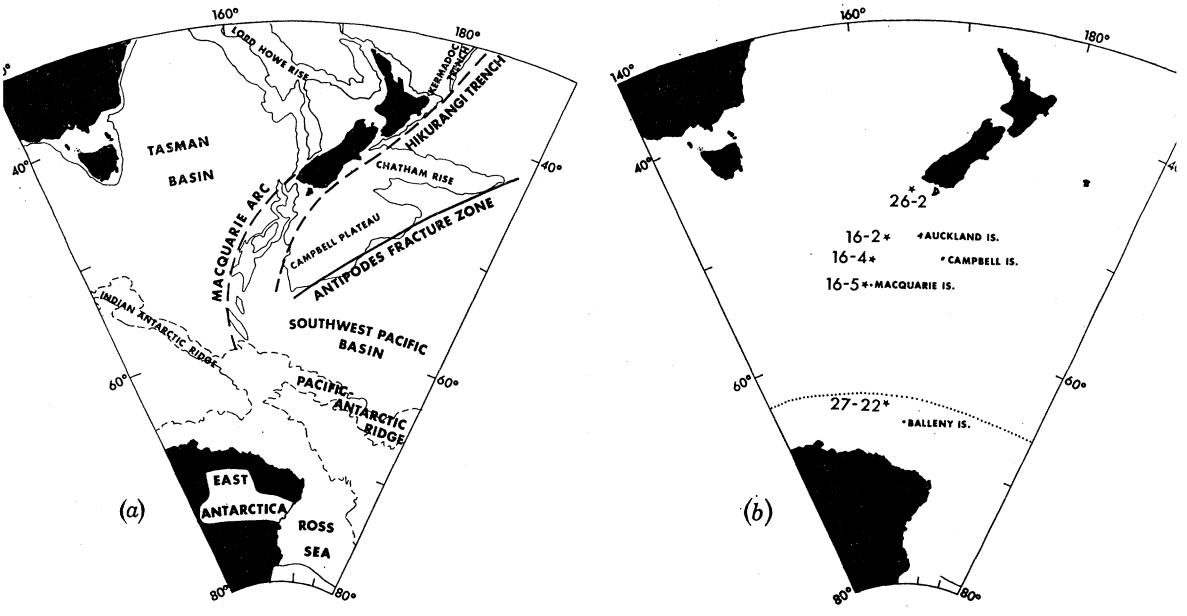

FIGURE 16. Map showing (left) location of the Macquarie Ridge and the adjacent major physiographic features and (right) location and numbers of dredge hauls.

NEW RESULTS

(a) *Dredged rocks from the Macquarie Ridge*

Figure 16 shows the location of dredged samples recovered from the Macquarie Ridge, during cruises of the U.S.N.S. *Eltanin*.

The geolo gy of Macquarie Island has recently been reviewed by Varne, Glee & Quilty (1969) They draw attention to the NW to SE linearity of the outcrops of harzbergites and basalts, implying a possible connexion between this geological configuration and sources of linear marine magnetic anomalies. Summerhayes (1969) has reviewed the known geology of the Macquarie Ridge, its islands, and adjacent regions. There have been recent speculations on the genesis of the ridge: it is thought to be an island arc by some (Cullen 1967), and a line of under-thrusting by others (Banghar & Sykes 1969). A strong normal magnetic anomaly marks the axis of the ridge over its northern half (Hatherton 1967).

Cores of 2.5 cm diameter were drilled from each of the recovered samples which were considered to be *in situ*. Only five such samples were recovered, most specimens being probably ice-rafted. These were sliced into specimens of 2.2 cm length for magnetic analyses, and later chemical analyses, the full details of which will be presented elsewhere (Watkins & Gunn 1970). Spinner magnetometers, a four-axis alternating field demagnetizing unit, and a 300 Hz susceptibility

bridge (Collinson, Molyneux & Stone 1963) were used to measure the magnetic parameters. Chemical analyses were made using a Phillips 1220 kV X-ray fluorescence spectrometer. The results, together with the normative petrological results are summarized in table 2.

TABLE 2. MAGNETIC PROPERTIES AND NORMATIVE PETROLOGICAL IDENTIFICATION OF DREDGED ROCKS FROM THE MACQUARIE RIDGE

specimen number	normative petrology	$10^4 J$ e.m.u. g^{-1}	$10^4 \chi$ c.g.s.	Q	J_{200}/J_0
E16–2 (3)	tholeiitic basalt	0.016	0.008	4.11	0.76
E16–2 (7)	harzburgite	16.60	4.710	7.03	0.35
E16–4 (1)	harzburgite	19.80	3.630	10.92	0.46
E 16–5 (1)	sodic olivine gabbro	12.60	1.430	17.61	0.85
E16–5 (2)	troctolite	7.30	3.390	4.30	0.71

For location of dredge hauls see figure 16. E16 refers to *Eltanin* cruise 16; 2, 4, or 5 refers to dredge station number; the number in brackets is our arbitrary sample number. The normative petrological identification is due to Watkins & Gunn (1970). J, intensity of magnetization; χ, mass susceptibility; $Q = J/\chi H$ where $H = 0.5$ G. J_{200}/J_0 = ratio of J after demagnetization treatment in alternating magnetic field of 200 Oe to J of n.r.m. Samples from other sites shown on figure 16 were considered to be ice-rafted.

The limited nature of the collection allows only minimal speculation about their meaning: the harzbergite, which we believe to be *in situ*, is clearly sufficiently magnetic to be considered as a potential source of strong magnetic anomalies over its parent body. This could be the axis of the Macquarie Ridge: speculations on the genesis of the Ridge and its magnetic signature (Hatherton 1967) are consistent with this possibility. The data from the other samples are less readily associated with the limited known geology of the Macquarie Ridge, but can be incorporated into models. There is clearly a need for more such data from this area.

(*b*) *Spilites from St Thomas, Virgin Islands*

The Lower Cretaceous spilites of the island of St Thomas have been well described by Donnolly (1959, 1960). There would appear to be little doubt of their submarine origin.

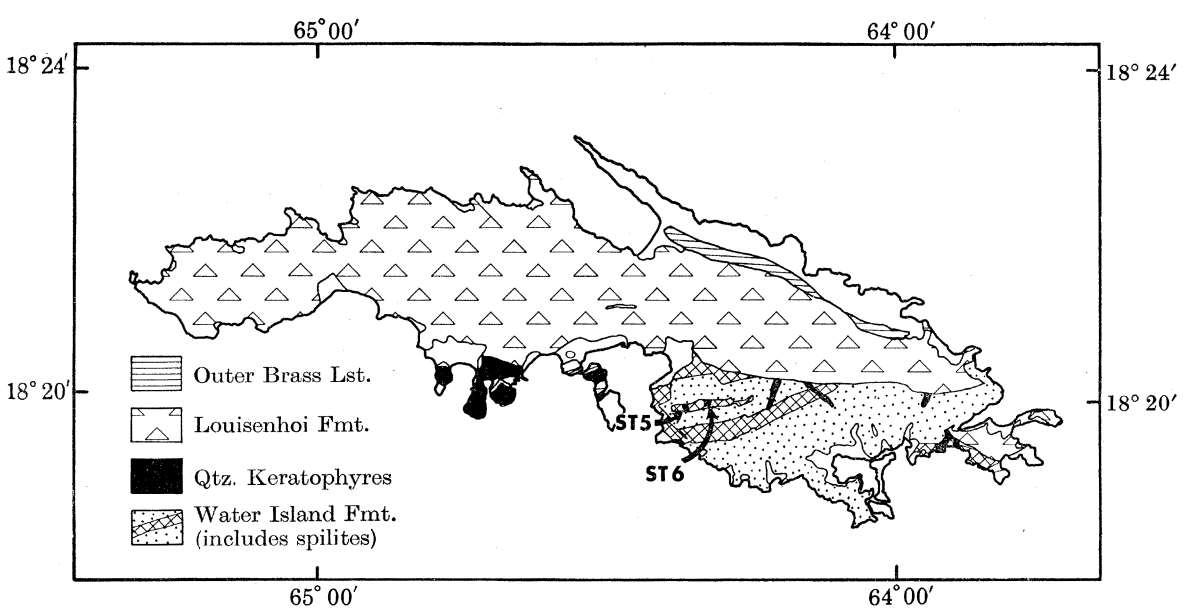

FIGURE 17. Geological map of St Thomas, Virgin Islands, showing location of two sampled spilite bodies (table 3). (Map after Connolly 1959).

Figure 17 shows the location of two of the spilite bodies, recently sampled by Watkins & Richardson as part of an attempted palaeomagnetic survey of the island. Speculations on the tectonic history of the Lesser Antilles are highly amenable to palaeomagnetic testing.

The bodies were sampled using a portable petrol-powered drill. The cores were oriented geographically *in situ* to an accuracy of 2°. The laboratory magnetic measurements utilized spinner magnetometers, a four-axis demagnetizing apparatus, and a 300 Hz susceptibility bridge. The results are presented in table 3.

TABLE 3. MAGNETIC PROPERTIES OF SPILITES FROM ST THOMAS, VIRGIN ISLANDS

specimen number	$10^4 J$ e.m.u. g^{-1}	$10^4 \chi$ c.g.s.	Q
ST 05–01	0.003	0.750	0.088
ST 05–02	0.004	0.067	0.121
ST 05–03	0.008	0.071	0.233
ST 05–04	0.020	0.870	0.047
ST 06–01	0.010	0.084	0.238
ST 06–02	0.002	0.011	0.399
ST 06–03	0.005	0.071	0.141
ST 06–04	0.020	1.005	0.040

For specimen location, see figure 17. 5 or 6 body number; 1 to 4 is core number. J, χ, Q as in table 2.

It can be seen that the St Thomas spilites, the petrological classification of which is undoubted are characterized by very low values of J, χ, and Q. In addition, the palaeomagnetic directions are scattered. The results of thermal demagnetization experiments, which were undertaken in order to attempt removal of any thermal overprint of an original t.r.m., were negative. It is clear that no trace of any original consistent t.r.m. remains in these rocks. The spilitization process would appear to be magnetically destructive, and therefore low magnetic anomalies may be characteristic of surveys over spilitized bodies.

(*c*) *Dredged pillow basalts from the South Pacific*

The location of eight submarine pillow basalt samples which were used for this study are shown in figure 18. They are all taken from the U.S.N.S. *Eltanin* collection, which is now stored at the Smithsonian Institute, Washington, D.C. The exact dredge locations, water depths and other data are included in table 4.

The samples range in size from 10 to 40 cm maximum dimension. Two are shown in figure 19, plate 7. Their shapes and chilled outer margins, as well as local sea-bottom photographs and available physiographic data convince us that the eight specimens are not ice-rafted. The largest sample (E05-05) is from the flank of a seamount in the Drake Passage.

(i) *Experimental methods and results*

Cores up to 30 cm length and 2.5 cm diameter have been drilled from each boulder sample, to provide a cross-section of each sample. These cores yield a total of 100 specimens of 2.2 cm length. The distribution of the specimens in each core and the nomenclature is summarized in figure 20.

(1) *Magnetic properties*. The specimens were all subjected to progressive demagnetization in alternating magnetic fields of up to 800 Oe peak, at intervals as small as 50 Oe, as well as measurement of the direction and magnitude of J, and the χ values, using the methods described earlier.

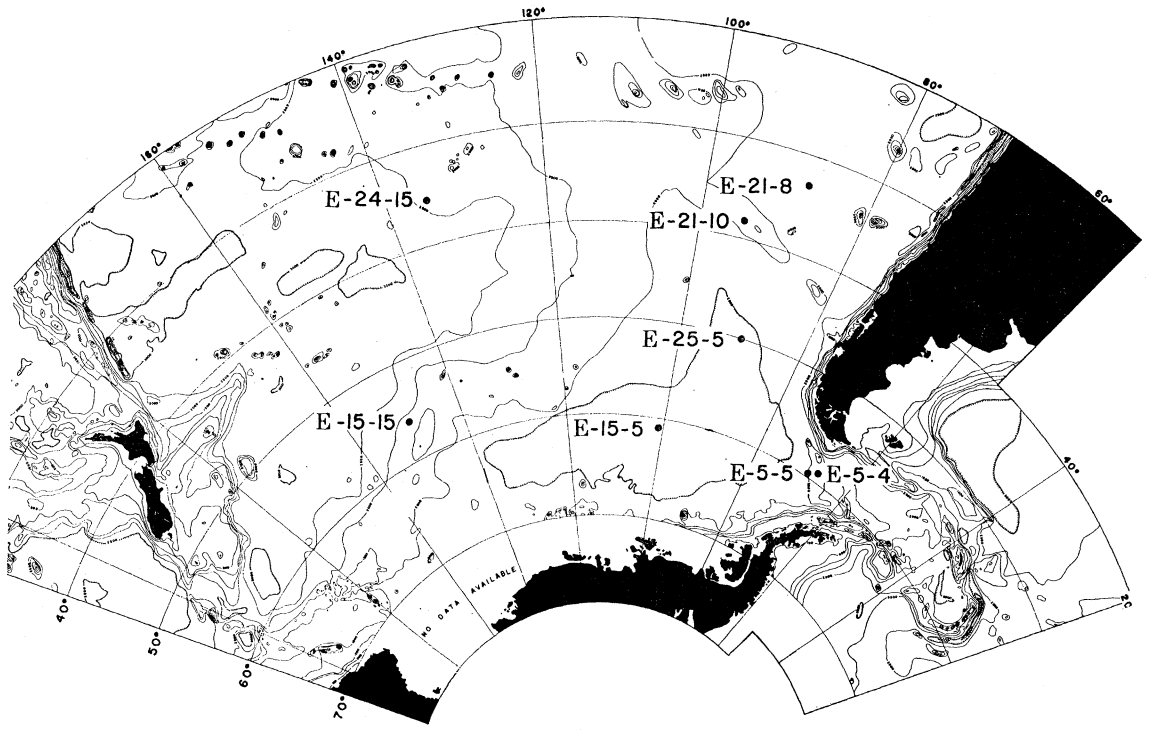

FIGURE 18. Map showing location and numbers of selected pillow basalts dredged from U.S.N.S. *Eltanin*. Bathymetry contours are at 500 fathom intervals.

TABLE 4. DETAILS OF SAMPLE SITES FOR THE SELECTED *ELTANIN* DREDGED BASALTS

sample number	location		water depth	remarks on sea-bottom relief
	lat. (°S)	long. (°W)	m	
E 05–04	59° 02′	67° 15′	3475	Scotia Ridge, 180 m relief
E 05–05	59° 45.5′	68″ 50′	1372	north slope of an unnamed seamount
E 15–05	61° 06′	104° 58′	4828	flat
E 15–15	56° 02′	149° 40.9′	3256	abyssal hills; 390 m relief
E 21–8	32° 58′	87° 59′	3621	rolling terrain; 55–70 m relief
E 21–10	37° 17′	94° 39′	3292	rugged hills on crest of Chile Rise; 550 m relief
E 24–15	35° 58′	134° 50′	4682	undulating; 20 to 90 m relief
E 25–05	49° 57′	89° 59′	4280	undulating; 550 m relief

The coercivity spectrum is obtained for each sample by the demagnetization treatment. Figure 21 shows three typical results. The slope of the curves are clearly a measure of the coercivity, or the capacity of the rock specimen to withstand demagnetization. The sign of the slope is seen to reverse in figure 21*c* where a high coercivity component is evident. Various functions of these J/J_0: H curves can be employed to express the magnitude of this high coercivity component. For example, $[(J_{300}+J_{350})/2-J_{250}]$ will be positive if a significantly higher coercivity component is present, but negative if it is not.

All magnetic results are presented graphically in figures 22*a* to 22*p*. There are no variations in polarity within each boulder: there are apparently no self reversals present. Directions of n.r.m. change very little in demagnetization.

(2) *Silicate petrology*. The polished thin sections were cut parallel to the cooling surface have been used for conventional transmitted light examination of the silicate mineralogy and petrology.

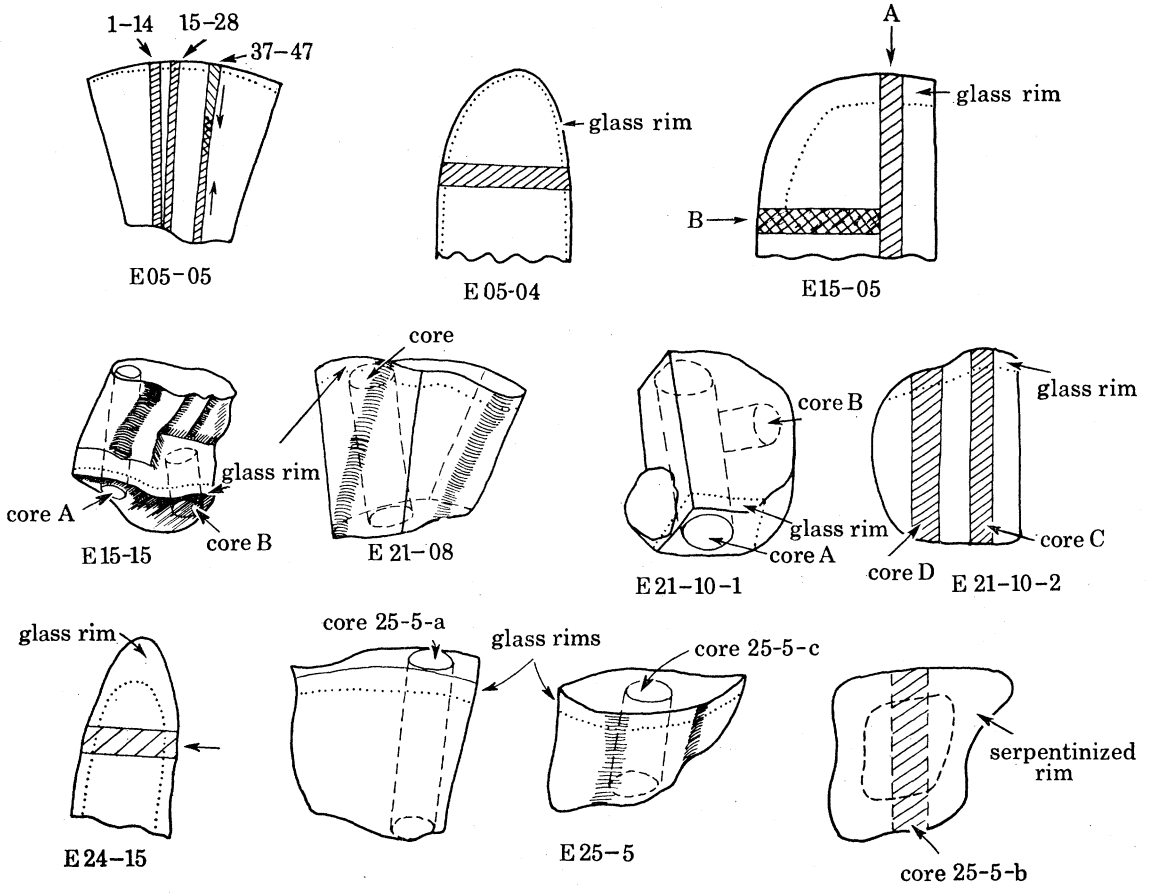

FIGURE 20. Diagrams showing the relation between specimens and sample surfaces in the studied samples of the *Eltanin* collection. In sample E 05–05, specimens 1–14 are in core 1; 15–28 in core 2; 29–36 in core 4, and 37–47 in core 3.

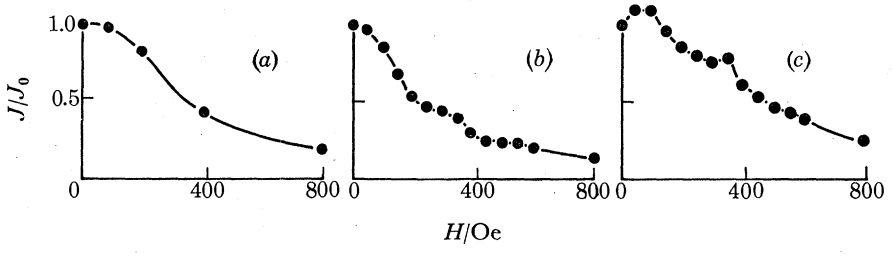

FIGURE 21. Three selected coercivity spectra from the *Eltanin* specimens, illustrating the different types of spectra: (*a*) shows a stable apparently single phase mineralogy; (*b*) shows a less stable component and a slight indication of a higher coercivity component; (*c*) shows an increase of J on demagnetizing (consistent with an antiparallel unstable phase) and a higher coercivity component. Sample (*a*) is specimen 11 from E 05–05 (1), sample (*b*) is specimen 37, and sample (*c*) is specimen 44, both from E 05–05 (4). J = intensity of magnetization after application of H; J_0 = original (untreated) intensity of magnetization. For specimen locations, see figure 20.

As figure 22 readily shows, the samples are characterized by changes in texture from the outer rim to the interior. In general, each sample exhibits the following textural sequence going from the outer rim to the centre: beneath a relatively thin manganese coating, an outer rim of hydrated glass gives way to unhydrated glass. This is succeeded by a variolitic zone. In the

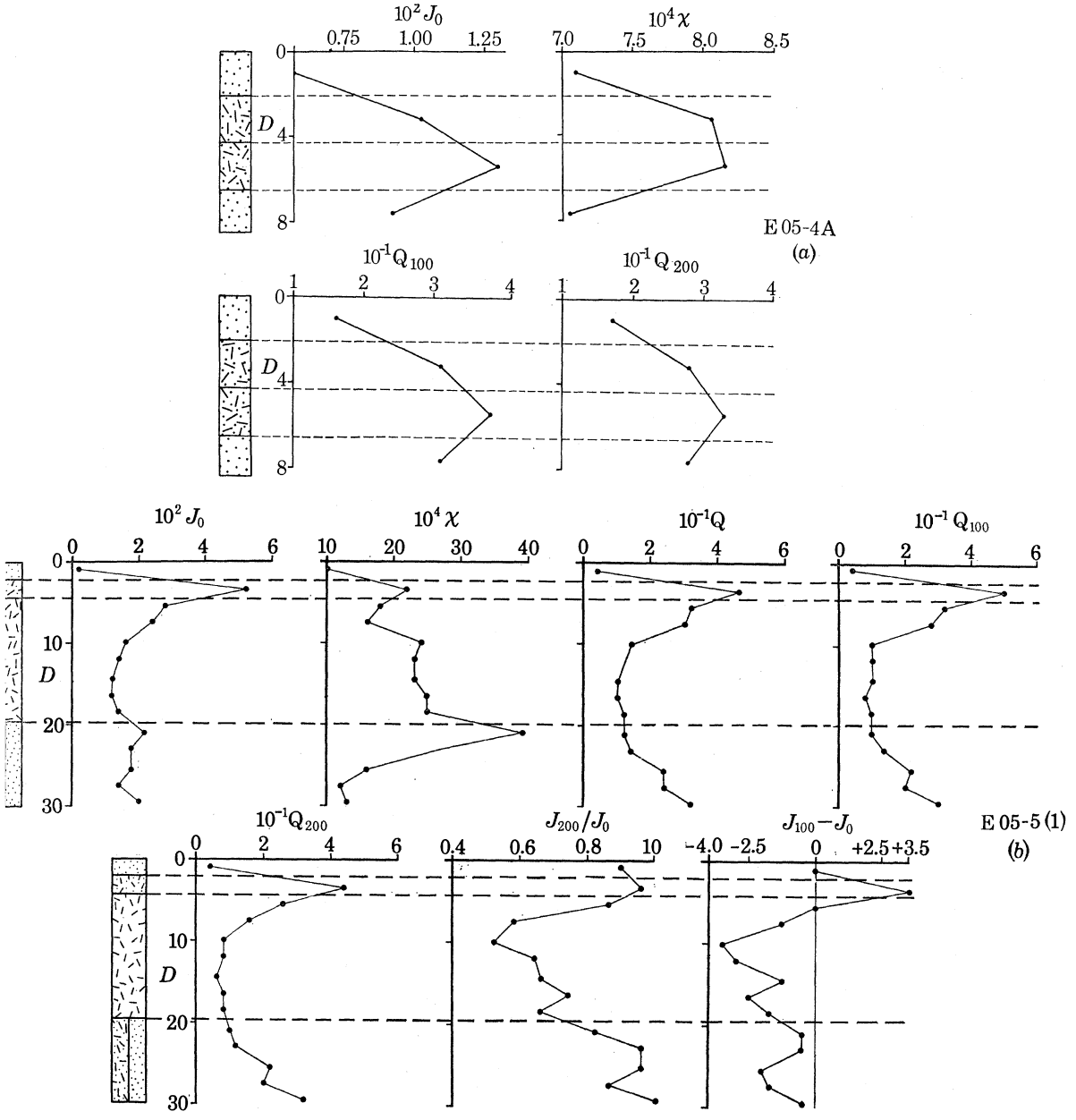

FIGURES 22*a* to 22*p*. Illustrations showing the variations of some magnetic properties with distance (D) from the outer glass edge of the dredged body. D is in cm. J_0, original (untreated) intensity of magnetization in e.m.u. g^{-1}; χ, mass susceptibility; Q, ratio of remanent to induced magnetism so that $Q = J_0/\chi H$ where H is the present ambient magnetic field intensity; J_x, intensity of magnetic field following demagnetization treatment in alternating magnetic field of x oersteds, $Q_x = J_x/\chi H$. Various functions of J_x are shown. These should be compared with figure 21, in order to understand their purpose, which in some cases includes graphical emphasis of the existence of high coercivity components. At the left of most diagrams are some graphically represented petrographic data; dots are glassy texture; dots and dashes are variolitic texture; dashes alone are aphanitic texture; solid black in a column indicates serpentinization of the given textural type; diagonal lines in column indicate chloritization.

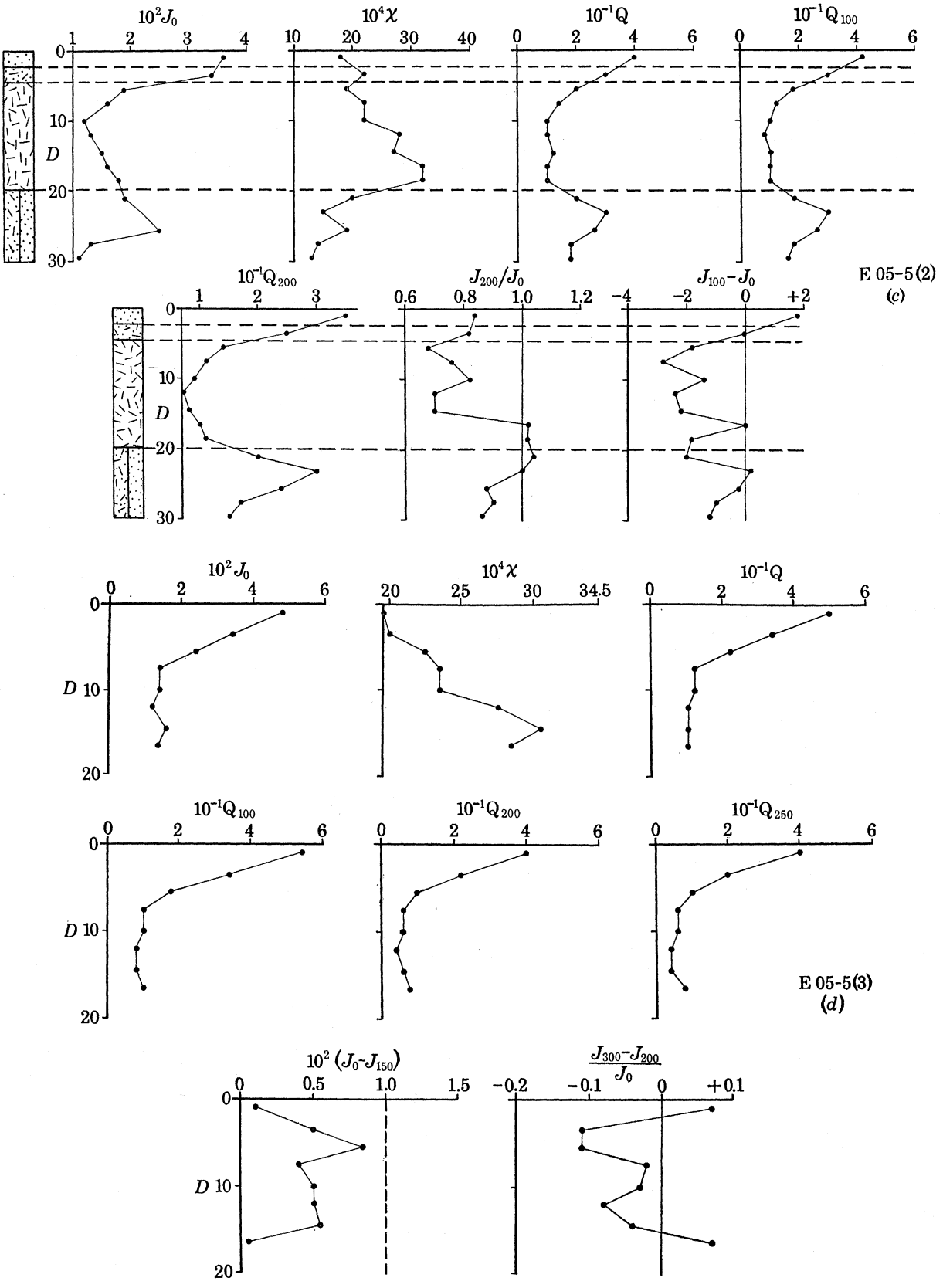

FIGURE 22 (*c*) and (*d*). For legend see facing page.

PHILOSOPHICAL TRANSACTIONS OF THE ROYAL SOCIETY A MATHEMATICAL, PHYSICAL & ENGINEERING SCIENCES

larger samples the interior is aphanitic. Figure 23, plate 8, shows the sequence diagramatically. The sequence is similar to the one in samples described by Moore (1966). His samples are generally smaller than ours.

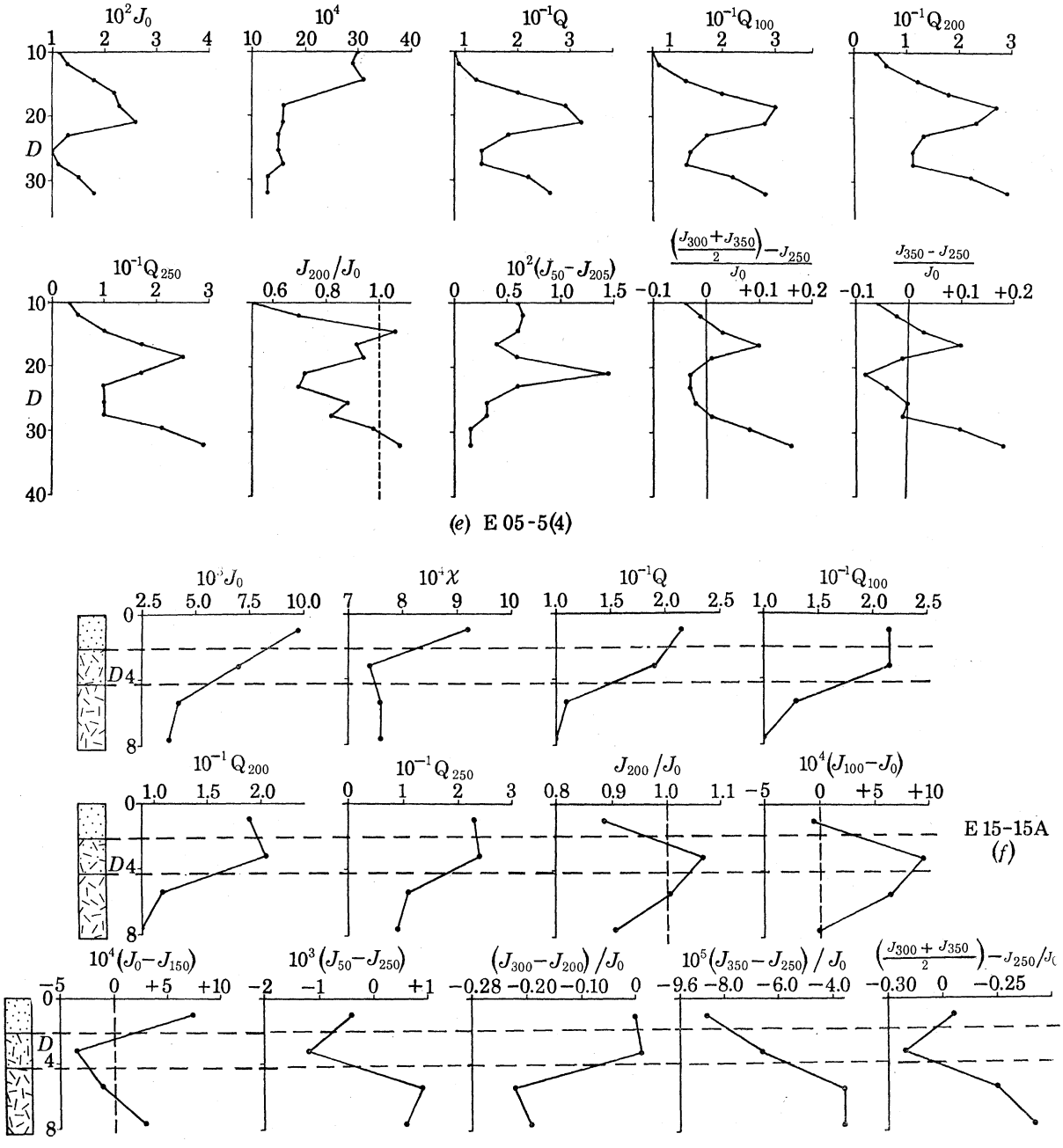

FIGURE 22 (*e*) and (*f*). For legend see p. 532.

In detail, this simple sequence is somewhat diversified. The clear glass zone often contains fibrous microlites with finely dispersed 'opaque dust' nucleating on phenocrysts of plagioclase and olivine (figure 24, plate 9). The variolitic zone consisting of subparallel fibres of clinopyroxene in polygonal units, is generally light brown in colour due to an increasing fraction of

titanomagnetite. The dispersed opaque dust of the glassy zone gives way to discrete skeletal grains which are less dispersed (and less in number), and which segregate at the peripheries of varioles (figure 25, plate 9). When present, the aphanitic interiors have patches of variolites (figure 25, plate 9). When present, the aphanitic interiors have patches of variolitic texture remaining, but plagioclase microlites and small clinopyroxene crystals are more common (figure 26, plate 9). The fibrous appearance and the parallelism of the feldspar phenocrysts with the pillow surface in the variolitic zone is far less apparent or absent in the aphanitic interiors.

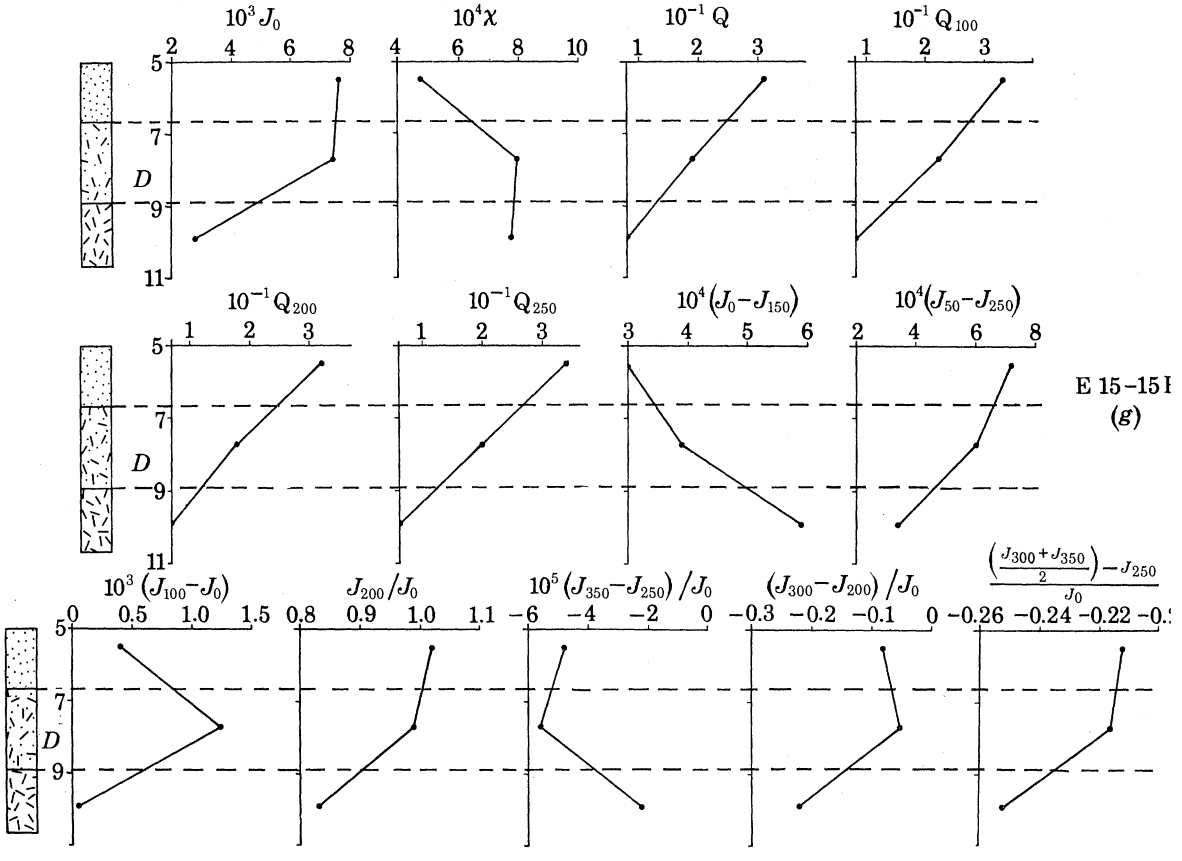

FIGURE 22 (*g*). For legend see p. 532.

Figure 27, plate 9, shows a thin section which includes all three major textures.

Deuteric minerals are very commonly recognized in submarine basalts: a few of the main examples are serpentine and haematite (Quon & Ehlers 1963); serpentinized oxides (Engel & Engel 1963); spongy iron hydroxide (Shand 1949); and serpentinized olivine and haematite (Poldervaart & Green 1965). In one pillow lava pile, Cann (1969) has recognized chloritized basalt, albitized basalt, augite replaced by actinolite, and iron oxide replaced by sphene. Kawai & Kang (1961) believe that submarine volcanism may be a common cause of maghaemitized basalts.

Alteration products in our eight samples constitute only about 2% by volume, except in E 05–05 and E 25–05 which contain up to 8% by volume of deuteric alterations. Two major alteration products are recognized: chloritization and serpentinization.

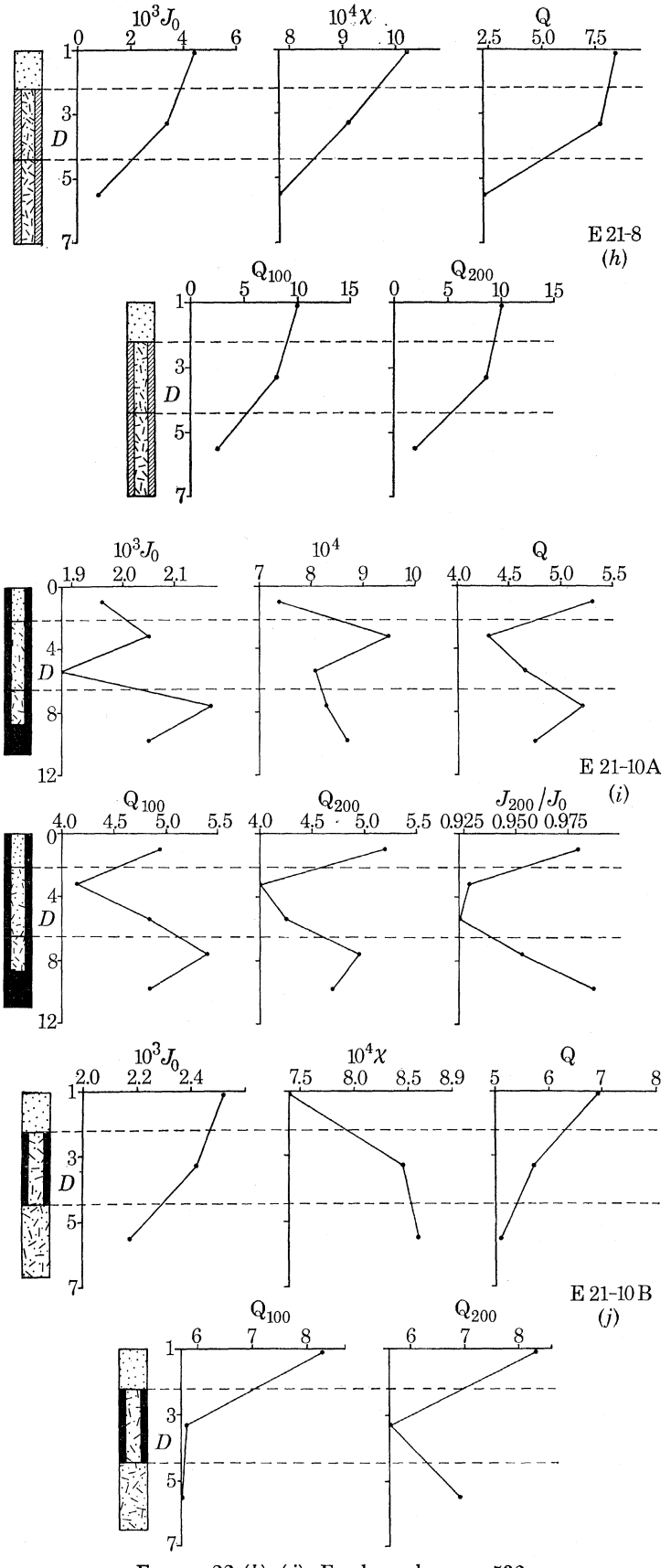

FIGURE 22 (*h*)–(*j*). For legend see p. 532.

PHILOSOPHICAL TRANSACTIONS OF THE ROYAL SOCIETY A MATHEMATICAL, PHYSICAL & ENGINEERING SCIENCES

Chlorite is generally associated with the hydrothermal alteration of ferromagnesium minerals, such as pyroxenes, amphiboles, or micas. In the *Eltanin* samples, chloritization is associated with the inner aphanitic zones, with none in the glass and very little in the variolitic parts. Chloritization of olivine was found in one sample but, in general, chlorite could not be associated with any particular mineral. Other alteration products included under the rank of 'chloritization' are talc (E21-8) and magnesite (E21-106) both replacing olivine.

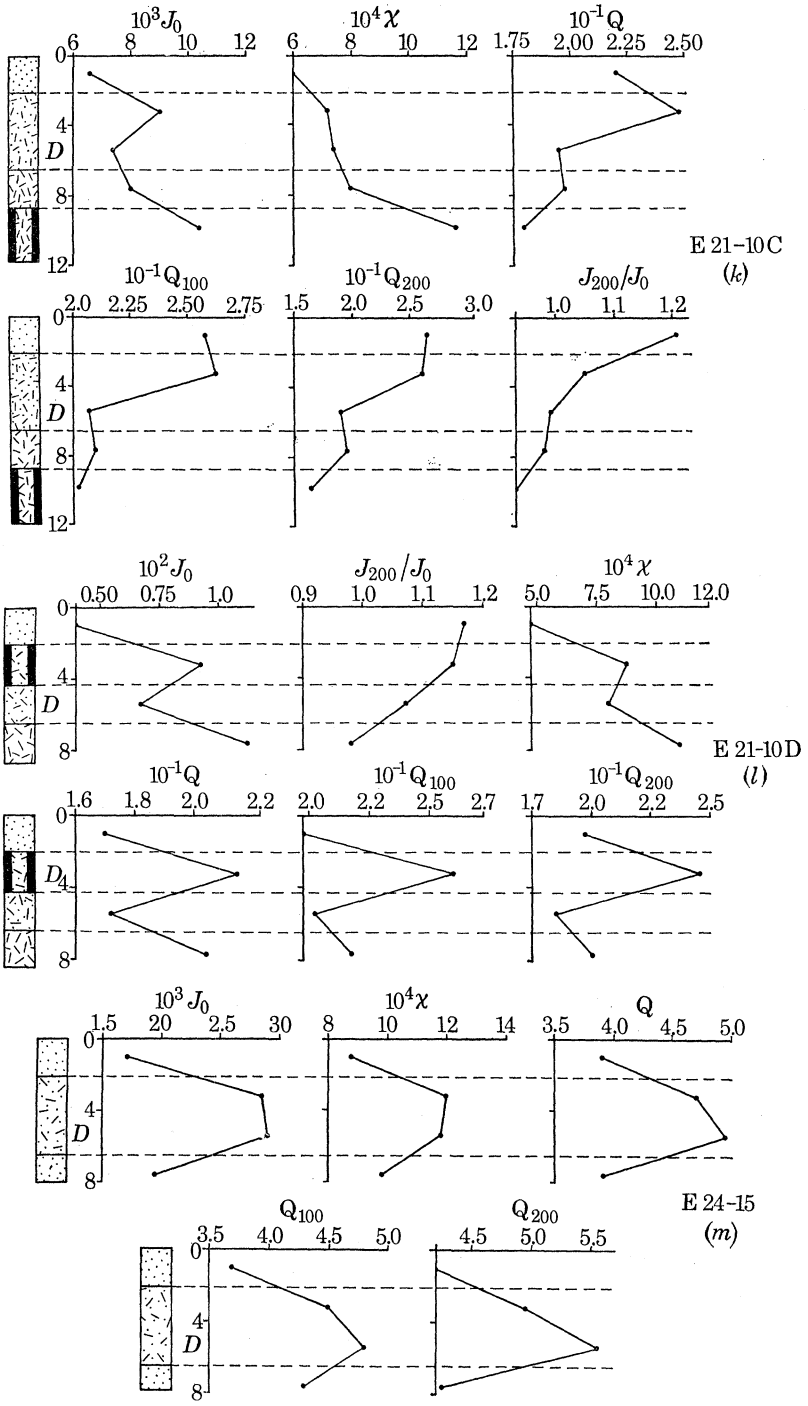

FIGURE 22 (*k*)–(*m*). For legend see p. 532.

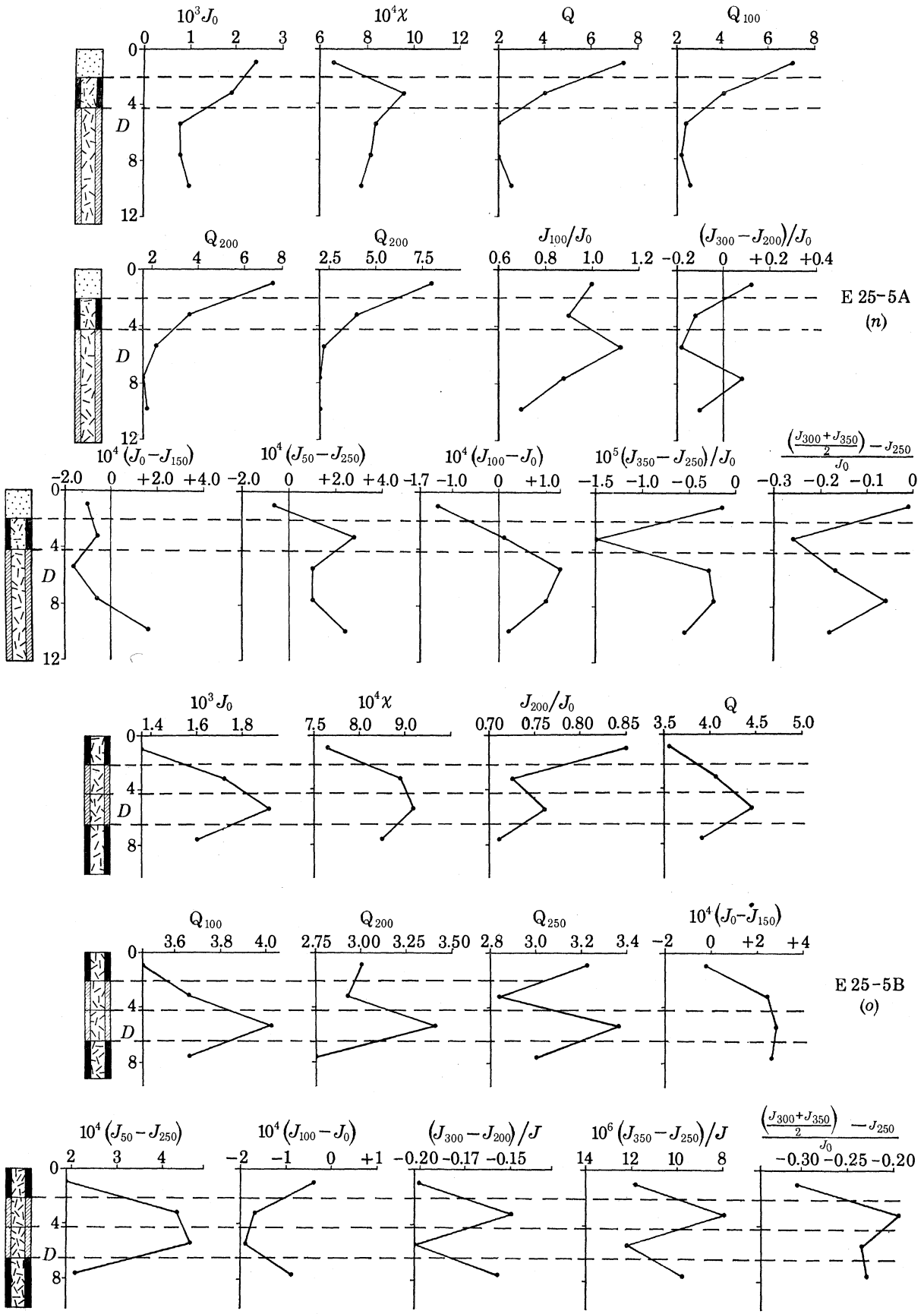

FIGURE 22 (*n*) and (*o*). For legend see p. 532.

Serpentinization generally occurs by the alteration of olivine and enstatite under low to medium metamorphism or hydrothermal activity. Assemblages of chrysolite serpentine plus brucite, or antigorite serpentine plus talc, can be expected (Brown 1968, p. 1527). In our *Eltanin* samples, serpentinization is observed in some of the aphanitic interiors and particularly next to joints (figure 28, plate 8). Magnetite is observed in some bright yellow-green serpentine near some joints, but other examples are stained reddish brown without secondary magnetite. Serpentine sometimes lines vesicle walls. In general, secondary ferric oxides increase towards the joints in the serpentinized zones.

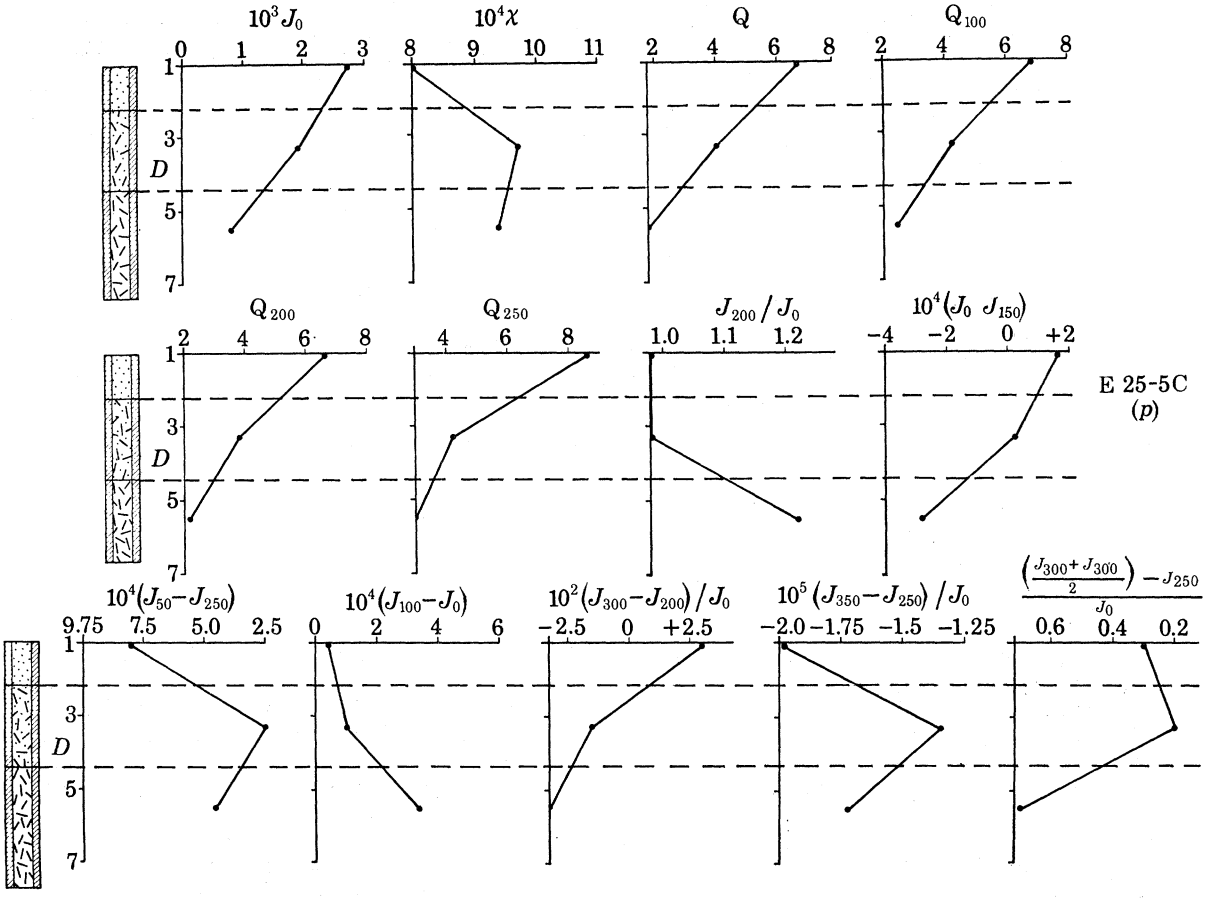

FIGURE 22 (*p*). For legend see p. 532.

Results of the silicate petrological examination are included graphically in figures 22*a* to 22*p*.

Paster (1970) has described the whole-rock chemistry of the samples. The details are not presented here, but mention is made of the major observations. With the exception of E 05–05, which is alkalic, all specimens (which include different parts of all samples) fall in the tholeiitic field of MacDonald & Katsura (1964). The fact that the single alkalic sample is from the shallowest source (table 4), which is a seamount, is probably significant. Basalts from seamounts and volcanic edifices in general tend to be more alkalic than deeper source basalts (Engel & Engel 1963; Luyendyk & Engel 1969). The iron content of the glass exterior is similar to that in Hawaiian tholeiites. The iron content of the aphanitic interior is much lower, however. This relative iron depletion in the interior is paralleled by a slight decrease in magnesium, but increases occur in most other oxides. The apparent iron loss in the tholeiites is manifested by the

norms which show undersaturation in the unhydrated glass and variolitic zones, but silica saturation in the interiors. Cann (1969) and Hart (1969) have described other chemical changes between the interior and exterior of submarine pillow basalts.

(3) *Opaque mineralogy*. At the time of writing the opaque minerals in each polished thin section have been examined only in specimens from E 05–05 (2). We feel that this single traverse of a boulder may provide typical data. A Reichert Zetopan-pol reflexion microscope has been used at magnifications up to 1200 times, with oil immersion. By observing 100 separate grains in each polished thin section, the following parameters have been measured; the 'magnetite oxidation number' (M) as defined in the summary at the beginning of this paper; the average size of the titanomagnetite grains in micrometres; and the fraction of the total observed field of view which is respectively titanomagnetite, ilmenite, and sulphide. This experimental method has been described by Wilson *et al.* (1968); Ade-Hall, Khan, Dagley & Wilson (1968); and Ade-Hall & Watkins (1970).

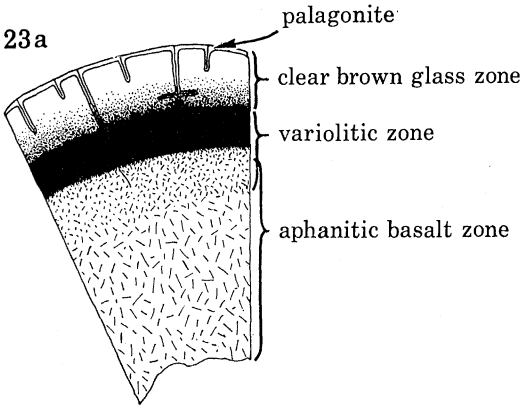

FIGURE 23. (*a*) Line diagram of pillow showing idealized relation between glass, variolitic, and aphanitic textures. Below are photographs of two thin sections. (*b*) (plate 8) Section through toe of E 24–15 showing concentric features lined with palagonite and phillipsite. The gradation from palagonite rim (white) to light grey unhydrated glass, to variolitic and aphanitic textures is illustrated. (*c*) (plate 8) Palagonite rim to slightly variolitic texture, at higher magnification. Scattered olivine and plagioclase agglomerates rimmed with incipient variolitic pyroxene are set in brown glass. Field of view in (*b*) 5 cm × 5.5 cm; in (*c*) 2 cm × 1.5 cm.

We have supplemented the opaque mineralogical description in E 05–05 (2) by measurement of the Curie point, using a modified Chevallier (1932) balance, in which the specimen is heated rapidly in air. The rapid heating inhibits the oxidation of low oxidation-state samples during heating, but the cooling process (which is not forced) will frequently be sufficiently slow so that new phases are created. Examples of the original Curie point curves and the creation of such new phases on cooling are given on figure 29. All Curie points are lower than that of magnetite.

The results of the opaque mineralogical examination and Curie point determination for E 05–05 (2) are given graphically in figure 30, where some magnetic data are also included, for ease of discussion. Four opaque mineralogical phases are found: brown skeletal titanomagnetite which tends to be euhedral in the rare larger grains; very rare small ilmenite laths; common very fine euhedral pyrite grains; and chrome or alumino-spinels as separate euhedral grains in phenocrysts of olivine (?), or as fringes on the titanomagnetites. Skeletal fronds are sometimes seen on the peripheries of small euhedral titanomagnetites, suggesting two phases of cooling. Deuteric oxidation is entirely absent; there also appears to be no maghaematization.

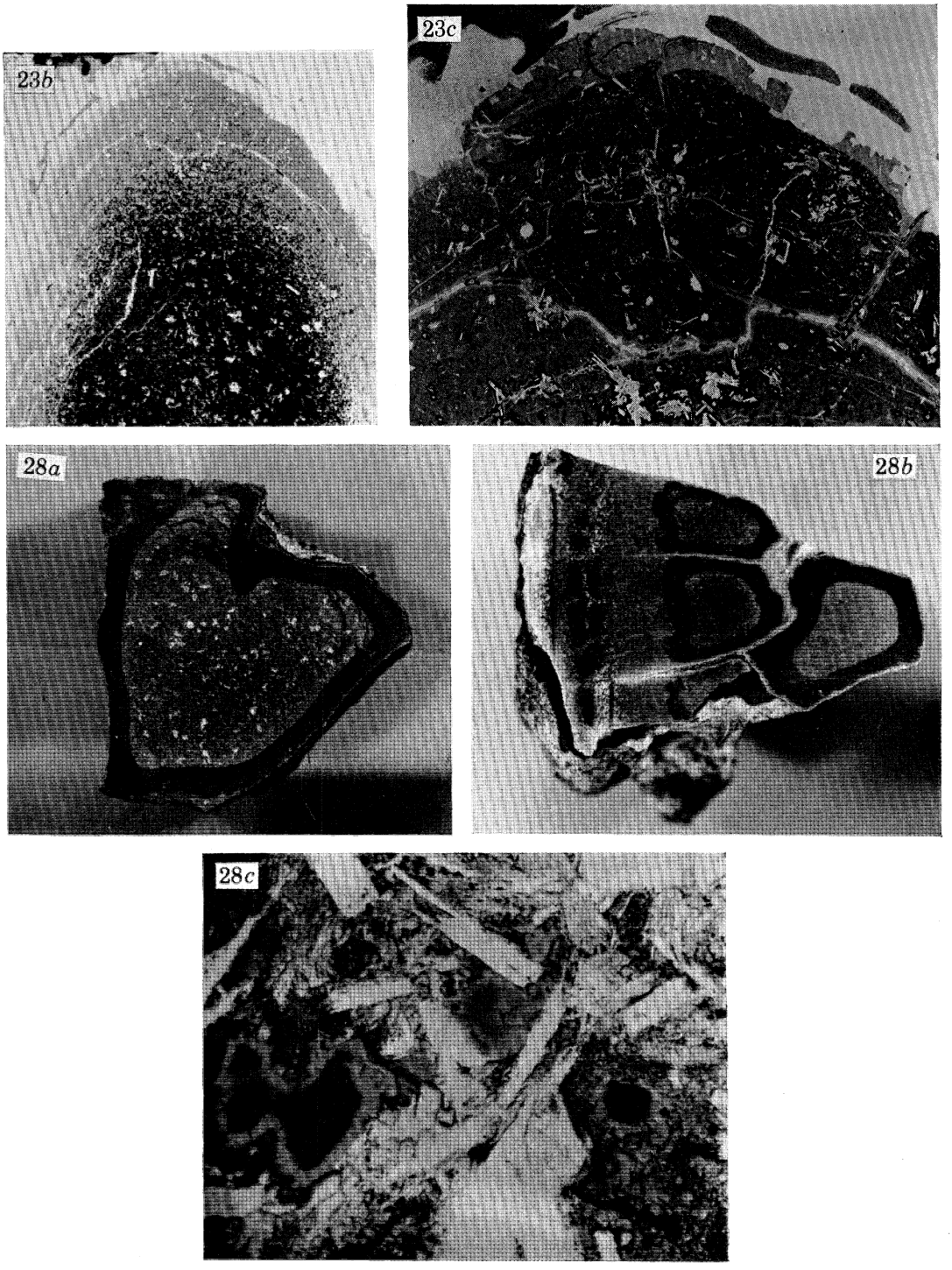

For legends to Figures 23 (*b*) and (*c*) see facing page.

FIGURE 28. Serpentinization of some of the *Eltanin* samples: (*a*) shows the 6 mm thick serpentinized rim in a section normal to the jointing in E 21–10 (2); (*b*) shows the darker sepentinized zones adjacent to fractures in the type wedge-shaped segment normal to the pillow surface of sample E 21–8; (*c*) shows a photomicrograph of a thin section of a specimen from E 21–10 (2), where serpentine (dark grey) lines vesicle walls. Specimen in (*a*) is 10 cm high. Specimen (*b*) is 9 cm wide. Field of view in (*c*) is 0.65 mm × 0.80 mm.

(*Facing p.* 540)

PHILOSOPHICAL TRANSACTIONS OF THE ROYAL SOCIETY A MATHEMATICAL, PHYSICAL & ENGINEERING SCIENCES

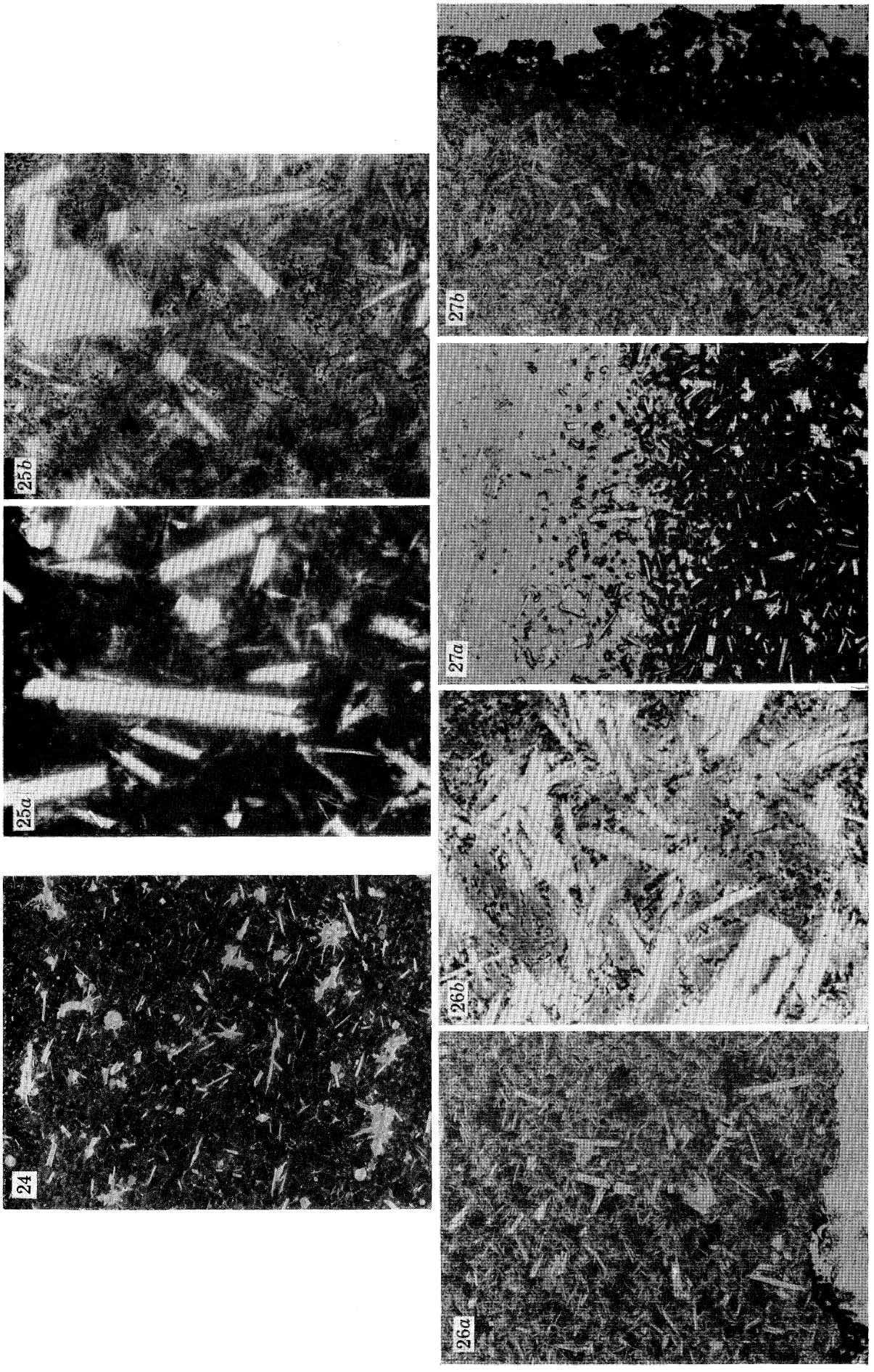

FIGURES 24 TO 27. For legends see facing page.

PHILOSOPHICAL TRANSACTIONS OF THE ROYAL SOCIETY A MATHEMATICAL, PHYSICAL & ENGINEERING SCIENCES

(4) *Discussion.* The magnetic and textural data in figure 22 shows very clearly the large variations which are found in single pillows. They appear to be closely related to distance below the cooling surface, but not in a totally consistent sense: in E 05–04, E 24–15, and E 25–5B, J increases below the surface, whereas the other pillow traverses exhibit a general decrease in J below the surface. At least one of these three samples feature serpentinization in the outer rim (figure 22): this could account for the direct relation between depth below the cooling surface and J. There is a general sharp increase in χ with depth below the surface: this is due to the

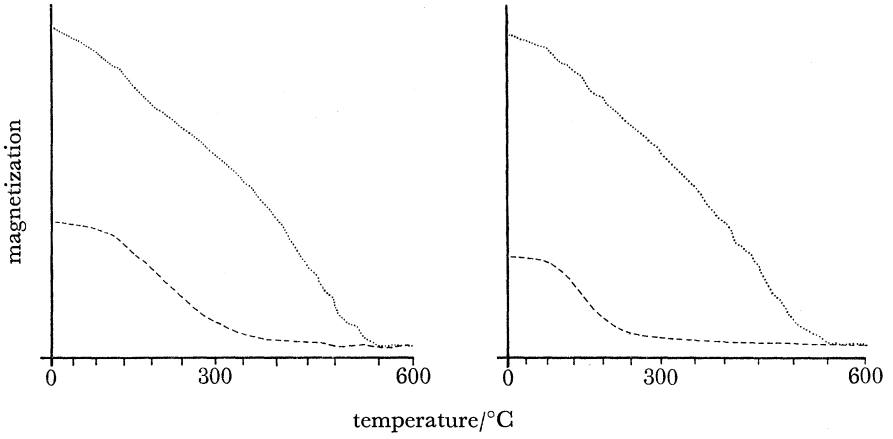

FIGURE 29. Two examples of Curie point curves for specimens from E 05–05 (2) dashed line is heating cycle; dotted line is cooling cycle. Vertical scale is function of the high field intensity of magnetization, in arbitrary units. Heating carried out in air.

increase in grain size or bulk ferromagnetic content with increasing crystallinity. Such a simple relation does not exist in E 05–05 (4), E 15–15A, or E 21–8, but thin section analysis chloritization is present in these samples. The effect of chloritization is very marked in all samples, as illustrated in figure 31.

Serpentinization, on the other hand, is not consistent in its apparent effect on the magnetic properties. For example, in E 21–10C and E 21–10D an increase in J (but little effect on χ) accompanies some serpentinization. In contrast a decrease in J appears to be associated with

DESCRIPTION OF PLATE 8

FIGURE 24. Photomicrograph of dark red-brown variolitic texture in specimen from dredged sample E 15–15. Field of view 6.5 mm × 8.0 mm.

FIGURE 25. Photomicrographs of opaque minerals in variolitic basalt: (*a*) shows fine fibrous pyroxenes and fine incipient opaques contributing to fuzzy appearance of groundmass. In (*b*) the groundmass pyroxene assumes fan-shaped forms and opaques are in the intervariolitic areas. Both from sample E 21–10(2). Field of view in (*a*) and (*b*) 0.65 mm × 0.80 mm.

FIGURE 26. Photomicrograph of aphanitic texture in sample E 21–10 (2): in (*a*) the groundmass is composed of plagioclase microlites and small discrete clinopyroxenes; but patches of turbid variolitic groundmass remain. In (*b*) the groundmass granules of pyroxene have lost the fibrous appearance, and are more equigranular. Opaques nucleate around the feldspars. Field of view in (*a*) is 6.5 mm × 8.0 mm; in (*b*) 0.65 mm × 0.80 mm.

FIGURE 27. Photomicrographs of transitional textural types: in (*a*) a specimen from sample E 21–10 (2) shows the transition from clear class to variolitic texture, with varioles nucleating around phenocrysts of olivine and plagioclase. In (*b*) a hydrated aphanitic texture is adjacent to sorbed iron and manganese hydroxide at a joint surface. Field of view in (*a*) and (*b*) is 6.5 mm. × 8.0 mm.

serpentinization in E21–10A and E25–5B, although the role of other factors is not clear. Only one generalization is possible about the observed magnetic effects of serpentinization: no *very* high J values are found in such specimens.

The Q values, which are all above 1.0 change very smoothly with distance below the cooling surface in many of the samples (figure 22).

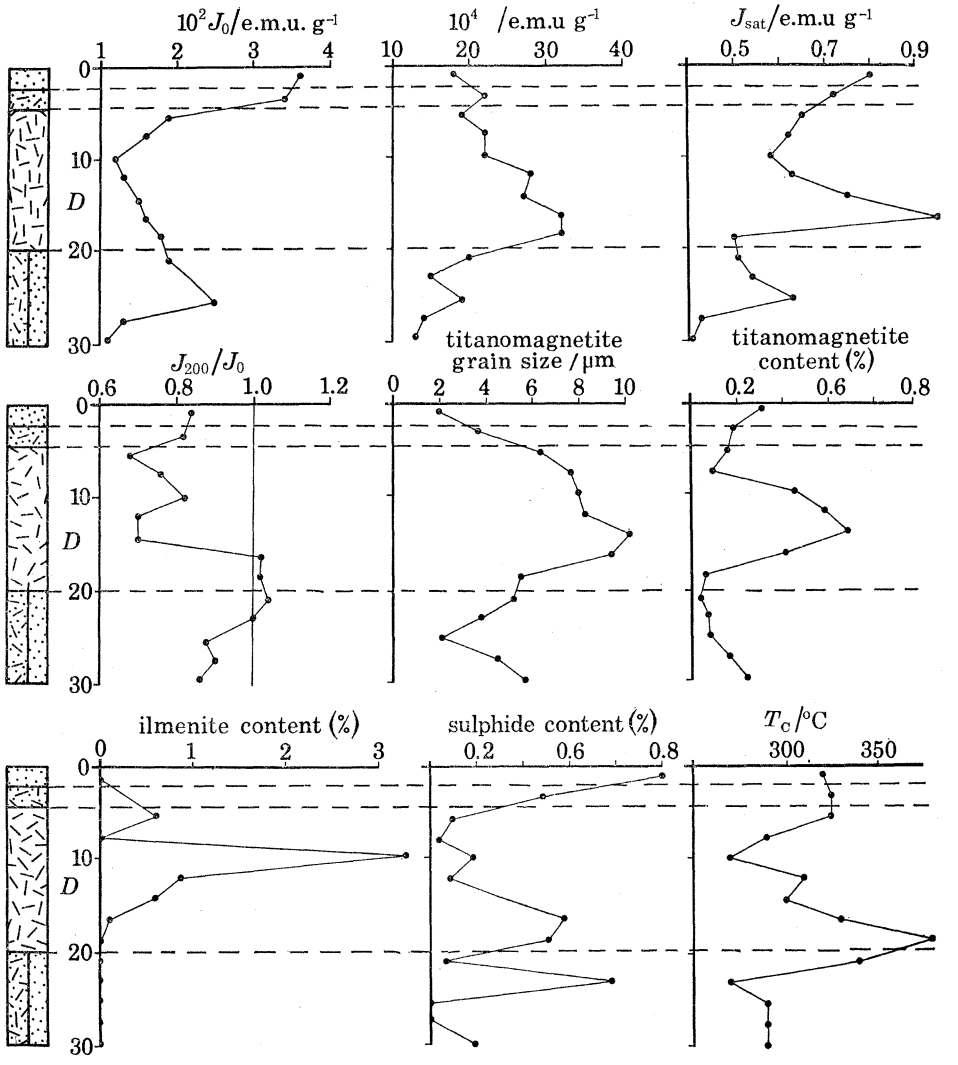

FIGURE 30. Opaque mineralogical parameters in E 05–05. For ease of comparison, several corresponding magnetic properties (already presented in figure 22) are shown. For definition of the parameters, and method involved in obtaining them, see text. J, J_0, J_{200}, and J_{sat} in e.m.u. g^{-1}. (From Watkins *et al.* 1970*b*.)

A simple function of the stability, such as J_{200}/J_0 increases inwards in some specimens, and decreases smoothly in others (figure 22). An increasing grain size would lead to a decrease in such functions (for example E21–10C). The change in slopes of the various other functions of J_x and J_0 may be interpreted in various ways, such as the possible development of higher coercivity phases during late stages of cooling (for example E05–05(4), and E15–15(A)). Such details are discussed elsewhere (Watkins *et al.* 1970*b*), but the point is made that considerable systematic variations exist in most pillows as the duration of cooling increases inwards.

Detailed interpretation of all magnetic variations in a pillow can only be satisfactorily made in conjunction with the opaque mineralogical and thermomagnetic data. Attention is therefore drawn to figure 30, which shows data for a core featuring upper and lower glassy parts. J decreases with distance below the surface, as χ, J_{sat}, titanomagnetite grain size and percentage, and ilmenite percentage increase to a maximum in the aphanitic interior. T_C and J_{200}/J_0 increase towards the lower edge of the aphanitic interior: a new higher coercivity phase has apparently developed during late stages of cooling, but is not visible optically.

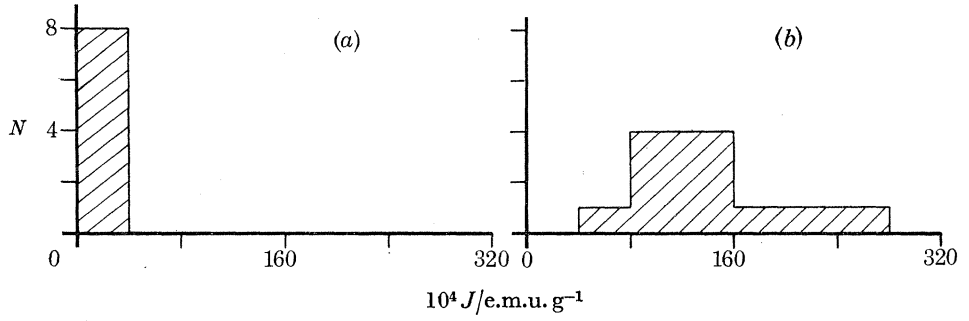

FIGURE 31. Histograms showing a comparison of the intensity of magnetization (J) of (*a*) chloritized and (*b*) non-chloritized basalt samples from the *Eltanin* submarine pillow basalts.

It is significant that a sulphide percentage minimum occurs within the T_C and J_{200}/J_0 maxima. Sulphides, which are common throughout the boulder are at a maxima towards the edge of the pillow, and a minimum in the aphanitic interior. This is consistent with the rest of the data: as described earlier, only minimum oxidation states (index I) are present throughout. Higher oxidation states would enhance removal of the sulphides. There is a tendency towards this only in the zone of T_C and J_{200}/J_0 maxima, which is very likely due to an oxidation maximum.

The data emphasize the dynamic processes existing in a cooling submarine extrusive, and the problem of selection of data for any appropriate study. Using reasonable assumptions (Jaeger 1968) the time for substantial cooling of all parts of E 05–05(2) would be of the order of 5 to 6 h. It appears that the rapid cooling, although providing strong gradients in several parameters, strongly inhibits oxidation in the titanomagnetites in pillow basalts: the quenching takes place faster than the oxidation. According to the potassium–argon data of Dalrymple & Moore (1968), quenching also inhibits degassing.

The rapid cooling could conceivably provide bodies convenient for application of the cooling-velocity concept of Winkler (1949). Figure 32 (*a*) shows the distribution of glass and major mineralogical functions as a function of distance beneath the cooling surface in one core from pillow E 05–05. Figure 32 (*b*) shows similar data, as a function of quenching temperature in a Hawaiian lava lake (Peck, Wright & Moore 1966): since cooling rates can be calculated for submarine pillows, it is therefore ideally possible to arrive at a semi-quantitative cooling history for separate pillow segments, in similar fashion to the inference of figure 32*b*.

(*d*) *Traverses of single Icelandic lavas and dykes*

The thickness (or time for complete cooling) of almost all submarine basalt samples so far collected is generally very limited. This may bias the conclusions possible from the observations. Therefore, as a supplement, we are including some unpublished results from a study of traverses of basaltic lavas and dykes outcropping above sea level.

Watkins & Haggerty (1965, 1967) have presented the detailed results from sampling, at an interval of about 30 cm, between the upper and lower cooling surfaces of a single Iceland lava of 11 m thickness. The results were repeated in part in figure 8. Mention was made of similar traverses of other bodies, and the major magnetic properties and titanomagnetite oxidation states were examined (as a whole) in a discussion of correlations between oxidation and polarity correlations in igneous rocks (Watkins & Haggerty 1968).

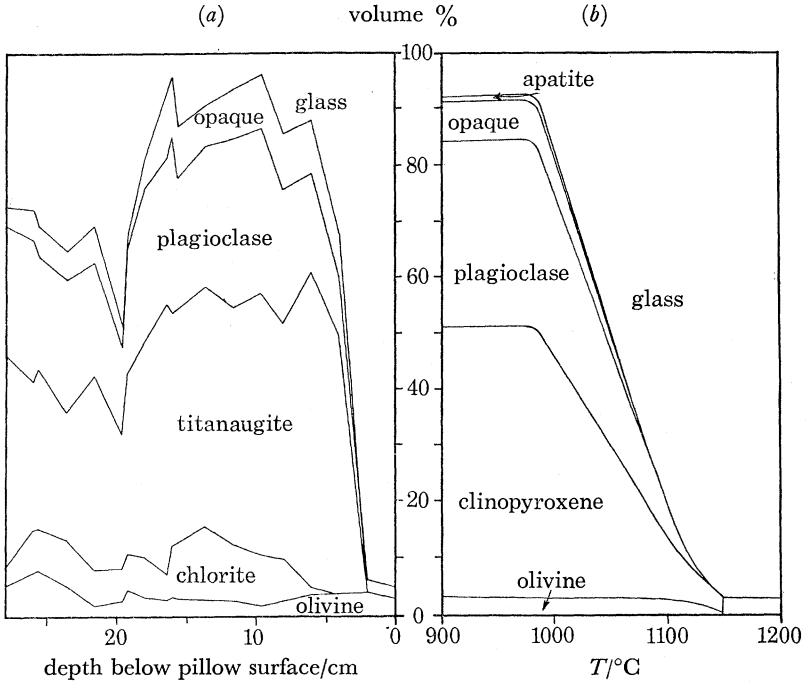

FIGURE 32. The volume percentage of various mineralogical or phase constituents as a function of depth beneath the cooling surface in core E 05–05 (3) in diagram (*a*), compared to the idealized fractions of various mineralogical or phase constituents in the Hawaiian lava lake, as a function of quenching temperature (Peck *et al.* 1966) in diagram (*b*). The vastly different environments during cooling prohibit direct comparison between (*a*) and (*b*).

In figures 33 and 34 we show the results from traverses of three lavas, and three dykes, respectively. Their exact locations are given elsewhere (Watkins & Haggerty 1968). In the case of the three lavas (figure 33) the lower limits were sampled, but the upper few tens of centimetres were not accessible. Samples from the eastern edge of two of the dykes (figure 34) similarly could not be obtained. Therefore of the six bodies, only samples from the western edges of the three dykes and the eastern edge of one dyke cooled adjacent to presumably cooler rock.

The three lavas range from 5 to 15 m in thickness. A cooling to lower temperatures will take of the order of 1 to 5 years.

The thinnest lava sampled, is part of a series of pillow basalts apparently extruded at short intervals (G. P. L. Walker, personal communication). The atypical increase in J, Q, and titanomagnetite oxidation index towards the upper edge could be due to the overlying lava being emplaced while the lower unit was still hot. Both other lavas (FS and LS) feature internal J, χ, Q, oxidation index, and stability maxima which are, in our opinion, typical of many lavas.

The generalizations which can be drawn from traverses of single lavas contrast with similar studies of single dykes (figure 34): although J, χ, and Q are variable, they are neither so high

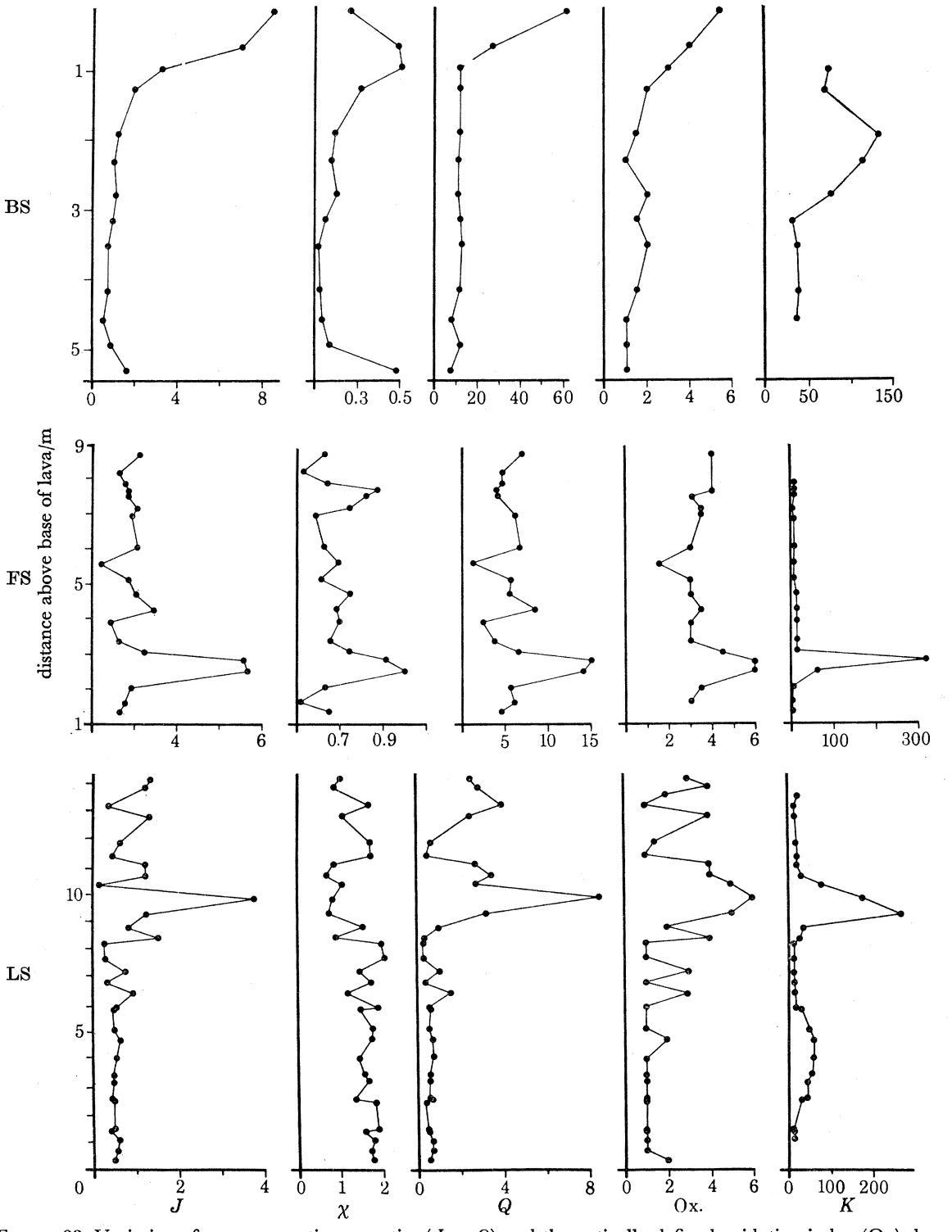

FIGURE 33. Variation of some magnetic properties (J, χ, Q) and the optically defined oxidation index (Ox). between the upper and lower surfaces of three Icelandic lavas. Also included is the precision parameter K: (Fisher 1953): this is defined as $K = N\text{–}1/N\text{–}R$ where R is the resultant vector applying unit vector per specimen. In the cases shown, $N = 5$. Therefore K expresses the scatter of directions of the natural remanent magnetism for groups of five specimens, being higher for less scatter of directions. The parameter is 'sliding' each successive point is obtained by dropping data from the specimen at the bottom of the group, and replacing it with one immediately above the group. For magnetic property definition see text. J is in e.m.u. $g^{-1} \times 10^{-3}$; χ is in c.g.s. $\times 10^{-6}$; Q and K are dimensionless; *Ox.* is defined in the text. Ordinate is position of specimen above the base of the lava in metres. For exact locations of the three lavas see Watkins & Haggerty (1968).

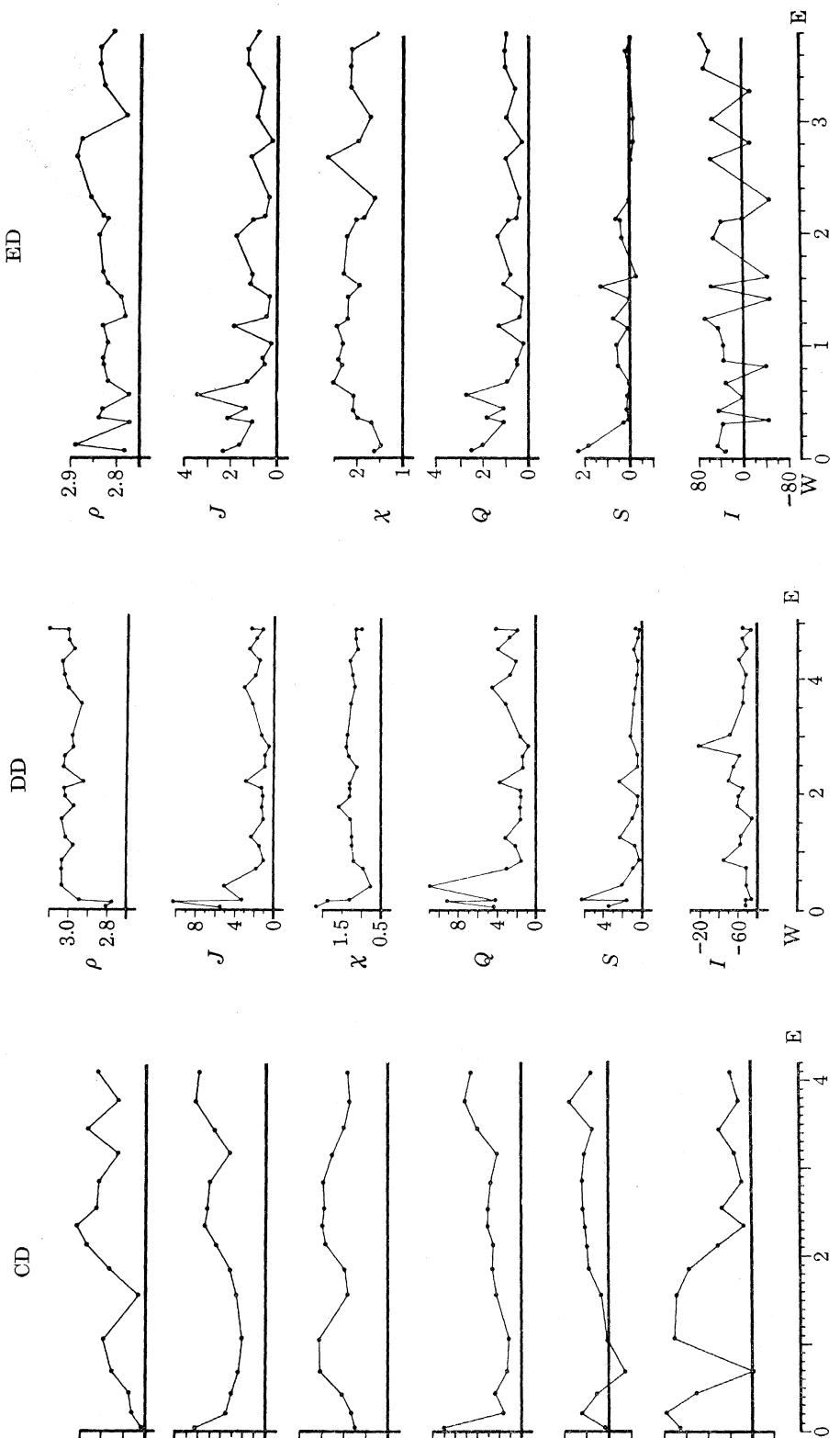

FIGURE 34. Variation of some magnetic properties, (J, χ, Q, S, I); and density (ρ) across three single Icelandic dykes. J, χ, Q, as in figure 33. S = a function of magnetic stability, where $S = J_{100}-J_{200}$ (see figure 21). I = inclination (in degrees) of direction of natural remanent magnetism; positive = down, negative = up. ρ in g cm^{-3}. Abscissa is distance of specimen from the west side of the dyke, in metres. For exact locations of these dykes, see Watkins & Haggerty (1968). The oxidation index data is excluded: it is non-varying and low.

absolutely, nor so variable as the data from lavas. The titanomagnetite oxidation indices are all low (Watkins & Haggerty 1968), and this fact is manifested in low stability and variable inclination (I) of natural remanent magnetism (figure 34). The slower cooling rates, different emplacement methods, and remoteness from the lower pressure of the surface environments, all contribute to low oxidation state of the titanomagnetites in dykes.

The gradients of the measured variables within both lavas and dykes is very low compared to that in submarine boulders, although the larger specimen spacing in the lava and dyke studies means that their outer rims were not sampled in detail. Different sources of gradient are detected: variation in the submarine pillows are very dominantly a function of quenching on a single low oxidation state titanomagnetite to the extent that sulphide development is enhanced, whereas magnetic variations in lavas and dykes reflect the development of higher oxidation state titanomagnetites, up to and including pseudobrookite, haematite, and secondary magnetite in any olivines present.

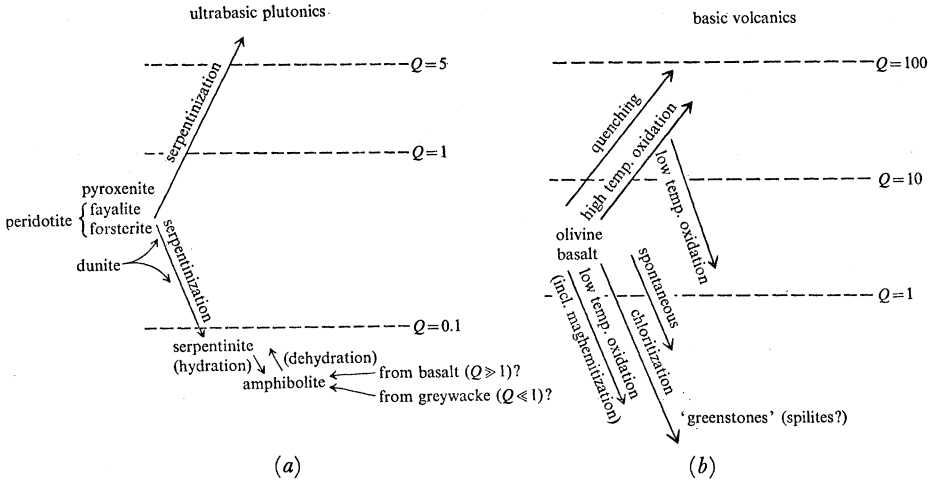

FIGURE 35. Empirically derived generalized 'flow' diagram showing some of the petrological factors observed to occur in association with changes n the Q factor in (a) basic and ultrabasic plutonic rocks and (b) basaltic rocks. For sources of these observations, see text. It is emphasized that no theoretical reasoning is involved, and therefore the diagram should not be interpreted at this time to be necessarily complete and universally applicable.

CONCLUSIONS

The limited number of studies of submarine igneous rocks provide several implications, which are summarized in figures 35a and 35b. The highly generalized nature of these two diagrams is stressed.

It is suggested that the basalt specimens so far examined are in all probability not generally representative of the oceanic crust. The collection method restricts the available specimens almost completely to the rapidly chilled outer surface of extrusives, so that the inherent very rapid cooling dominates the magnetic property variation, which are systematic and considerable between glassy rim and aphanitic interior. It is highly unlikely that the ocean floor is built up of extrusives of such limited thickness that the bulk magnetic properties are determined by quenching, as opposed to the processes which cause the magnetic variations observed in lavas outcropping above sea level, despite obvious environmental pressure differences. This belief is supported by the recovery, however rare, of basalts with coarse (and

therefore relatively slowly cooled) titanomagnetites, as illustrated by Carmichael (1970). Of course, much non-quenched igneous and metamorphic material has been recovered from faulted areas. Nevertheless, basalts with $Q > 1$ would still be characteristic, according to data from lavas and dykes outcropping above sea level.

The problem of 'representative sampling' of submarine rocks which are quenched may be a considerable one, according to the magnetic data. Some chemical variations must parallel these magnetic differences. Until improved upon, we propose that a variolitic texture can be used as an acceptability criterion. For reasons not clear to us, in the collection of submarine rocks which we have examined, there is far less between-pillow chemical variation if the non-variolitic specimens are rejected (Paster 1970). This also leads to more uniform magnetic data. The fact that the aphanitic interiors of our specimen frequently feature chloritization, whereas the variolitic zones do not, may be relevant to the contrast in between-pillow chemical consistencies of the different textural zones.

Conflict exists in data relevant to the magnetic properties of ultrabasic igneous rocks, most likely because of their varying degrees of alteration. The effect of serpentinization, in particular, is inconsistent. It can lead to either an increase or a decrease in J. It is clear that the term serpentinite is a very wide petrological category: magnetic properties and density measurements could be profitably utilized for finer definition. Our data show that definition of chloritization can utilize magnetic properties: low J and Q are characteristic. 'Greenstones' and spilite appear to possess similar properties, but not uniquely so.

Recovery of several cores from the ocean crust will undoubtedly lead to a greater understanding of the limits of magnetic properties in the oceanic crust. An assumption of a basaltic layer with $Q > 1$ as the magnetically dominant horizon is valid according to the available data. A lack of classical anomaly pattern would not be sufficient to remove the possibility of local crustal spreading, however, since there clearly exist several natural means to diminish magnetic intensities in submarine igneous rocks.

The new data presented in this paper are based on samples from three sources. The dredged pillow basalts from the South Pacific and Macquarie Ridge were obtained during cruises of the U.S.N.S. *Eltanin* as part of its continuing programme for the Antarctic Branch of the National Science Foundation. Laboratory examination of these materials was carried out using apparatus provided in part by National Science Foundation grant numbers GA 582, GA 602, and GA 1620, to N. D. Watkins. One of us (T. P.) was supported by National Science Foundation grant numbers GA 523 and GA 1066, and also by an N.D.E.A. graduate fellowship. The Icelandic lavas and dykes were sampled by one of us (N.D.W.) during field work in 1964 and 1965. This was supported by D.S.I.R. (England) and in 1965 was carried out in conjunction with Dr S. E. Haggerty, who made the oxidation index determination in the three Icelandic lavas presented in this paper. The spilites on the island of St Thomas were sampled by N.D.W. with the assistance of Dr A. Richardson. Several authors have allowed reproduction of illustrations from their papers in the review segment of our paper. This permission is gratefully acknowledged.

PHILOSOPHICAL TRANSACTIONS OF THE ROYAL SOCIETY A MATHEMATICAL, PHYSICAL & ENGINEERING SCIENCES

References (Watkins & Paster)

Ade-Hall, J. M. 1964 *Geophys. J.* **9**, 85.
Ade-Hall, J. M., Khan, M. A., Dagley, P. & Wilson, R. L. 1968 *Geophys. J.* **16**, 375.
Ade-Hall, J. M. & Watkins, N. D. 1970 *Geophys. J.* **19**, 351.
Akimoto, S. 1957 *Adv. Phys.* **6**, 288.
Akimoto, S. & Katsura, T. 1960 *J. Geomag. Geoelect. Kyoto* **9**, 94.
Amstutz, G. C. 1968 *Poldervaart treatise on rocks of basaltic composition* (ed. H. H. Hess and A. Poldervaart), p. 737. New York: Wiley and Sons.
Angenheister, G. & Turkowsky, C. 1964 *Boll. Geofis. teor. appl.* **6**, 310.
Banghar, A. R. & Sykes, L. R. 1969 *J. geophys. Res.* **74**, 632.
Barnes, I., Lamarche, V. C. & Himmelberg, G. 1967 *Science, N.Y.* **156**, 830.
Beck, M. E. 1966 *U.S. Geol. Surv. Prof. Paper* 500–*D*, D 109.
Brown, G. M. 1968 *Poldervaart treatise on rocks of basaltic composition* (ed. H. H. Hess and A. Poldervaart), p. 103. New York: Wiley and Sons.
Buddington, A. F. & Lindsley, D. H. 1964 *J. Petrology* **5**, 310.
Bull, C., Irving, E. & Willis, I. 1962 *Geophys. J.* **6**, 320.
Bullard, E. C. 1968 *Phil. Trans. Roy. Soc. Lond.* A **263**, 481.
Bullard, E. C. 1969 *Scient. Am.* **221**, 66.
Bullard, E. C. & Mason, R. G. 1963 *The sea* (ed. M. N. Hill), **3**, 175.
Cann, J. R. 1969 *J. Petrology* **10**, 1.
Carmichael, C. M. 1970 *Can. J. Earth Sci.* **7**, 239.
Chevallier, R. & Pierre, J. 1932 *Ann. Phys.* **10**, 383.
Clark, H. C. 1969 *J. geophys. Res.* **74**, 3143.
Collinson, D. W., Molyneux, L. & Stone, D. B. 1963 *J. scient. Instrum.* **40**, 310.
Cox, A. & Doell, R. R. 1962 *J. geophys. Res.* **67**, 3397.
Cox, A., Doell, R. R. & Thompson, G. 1964 *A study of serpentinite* (NAS–NRC Publ. no. 1188), p. 53.
Cullen, D. J. 1967 *N.Z. Jl Sci.* **10**, 813.
Dalrymple, G. B. & Moore, J. G. 1968 *Science, N.Y.* **161**, 1132.
DeBoer, J., Schilling, J. G. & Krause, D. C. 1969 *Science, N.Y.* **166**, 996.
DeBoer, J., Schilling, J. G. & Krause, D. C. 1970 *Earth Planet. Sci. Lett.* **9**, 55.
Donnolly, T. W 1959 Geology of St Thomas and St John, Virgin Islands. Unpublished Ph.D. Thesis, Princeton University.
Donnolly, T. W. 1960 Petrologic and tectonic evolution of St Thomas and St John, Virgin Islands (abstract) *Bull. Geol. Soc. Am.* **71**, 1851.
Dymond, J. R., Watkins, N. D. & Nayudu, Y. R. 1968 *J. geophys. Res.* **73**, 3977.
Engel, C. G. & Engel, A. E. J. 1963 *Science, N.Y.* **140**, 1321.
Gheith, M. A. 1952 *Am. J. Sci.* **250**, 677.
Gottshalk, V. H. 1935 *Physics* **6**, 127.
Grommé, C. S. & Gluskoter, H. J. 1965 *J. Geol.* **73**, 74.
Hart, S. R. 1969 *Earth Planet. Sci. Lett.* **6**, 295.
Hatherton, T. 1967 *N.Z. Jl Geol. Geophys.* **10**, 1204.
Heirtzler, J. R., Le Pichon, X. & Baron, J. G. 1966 *Deep Sea Res.* **13**, 437.
Heirtzler, J. R., Dickson, G. O., Herron, E. M., Pitman, W. C. & Le Pichon, X. 1968 *J. geophys. Res.* **73**, 2119.
Hess, H. H. 1964 *A study of serpentinite* (NAS-NRC Publ. no. 1188), p. 171.
Hess, H. H. 1966 *Geol. Surv. Can. Pap.* 66–13, p. 149.
Hess, H. H. & Otalora, G. 1964 *A study of serpentinite* (NAS–NRC Publ. no. 1188), p. 152.
Irving, E. 1968 *Can. J. Earth Sci.* **5**, 1319.
Jaeger, J. C. 1968 *Poldervaart treatise on rocks of basaltic composition* (ed. H. H. Hess and A. Poldervaart), p. 503. New York: Wiley and Sons.
Jaeger, J. C. & Green, R. 1962 *Dolerite, a symposium*, University of Tasmania (Hobart), p. 26.
Jaeger, J. C. & Joplin, G. 1955 *J. geol. Soc. Aust.* **2**, 1.
Kawai, N. & Kang, Y. 1961 *Mem. Coll. Sci. Univ. Kyoto* B **28**, 285.
Kazmi, S. A. A. 1961 *J. Proc. R. Soc. N.S.W.* **94**, 223.
Komarov, A. G. 1962 *Isv. Geophys. Ser.* p. 986.
Komarov, A. G., Moskaleva, S. V., Belyayev, V. M. & Ilyina, V. I. 1962 *Dokl. Akad. Nauk. SSSR* **143**, 1166.
Konigsberger, J. G. 1938 *Terr. Magn. Atmos. Elec.* no. 119.
Lepp, R. 1957 *Am. Miner.* **42**, 679.
Luyendyk, B. P. & Melson, W. G. *Nature, Lond.* **215**, 147.
Luyendyk, B. P. & Engel, C. G. 1969 *Nature, Lond.* **223**, 1050.
MacDonald, G. A. & Katsura, J. 1964 *J. Petrology* **5**, 82.
Manley, H. 1956 *Pure and appl. Geophys.* **33**, 86.

PHILOSOPHICAL TRANSACTIONS OF THE ROYAL SOCIETY A MATHEMATICAL, PHYSICAL & ENGINEERING SCIENCES

Matthews, D. H. 1961 *Nature, Lond.* **196**, 158.
Meitzner, W. 1963 *Beitr. Miner. Petrogr.* **9**, 320.
Mikhailova, N. P. 1961 *Isv. Geophys. Ser.* 1599.
Moore, J. G. 1965 *Am. J. Science*, **263**, 40.
Moore, J. G. 1966 *U.S. Geol. Surv. Prof. Paper* 475-*B*, B 153.
Muratov, D. I. 1964 *Isv. Geophys. Ser.* p. 1801.
Nagata, T. 1961 *Rock magnetism*, 225 pp. Tokyo: Maruzen Co. Ltd.
Opdyke, N. D. & Hekinian, R. 1967 *J. geophys. Res.* **72**, 2257.
Ozima, M. & Ozima, M. 1967 *Earth Planet. Sci. Lett.* **3**, 213.
Ozima, M., Ozima, M. & Kaneoka, I. 1968 *J. geophys. Res.* **73**, 711.
Paster, T. 1970 *Am. Geophys. Un., Antarctic Series Monog.* (in the Press).
Peck, D. L., Wright, T. L. & Moore, J. G. 1966 *Bull. Volc.* **29**, 629.
Poldervaart, A. & Green, J. 1965 *Am. Miner.* **50**, 1723.
Quon, S. H. & Ehlers, E. G. 1963 *Bull. Geol. Soc. Am.* **74**, 1.
Rösler, H. J. 1962 *Geophysik Geologic* **3**, 3.
Sato, M. & Wright, T. L. 1966 *Science, N.Y.* **153**, 1105.
Shand, S. J. 1949 *J. Geol.* **57**, 89.
Smith, P. J. 1967 *Geophys. J.* **12**, 123.
Summerhayes, C. P. 1969 *N.Z. Ocean Inst. Mem.* **50**, 94 pp.
Thellier, E. 1959 *Ann. Geophys.* **15**, 285.
Van Andel, Tj.H. & Bowin, C. O. 1968 *J. geophys. Res.* **73**, 1279.
Varne, R., Glee, R. D. & Quilty, P. G. J. 1969 *Science, N.Y.* **166**, 230.
Verhoogen, J. 1959 *J. geophys. Res.* **61**, 201.
Vine, F. J. 1966 *Science, N.Y.* **154**, 1405.
Vine, F. J. & Matthews, D. H. 1963 *Nature, Lond.* **199**, 947.
Vogt, P. R. & Ostenso, N. A. 1966 *J. geophys. Res.* **71**, 4389.
Wagner, F. C. 1967 *Z. Geophys.* **33**, 262.
Wasilewski, P. J. 1968 *J. Geomag. Geoelect. Kyoto* **20**, 129.
Watkins, N. D. 1967 *J. Geomag. Geoelect. Kyoto* **19**, 63.
Watkins, N. D. 1968 *Pure and appl. Geophys.* **69**, 179.
Watkins, N. D. 1969 *Geophys. J.* **17**, 121.
Watkins, N. D. & Haggerty, S. E. 1965 *Nature, Lond.* **206**, 797.
Watkins, N. D. & Haggerty, S. E. 1967 *Contrib. miner. Petrol.* **15**, 251.
Watkins, N. D. & Haggerty, S. E. 1968 *Geophys. J.* **15**, 305.
Watkins, N. D., Holmes, C. W. & Haggerty, S. E. 1967 *Science, N.Y.* **155**, 579.
Watkins, N. D. & Richardson, A. 1969 *Trans. Am. Geophys. Un.* **50**, 606 (abstract).
Watkins, N. D. & Gunn, B. M. 1970 *New Zealand J. Geol. Geophys.* (in the Press).
Watkins, N. D., Gunn, B. M. & Coy-Yll, R. 1970*a* *Am. J. Sci.* **268**, 24.
Watkins, N. D., Ade-Hall, J. & Paster, T. 1970*b* *Earth Planet. Sci. Lett.* **8**, 322.
Wilson, R. L., Haggerty, S. E. & Watkins, N. D. 1968 *Geophys. J.* **16**, 179.
Wilson, R. L. & Watkins, N. D. 1967 *Geophys. J.* **12**, 405.
Winkler, H. 1949 *Miner. Mag.* **28**, 557.

Note added in proof (September 1970): since submitting the original manuscript, several other studies of the magnetic properties or magnetic mineralogy of submarine basalts have been published or presented. They are:

Haggerty, S. E. 1970 *Trans. Am. Geophys. Un.* **51**, 273 (abstract).
Haggerty, S. E. & Irving, E. 1970 *Trans. Am. Geophys. Un.* **51**, 273 (abstract).
Irving, E., Robertson, W. A. & Aumento, F. 1970 *Can. J. Earth Sci.* **7**, 226.
Marshall, M. & Cox, A. 1969 *Trans. Am. Geophys. Un.* **50**, 606 (abstract).
Marshall, M. & Cox, A. 1970 *Trans. Am. Geophys. Un.* **51**, 273 (abstract).
Ozima, M. & Larson, E. E. 1970 *J. geophys. Res.* **75**, 1003.
Schaeffer, R. M. & Schwartz, E. J. 1970 *Can. J. Earth. Sci.* **7**, 268.

PHILOSOPHICAL TRANSACTIONS OF THE ROYAL SOCIETY A MATHEMATICAL, PHYSICAL & ENGINEERING SCIENCES

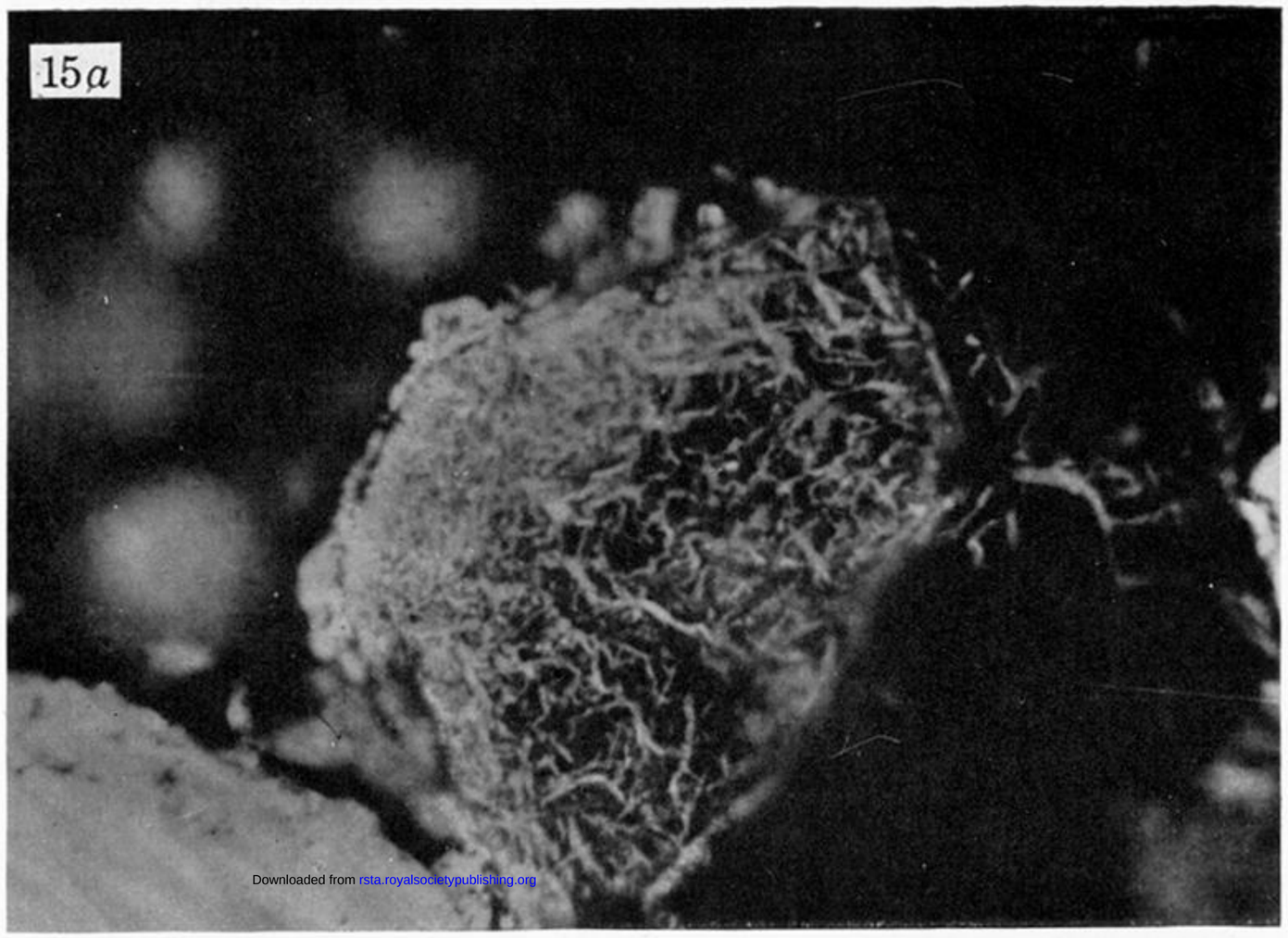

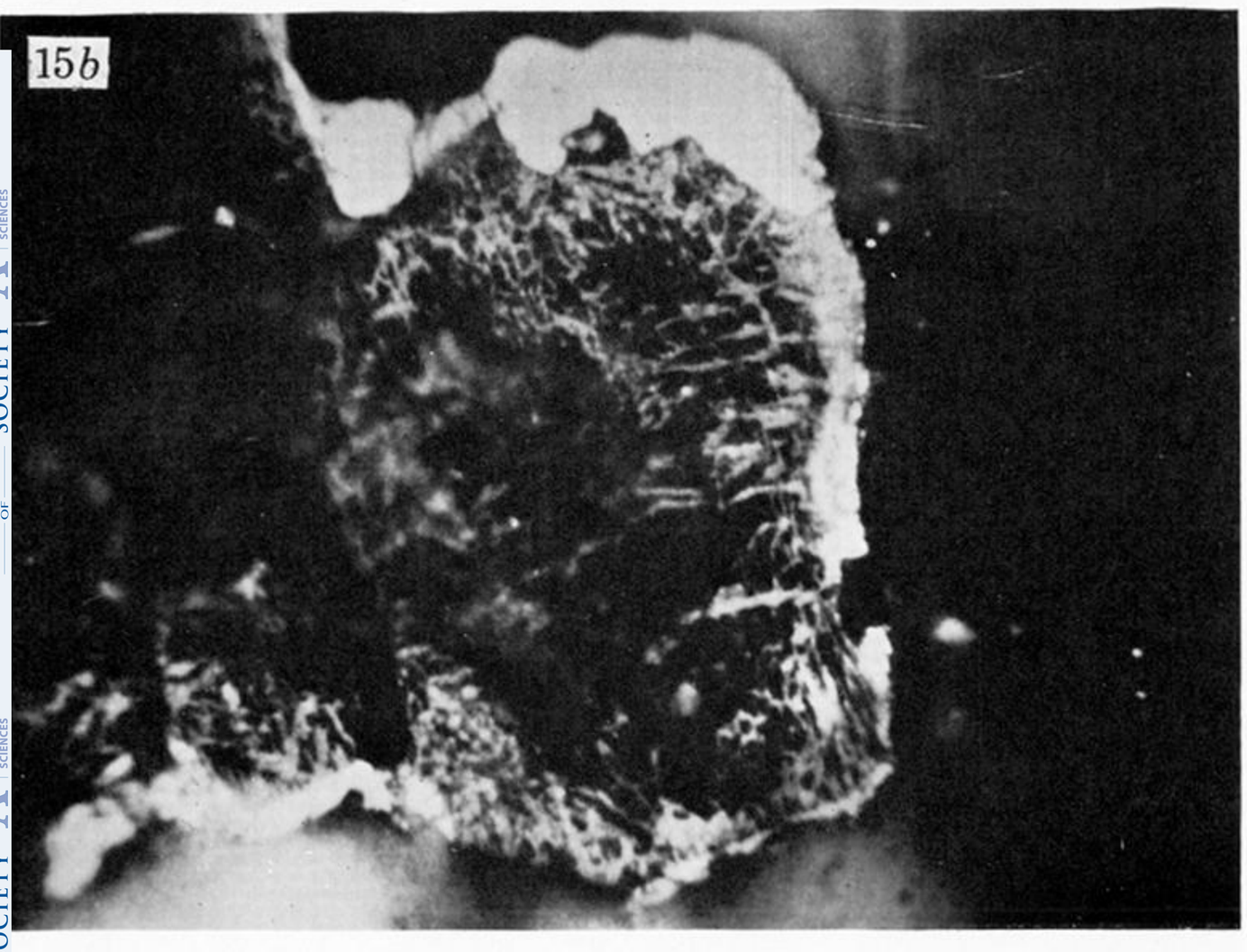

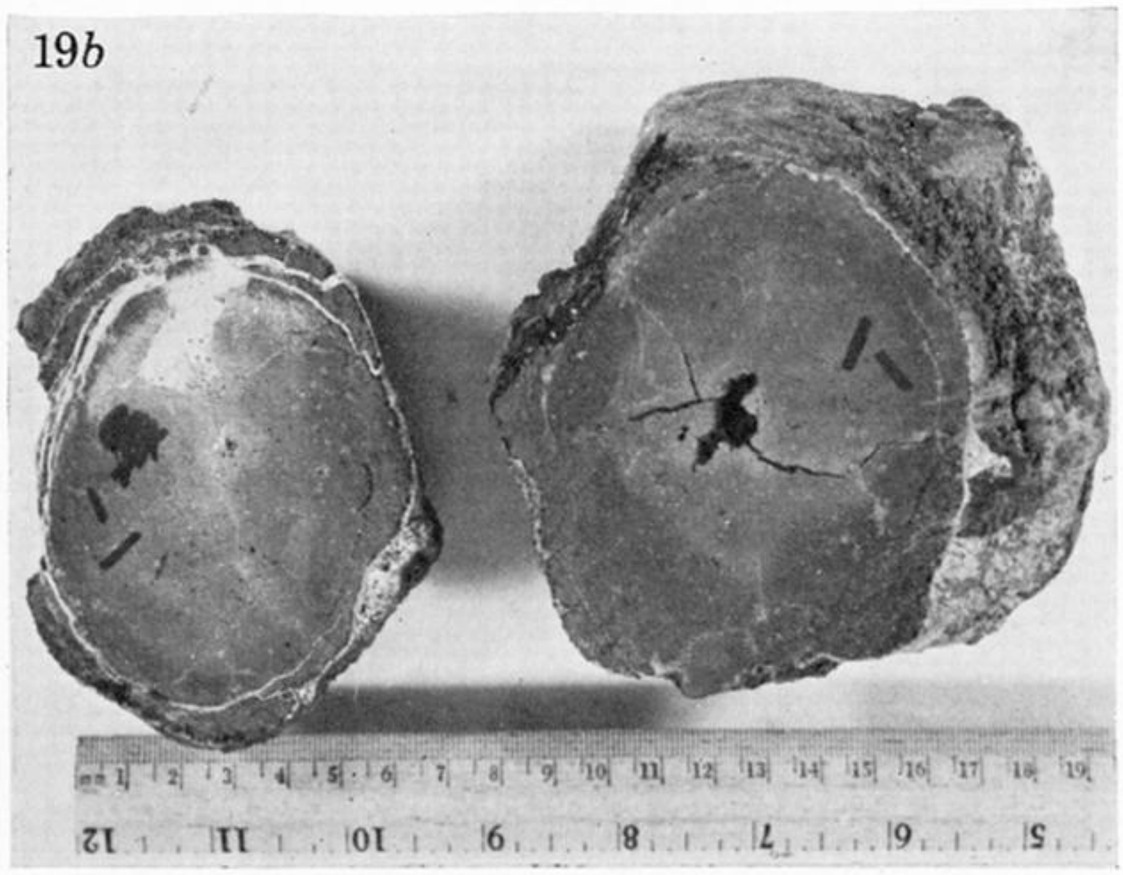

FIGURE 15. Photomicrographs of secondary magnetite and haematite in olivine grains. The magnetite is light grey and has a web-like texture. The haematite increases towards and at the rim of the grains. Conversely, the fraction of magnetite decreases towards the centres of the grains. (From Watkins (1969); field of view 140 μm $\times$ 100 μm.)

FIGURE 19. Photographs of two samples: (*a*) is pahochoe toe E24–15 with a ferromanganese crust from 1.0 to 1.4 cm thick and (*b*) is section through toe E 05–04 showing central cavity and concentric fractures in glass rim, filled with phillipsite.

PHILOSOPHICAL TRANSACTIONS OF THE ROYAL SOCIETY A MATHEMATICAL, PHYSICAL & ENGINEERING SCIENCES

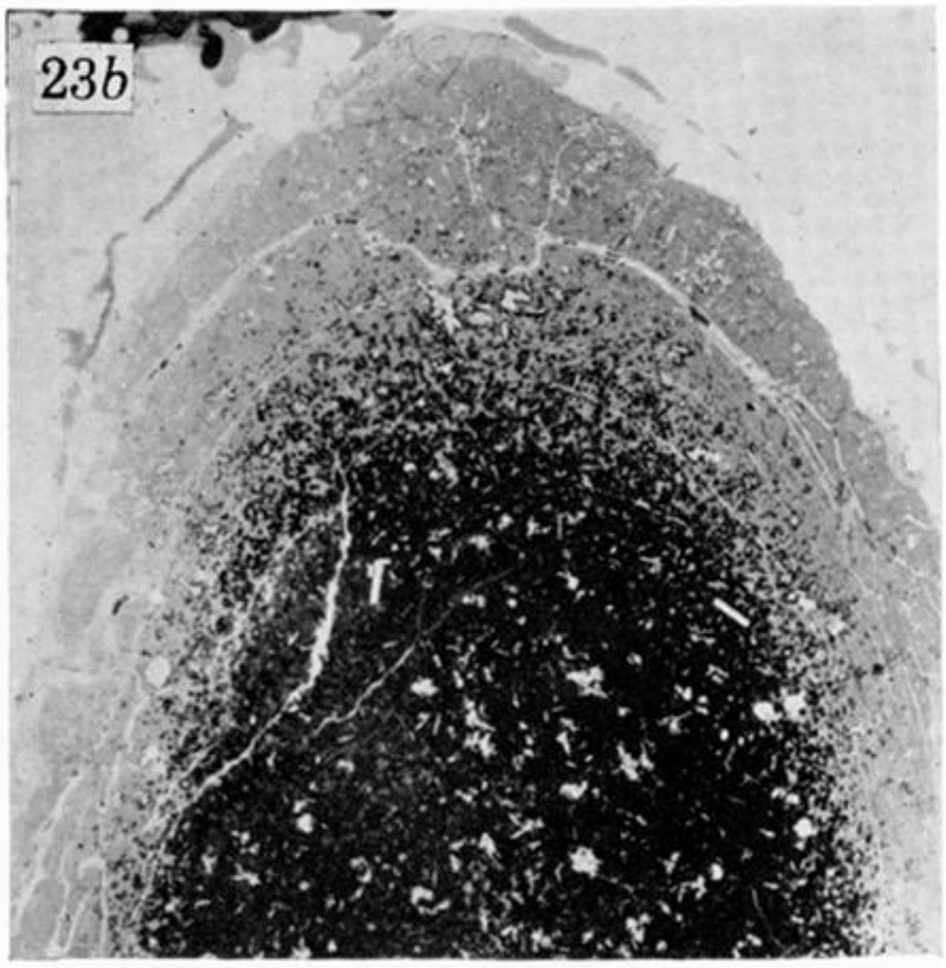

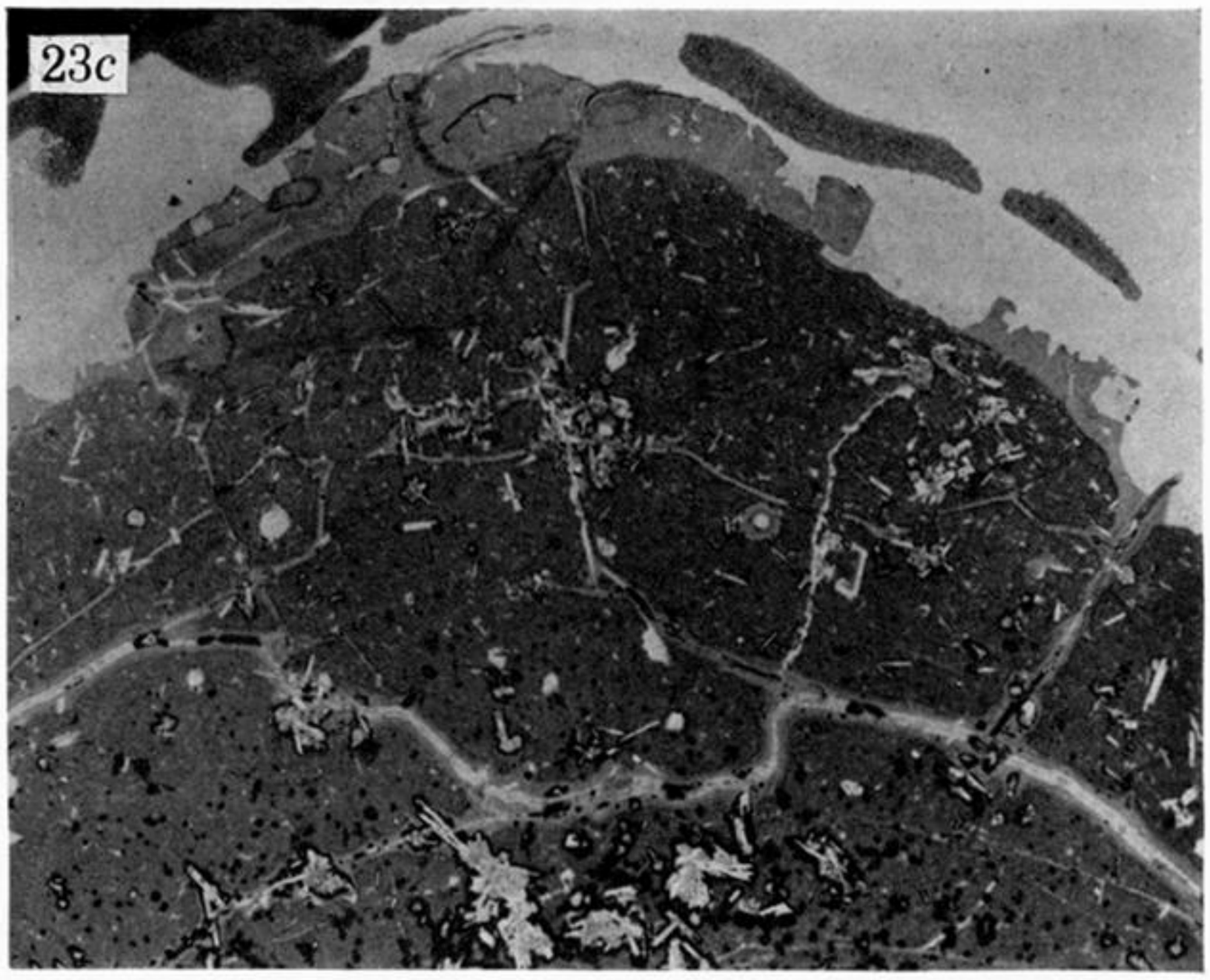

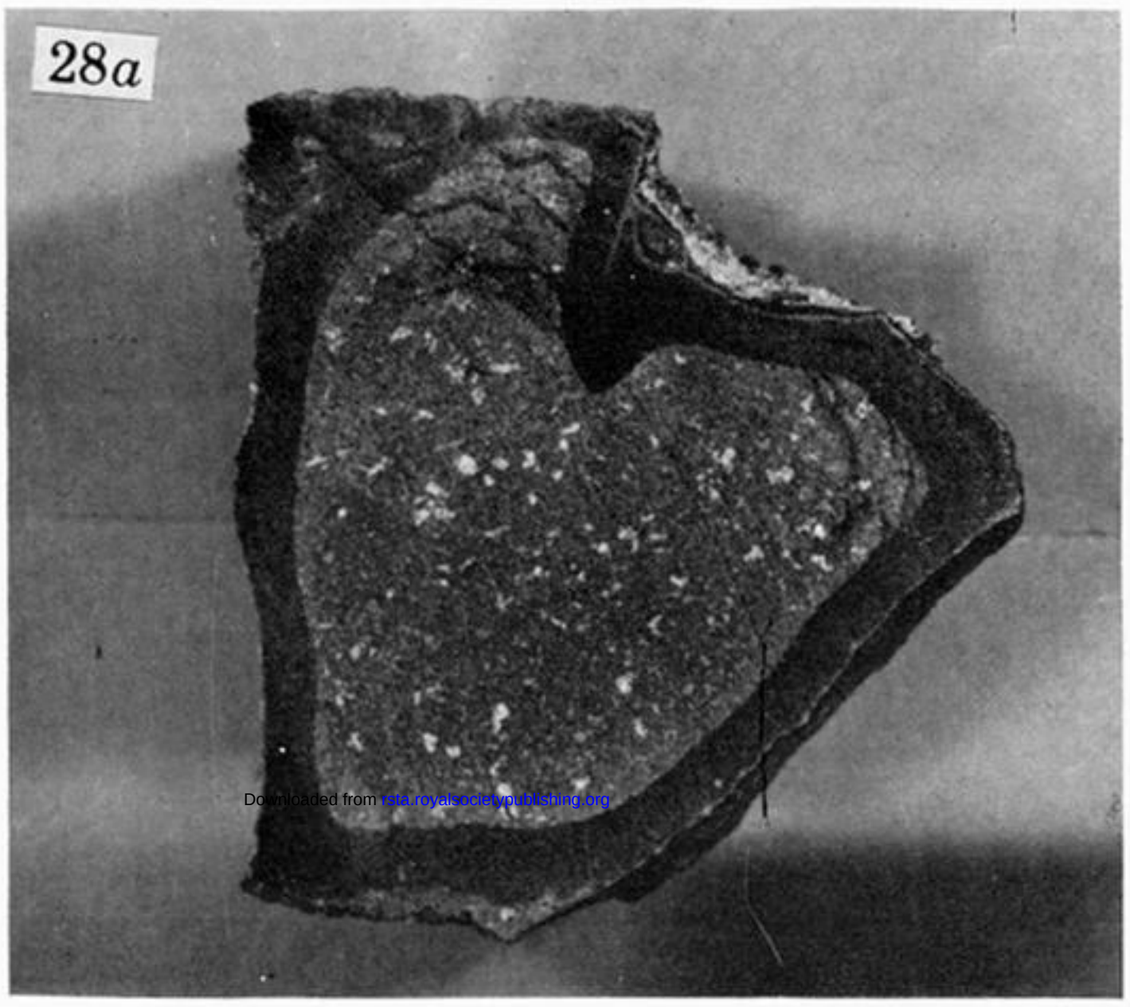

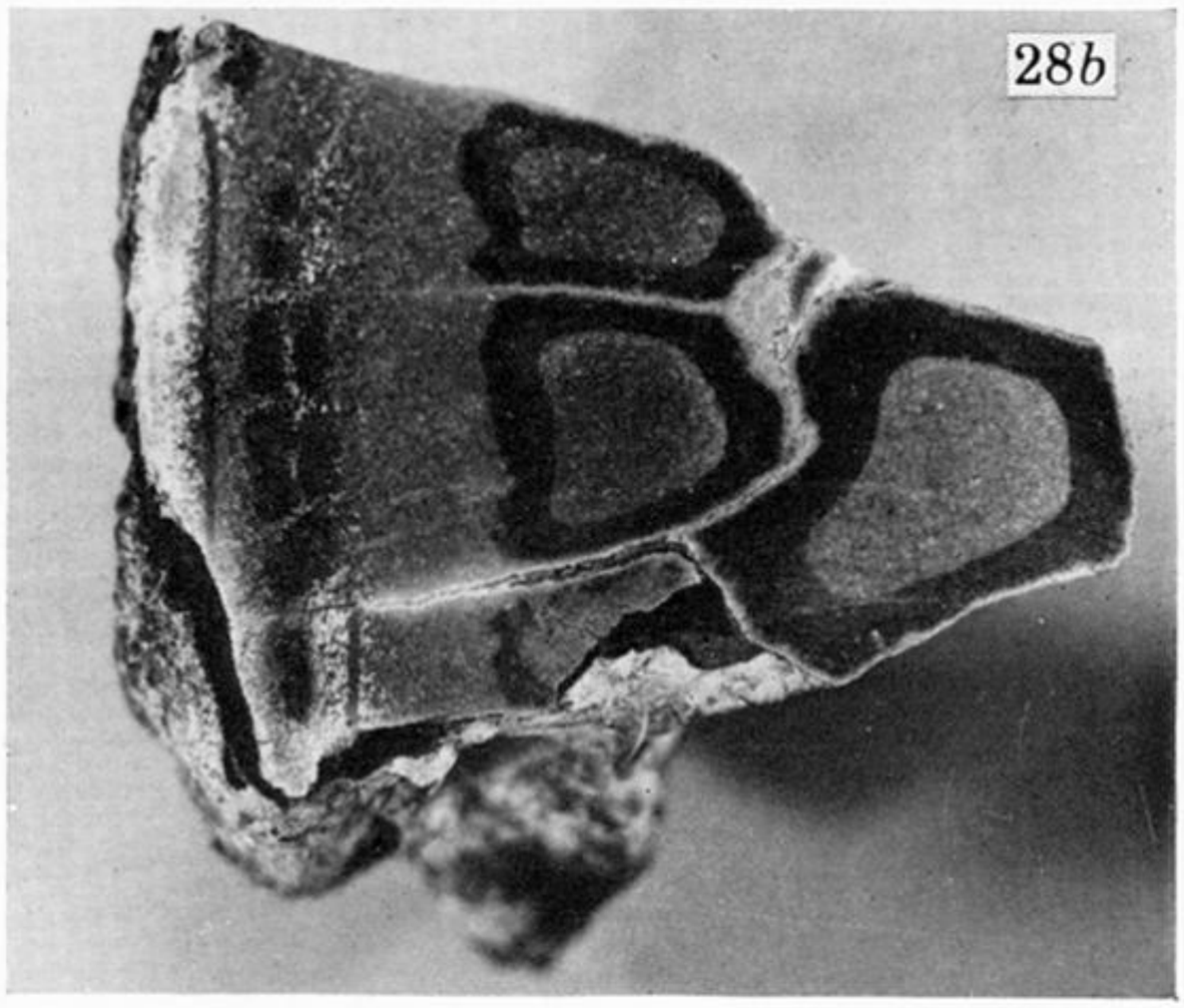

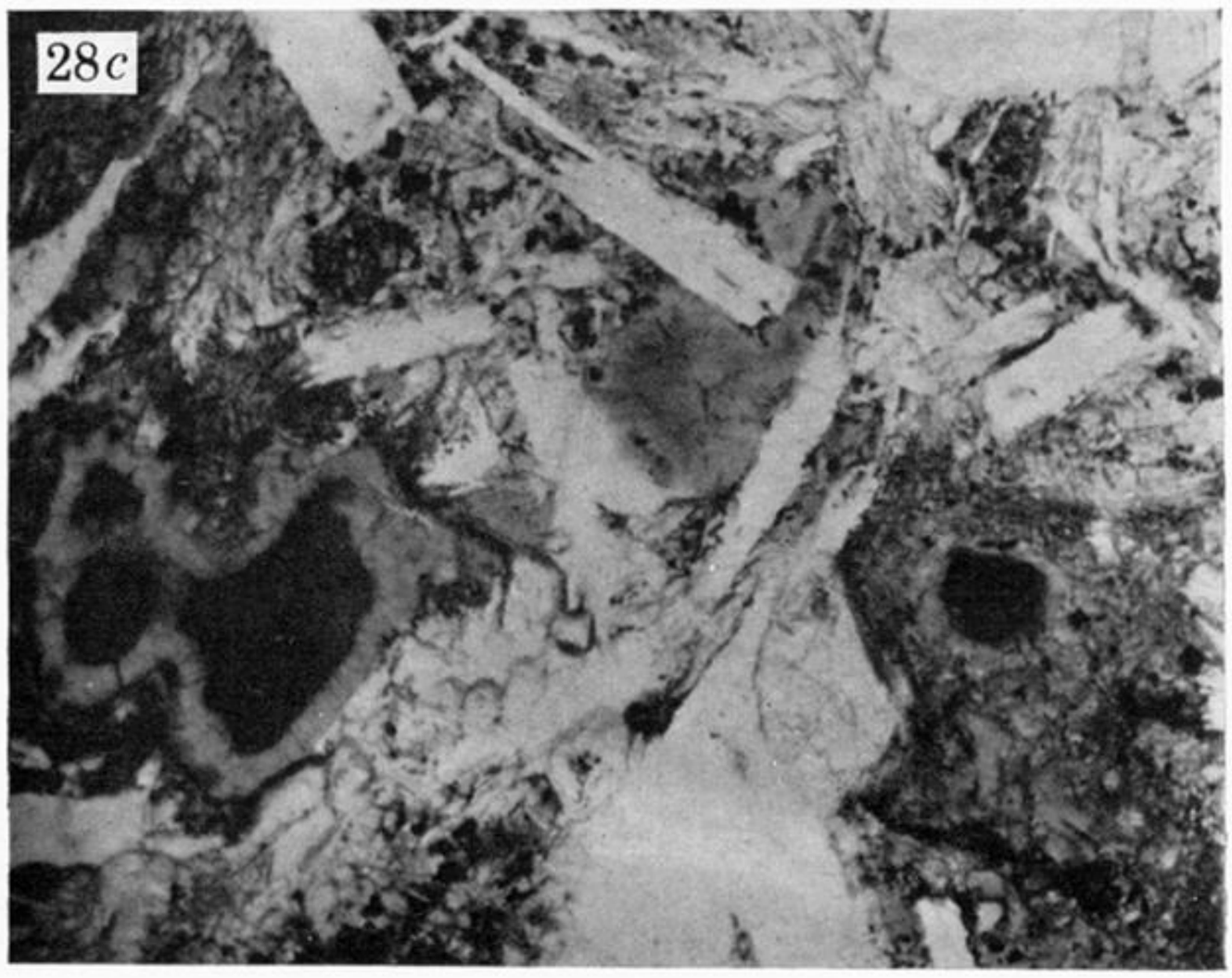

For legends to Figures 23 (*b*) and (*c*) see facing page.

FIGURE 28. Serpentinization of some of the *Eltanin* samples: (*a*) shows the 6 mm thick serpentinized rim in a section normal to the jointing in E 21–10 (2); (*b*) shows the darker sepentinized zones adjacent to fractures in the type wedge-shaped segment normal to the pillow surface of sample E 21–8; (*c*) shows a photomicrograph of a thin section of a specimen from E 21–10 (2), where serpentine (dark grey) lines vesicle walls. Specimen in (*a*) is 10 cm high. Specimen (*b*) is 9 cm wide. Field of view in (*c*) is 0.65 mm × 0.80 mm.

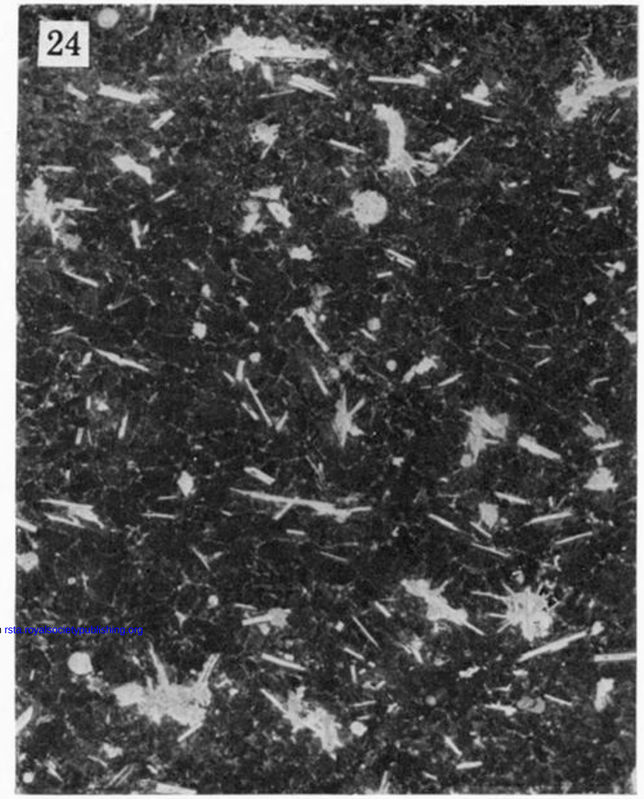

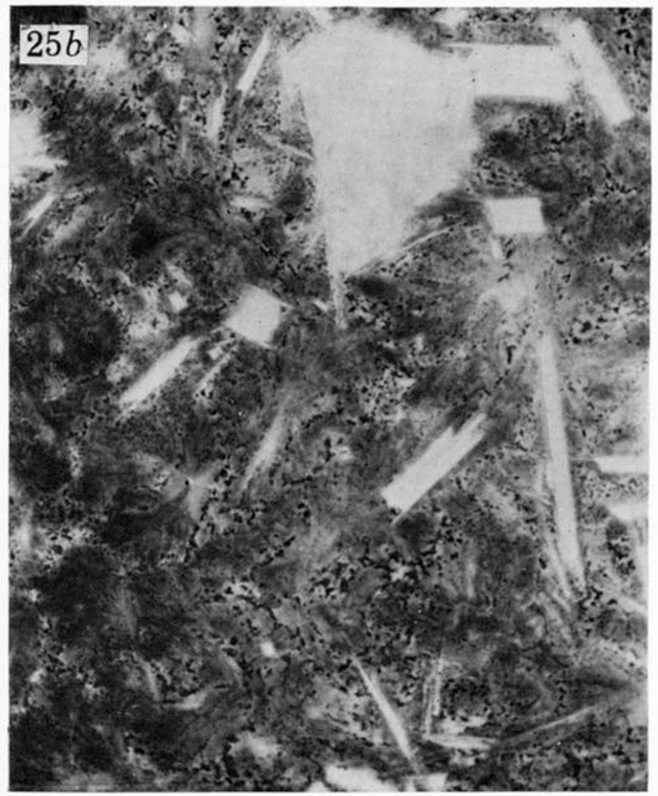

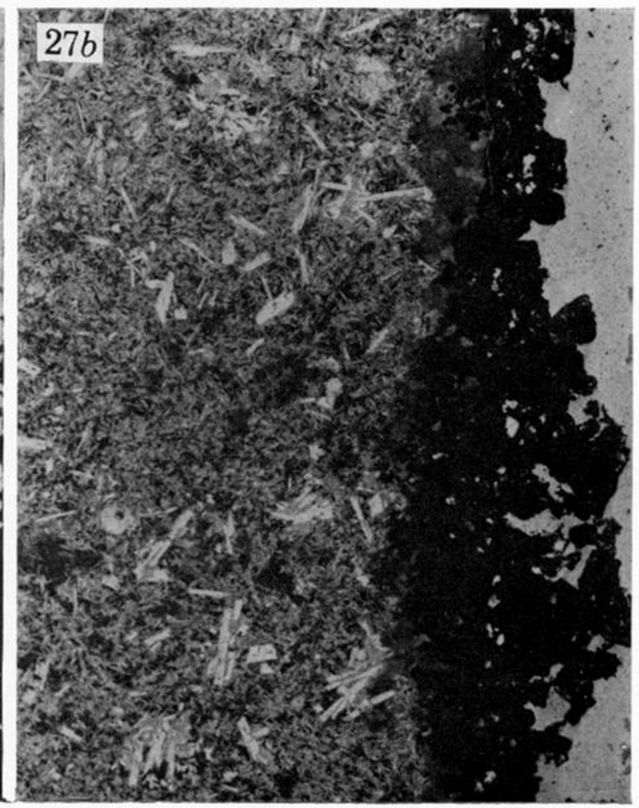

FIGURES 24 TO 27. For legends see facing page.

PHILOSOPHICAL TRANSACTIONS OF THE ROYAL SOCIETY A MATHEMATICAL, PHYSICAL & ENGINEERING SCIENCES